

FOUNDED 1925  
INCORPORATED BY  
ROYAL CHARTER 1961

*"To promote the advancement  
of radio, electronics and kindred  
subjects by the exchange of  
information in these branches  
of engineering."*

# THE RADIO AND ELECTRONIC ENGINEER

The Journal of the Institution of Electronic and Radio Engineers

VOLUME 35 No. 4

APRIL 1968

## Anticipating the Future

CONFERENCES usually have a clearly defined theme which is explored in depth rather than in breadth. The policy of the I.E.R.E. over the years has been to organize conferences of such a specialized nature only when developments point to a real need for a major meeting as a result of which there will be substantial additions to existing knowledge.

Occasionally, however, every engineer should stand back from his particular specialization and take a broad view of the whole of his professional field, particularly the areas in which notable advances have recently been made or are imminent. It was with the intention of providing such an opportunity for electronic and radio engineers that the I.E.R.E. Council planned the 1968 Convention 'Electronics in the 1970s'—which is to be held in Cambridge from 2nd to 5th July. The outline programme and the preliminary details of the first thirty or so main papers printed on pages 186 and 187 of this issue will indicate the extent to which the Council's aims are being achieved.

It is manifestly impossible in a convention of realistic length to cover *all* the areas in electronic engineering which meet the criterion stated above. The selection which has been made will, however, provide opportunity for engineers to appreciate, in a way not possible at a more specialized meeting, the trends and the more important implications in five main 'growth areas'. These will be covered in symposia on computer applications, communications, automatic testing, materials and components, and education. Equally important, though not covered quite so comprehensively, are the subjects on which single authoritative survey papers are being presented, namely underwater acoustics, electronics in oceanography, ultrasonics, and applications of lasers.

For this new kind of broad convention, the choice of venue is important in that the opportunity of seeing and hearing about work on the 'frontiers of electronics' adds to the forward-looking theme of the Convention. Thus those taking part will learn at first hand, in short symposia, about the present research programmes of both the Cavendish Laboratory and the Engineering Laboratory, two of Britain's leading university research establishments.

The proceedings during previous Institution Conventions in Cambridge have included the presentation of the Clerk Maxwell Memorial Lecture. Monsieur M. Ponte, head of the well known French electronics company, C.S.F., has accepted an invitation to give the Sixth Lecture in this series on Wednesday, 3rd July. The Convention Banquet will take place on the following evening in the Hall of King's College and will represent the Institution's main social function of 1968.

As this preliminary description of the programme shows, the Convention will provide an unrivalled opportunity for all members, but especially those in what is usually termed middle and upper management, to take a broad view of the way in which electronics will develop in the next decade.

F. W. S.

# Institution Convention at Cambridge University

Tuesday 2nd July to Friday 5th July 1968

## *Electronics in the '1970s'*

The purpose of this Convention is to 'up-date' engineers over a large sector of the field of electronics with particular emphasis on those developments which will have the greatest impact during the next decade. At the time of printing the programme is not finalized, but a provisional programme is given below. Further details will, from time to time, be given in the Institution's publications, *The Radio and Electronic Engineer* and the *Proceedings* of the I.E.R.E., and will also be sent to all persons who register for the Convention.

Accommodation, both in the lecture theatres and in King's College, is limited and applications to attend will be dealt with in strict rotation as received.

### PROVISIONAL PROGRAMME

<b>Monday, 1st July</b>	1600 onwards	Registration in the Convention Office in King's College.
<b>Tuesday, 2nd July</b>	0915	Opening by the President, MAJOR GENERAL SIR LEONARD ATKINSON, K.B.E.
Session 1	0930–1230	Computers and Automation.
Session 2	1415–1745	Electronic Engineering Education.
<b>Wednesday, 3rd July</b>		
Session 3	0900–1230	Survey papers.
Session 4	1415–1715	Automatic Test Equipment.
	1730–1830	The Sixth Clerk Maxwell Memorial Lecture.
<b>Thursday, 4th July</b>		
Session 5	0900–1230	} Communications.
	1415–1600	
Session 6	1615–1745	Electronics in the Cavendish Laboratories.
	1930	Convention Banquet in King's College.
<b>Friday, 5th July</b>		
Session 7	0900–1230	Future Materials and Components.
Session 8	1415–1630	Electronics in the University Engineering Laboratory.

### ***Among the Papers to be presented are the following:***

#### **Session 1. COMPUTERS AND AUTOMATION**

'Progress in On-line Control by Computer' by D. BEST, O.B.E., *Manager, Automation Systems Division, Ferranti Ltd.*

'Simulation Techniques for Traffic Studies' by M. G. HARTLEY, *University of Manchester Institute of Science and Technology.*

Two further papers will be presented by engineers concerned with the application of computers in industry.

#### **Session 2. ELECTRONIC ENGINEERING EDUCATION**

'A New Approach to Post-Graduate Courses' by Professor G. D. SIMS, *Southampton University.*

'Training after Graduation' by Professor W. E. J. FARVIS, *Edinburgh University.*

'The Role of the Polytechnics' by N. L. GARLICK, *Vice-principal, Brighton College of Technology.*

'Teaching Microcircuits' by D. F. DUNSTER, *Principal Lecturer, West Ham College of Technology.*

'Microelectronics Developments in the 1970s' by Dr. B. H. VENNING, *Brighton College of Technology.*

**Session 3. SURVEY PAPERS**

- 'Applications of Lasers in Electronic and Radio Engineering' by Professor W. A. GAMBLING and Dr. R. C. SMITH, *University of Southampton.*
- 'Underwater Acoustics' by Professor D. G. TUCKER, *University of Birmingham.*
- 'High Power Ultrasonics in Industry' by A. E. CRAWFORD, *Manager, Ultrasonics Products Group, Radyne-Delapena Ltd.*
- 'Electronic Measurements in Oceanography' by R. BOWERS, *National Institute of Oceanography.*

**Session 4. AUTOMATIC TEST EQUIPMENT**

(Papers will be presented by engineers from the Armed Services and from the aircraft and electronic industries.)

**The Sixth Clerk Maxwell Memorial Lecture**

To be delivered by M. MAURICE PONTÉ, *President of the C.S.F. Group of Companies (Compagnie Générale Télégraphique Sans Fils.)*

**Session 5. COMMUNICATIONS**

- 'Global Communications—Current Techniques and Future Trends' by R. W. CANNON, *Deputy Engineer-in-Chief, Cable and Wireless Ltd.*
- 'Communication Services in the United Kingdom' by a *Deputy Director of Engineering, G.P.O.*
- 'The Impact of Pulse Code Modulation on the Telecommunications Network' by Professor K. W. CATTERMOLE, *University of Essex.*
- 'A Communication Network for Real-Time Computer Systems' by D. W. DAVIES, *Head of Division of Computer Science, National Physical Laboratory.*
- 'The Control System of the National Grid and its Communication Links' by P. F. GUNNING, *Central Electricity Generating Board.*
- 'Future Broadcasting Techniques' by Dr. K. R. STURLEY, *British Broadcasting Corporation.*

**Session 6. ELECTRONICS IN THE CAVENDISH LABORATORY**

Contributions will be made by Dr. D. M. A. WILSON, D. W. J. BLY and H. BETT on 'Electronics in the Cavendish Laboratory' including the work of the Mond Laboratory (low-temperature physics), the Electron Microscope group, the Meteorological Physics group and the Radio Astronomy group.

**Session 7. FUTURE MATERIALS AND COMPONENTS**

- 'Two Dimensional Electronics' by Professor J. C. ANDERSON, *Imperial College of Science and Technology.*
- 'The Monolithic Linear Integrated Circuit' by Professor W. GOSLING, *University College of Swansea.*
- 'The Interconnexion of Integrated Circuits' by Dr. S. S. FORTE, *The Marconi Co. Ltd.*
- 'The Impact of the Burghard Scheme' by T. M. BALL, *I.E.R.E. Representative on B.S.I. Microelectronics Panel.*

**Session 8. ELECTRONICS IN THE CAMBRIDGE UNIVERSITY ENGINEERING LABORATORY**

An introductory talk by Professor C. W. OATLEY, followed by a tour of the Laboratories and discussion.

**Preprints.** Preprints of papers or extended summaries will be available at the Convention Office at Cambridge.

**Registration.** Persons wishing to attend this Convention should register without delay as accommodation in the Lecture Theatre is limited. An application form is contained on page (xv) of this issue. The registration fee is: £5 for members; £8 for non-members. These charges include: preprints, attendance at all lecture sessions, Convention badge, light refreshments in the morning and afternoon.

**Residential Accommodation.** Residential accommodation for men and women will be available in King's College. The charge for accommodation, including all meals from dinner on Monday, 2nd July to lunch on Friday, 5th July and including the Convention Banquet, will be £18.

## INSTITUTION NOTICES

### Dinner of Council and Committees

As announced in the March *Journal*, the Twelfth Dinner of Council and Committees is being held on Thursday, 16th May. This Dinner, a traditional function, will be an occasion at which to thank the Immediate Past President, Professor Emrys Williams, for his work for the Institution. It also provides an excellent opportunity for all the members who assist the Institution to meet socially and be accompanied by their ladies, and one or two personal guests.

The charge, including wines with Dinner, is £3 17s. 6d. per ticket.

### NELCON II

Full details and registration forms are now available for the Second National New Zealand Electronics Convention to be held at the University of Auckland from 20th to 23rd August, 1968. The Convention is sponsored by the New Zealand Section of the I.E.R.E. and the New Zealand Electronics Institute (Inc.).

There will be three symposia, on Integrated Circuits and the Electronics Designer, Communications for Computers, and Automation for Primary Production in New Zealand. The papers have been grouped into five sections: components and instruments; applied electronics (including industrial, medical and aviation applications); research electronics; communications; and data handling. During the four days of the Convention there will be ample time for general discussions and professional meetings, as well as social functions and a trade exhibition.

Enrolment fees are \$9 and \$7 for students. Enrolment forms and full details may be obtained on direct application to the Secretary, NELCON II, P.O. Box 3266, Auckland 1, New Zealand.

### Conference on Stress Analysis

The Fourth International Conference on Experimental Stress Analysis will be held at Cambridge University from 7th to 10th April, 1970. The Conference is being organized again by the Institution of Mechanical Engineers, and the main theme will be the influence of experimental stress analysis on design.

Original papers in any branch of experimental stress analysis are welcomed, although preference will be given to papers concerned with the following: application of experimental techniques to design problems and new production methods; the correlation between theoretical and experimental techniques for design purposes; data processing and presentation of information; methods of retrieval for design purposes; the influence of new prototype or model materials on experimental stress analysis;

and influence of experimental stress analysis on design philosophy.

Summaries of about 600 words, together with a short resumé of about 100 words, in English, French or German, giving an outline of the technique used with the results obtained and stating which parts, if any, of the contribution are original, should be submitted to Mr. R. J. Millson, Institution of Mechanical Engineers, Birdcage Walk, London, S.W.1, before 1st April 1969.

### Royal Society Research Fellowships

The Royal Society invite applications for two Scientific Information Research Fellowships for research in the general field of scientific information.

The fellowships are intended for young men and women of any nationality, and appointments will be for two years in the first instance, from 1st October 1968, and may be renewed annually. The stipend will be in the range from £2275 to £2675 per year, rising by annual increments of £100, and will depend upon qualifications. There will be a contributory super-annuation benefit scheme.

Applications, which should be received not later than 31st May 1968, should be made on forms obtainable from the Executive Secretary, The Royal Society, 6 Carlton House Terrace, London, S.W.1. The subject of the proposed research and the place at which it would be carried out, together with the name of the Head of the Department, whose permission should first be obtained, must also be stated.

### Royal Charter and Bye-laws

A revised edition of the Institution's Royal Charter and Bye-laws, incorporating amendments made recently to allow for changes in membership designation, is now available, price 5s. Requests for this publication, which should be accompanied by a remittance, should be addressed to the Secretary, I.E.R.E., 9 Bedford Square, London, W.C.1.

### Correction

The following amendments should be made in the paper 'System Engineering for Reliability and Ease of Maintenance', published in the February issue of *The Radio and Electronic Engineer*:

Page 79, Table 1 (contd.): The seventh item should read:

CARBON GRADE I RESISTORS

522 267 11600·882 etc.

The accidental failure rate per 1000 hours for the fourteenth item, CARDS, should read:

0·00053%.

# Standards for Electrical Circuit Properties at Radio Frequencies: A Survey of Some U.K. Developments

By

I. A. HARRIS,

C.Eng., M.I.E.E., M.I.E.R.E.†

*Reprinted from the Proceedings of the Joint I.E.R.E.-I.E.E. Conference on 'R.F. Measurements and Standards' held at the National Physical Laboratory, Teddington, on 14th-16th November 1967.*

**Summary:** The choice of properties for basic r.f. standards and their precise definitions are discussed. The differences in approach of lumped circuit-element and wave transmission languages are noted and reasons are given for adopting the latter in the definitions of properties measured. The importance of precision coaxial connectors to realize well-defined cross-sections in a circuit is stressed. The basic properties chosen are impedance (and equivalent properties), attenuation and power. Brief descriptions of standards for these three properties are given, together with some comments on making comparisons.

## 1. Introduction

Measurement standards are needed as a foundation on which to base the calibration of instruments for the measurement of a range of properties. There are two main uses for measurements; first, as part of scientific method on which the establishment of standards and their inter-connection is founded, and secondly, to satisfy the need for quantitative functional tests on items or assemblies of apparatus for commercial or operational purposes.

The principle which governs the choice of radio frequency electrical properties to form the set of basic standards is to choose those properties that can be realized most accurately while taking account of the need to have them connected by well-established linear circuit theory. The set of basic properties which satisfies these requirements comprises impedance, attenuation and power. Impedance includes complex admittances at frequencies up to 300 to 400 MHz and the magnitude and angle of complex voltage reflection coefficients for higher frequencies. Attenuation here includes both ratio of magnitudes and phase change through a two-port element. Frequency and noise are not included in this paper.

The range of frequencies considered embraces the range of radio frequency phenomena described by alternating voltages and currents in lumped-element circuits and the higher frequency range in which the dimensions of the apparatus are not very small compared with a wavelength, where the phenomena are necessarily described in terms of guided electromagnetic waves. In precision measurements, it is

† Electrical Inspection Directorate, Ministry of Technology, Harefield, Middlesex.



LUMPED-ELEMENT LANGUAGE	WAVE LANGUAGE
Voltage reflection coefficient in terms of impedance	Impedance in terms of voltage reflection coefficient
$\rho = \frac{Z - R_0}{Z + R_0}$	$Z = R_0 \frac{1 + \rho}{1 - \rho}$
Elementary incident wave voltage in terms of source e.m.f.	Source e.m.f. in terms of elementary wave voltage
$a = \frac{E_s R_0}{Z_s + R_0}$	$E_s = \frac{2a}{1 - \rho_s}$
Power absorbed in load	
$P_L = \frac{ E_s ^2 R_L}{ Z_s + Z_L ^2}$	$P_L = \frac{ a ^2}{R_0} \cdot \frac{(1 -  \rho_L ^2)}{ 1 - \rho_s \rho_L ^2}$
Available power from source	
$P_{av.} = \frac{ E_s ^2}{4R_s}$	$P_{av.} = \frac{ a ^2}{R_0(1 -  \rho_s ^2)}$

Fig. 1. Comparison of lumped circuit-element and wave languages for the description of radio-frequency networks.

necessary to use the 'wave' language instead of the 'lumped-element' language down to much lower frequencies than is customary in measurements of only moderate accuracy. Both languages give the same information in any problem that can be described by the lumped-element concepts. For instance, Fig. 1 shows the connection at a cross-section between a source and a load. Everything to the left of the cross-section constitutes the source while everything to the right constitutes the load. This enables relations to be established between the voltage  $a$  associated with an

elementary incident wave in an ideal transmission line of purely resistive characteristic impedance  $R_0$  and the source e.m.f.  $E_s$  of a lumped-element circuit representation. It should be noted that what is usually termed the voltage between the two conductors of a transmission line, at any cross-section, is the sum of the voltage of the resultant incident (forward) wave and the voltage of the resultant reflected (backward) wave at the cross-section. Similar considerations apply to currents in the conductors, except that the current associated with an elementary incident wave is  $a/R_0$ .

Two-port and more complicated components are described by scattering coefficients in the wave language, these being voltage reflection coefficients and voltage transmission coefficients or corresponding coefficients for current. The current transmission coefficients are the same while the reflection coefficients are negative in sign compared with the voltage coefficients.

When using actual precision coaxial transmission lines there will be a small loss and the actual characteristic impedance will have a very small imaginary component. Nevertheless, the scattering coefficients are still best referred to the ideal  $R_0$  instead of the complex  $Z_0$ , small corrections being made to allow for the actual conditions.

Properties measured are referred to definite cross-sections in a transmission line and such cross-sections must be realized physically and be accessible. It is therefore necessary to be able to connect and disconnect coaxial lines at precisely defined cross-sections while maintaining a substantially uniform characteristic impedance throughout. Recognition of this need has led to the development of precision coaxial connectors for use in all measurements concerned with the establishment of standards and the best calibration work. Precision connectors produced for embodiment in measuring apparatus usually include an insulating support for the inner conductor (general precision connectors), while precision connectors for certain standardizing applications are usually made integral with lengths of standard line and have no support for the inner conductor (laboratory precision connectors). The most important properties of a precision connector pair are that both inner and outer conductors break at a common cross-section and have a very small contact impedance.<sup>1</sup>

When precision connectors are employed it is possible to make precise definitions of the properties relative to the well-established linear circuit theory (particularly in terms of scattering coefficients and power flow across a cross-section) and to realize the necessary conditions physically. This is essential for the establishment of meaningful standards of measurement.

## 2. Impedance

### 2.1. Bridge Methods at Frequencies up to 250 MHz

An extensive study to determine the most suitable type of bridge for precision impedance or admittance measurement in the h.f. and v.h.f. bands, led to the conclusion that the most promising type was the twin-T bridge.<sup>2</sup> The following requirements can all be met only with a dual twin-T bridge:

- (a) The effects of unwanted residual circuit parameters should be calculable. For instance, the accurate r.f. calibration of the two main standard variable capacitors must be determined by calculation of corrections to the calibration made at 1 kHz. This requirement is in general met by constructing the bridge circuit entirely from machined metal and insulating material parts, using a straight cylindrical carbon film resistor without wire ends for the standard resistor and using no wire connections at all.
- (b) A fixed value of standard conductance or resistance has to be employed in the bridge and it is necessary to determine its precise r.f. value ( $\pm 0.2\%$ ) by measurement. This can be done by making the bridge 'dual', i.e. by providing for an unknown admittance to be connected in the lower limb of either T of the twin-T bridge, so that the r.f. conductance of the standard can be determined in terms of capacitance and frequency.
- (c) The design must be such that the residual circuit parameters associated with the series connecting elements and the neighbourhood of the common junction point can all be compensated.
- (d) Precision coaxial connectors with co-planar inner and outer conductor faces must be employed for connection to the unknown, to ensure the realization of a definite reference-plane for the measured admittance.
- (e) The bridge should provide a range of conductance measurement that is independent of frequency.

The basic circuit of the bridge design adopted<sup>2</sup> is shown in Fig. 2. The balance equations for this circuit for a null at the detector D are

$$\frac{1}{\omega^2 L_a} = C_a + C_1 + C_2 + \left[ \frac{C_1 C_2}{C_3} \right] \left[ 1 + \frac{g_b}{G_s} \right] + \frac{g_a C_{sg}}{G_s}$$

$$\frac{1}{\omega^2 L_b} = C_b + C_3 \left[ 1 - \frac{g_a}{\omega^2 R_s C_1 C_2} \right] - \frac{g_b C_{sg}}{G_s} \quad \dots\dots(1)$$

In the circuit,  $C_a$  and  $C_b$  are calibrated, coaxial variable capacitors associated respectively with the coaxial terminals A and B.  $L_a$  and  $L_b$  are inductors which are adjusted to obtain initial balance of the bridge (i.e. a null at D) when A and B are open-circuited.  $g_a$  and

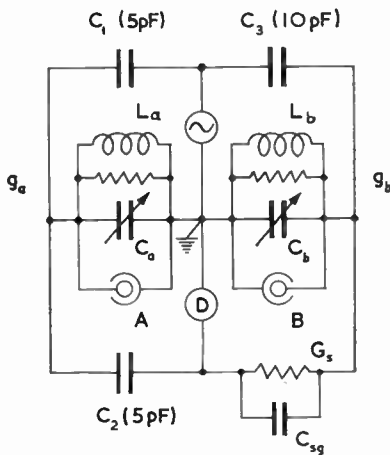


Fig. 2. Circuit diagram of dual twin-T admittance bridge. The residual junction impedances have been omitted to simplify the diagram.

$G_b$  are conductances to account for losses in the inductor and capacitor assemblies.  $G_s$  and  $C_{sg}$  are the effective conductance and shunt capacitance of the 'standard' resistor in its coaxial mount. The effective series resistance of this is

$$R_s = 1/[G_s(1 + \omega^2 C_{sg}^2/G_s^2)]$$

With the 'unknown' admittance  $Y_{xb} = G_{xb} + j\omega C_{xb}$  connected to B, the components are given in terms of the decrements  $\Delta C_a$  and  $\Delta C_b$  of the variable capacitors in the bridge required to regain balance, by the relations

$$G_{xb} = (C_3/C_1 C_2)G_s \cdot \Delta C_a \quad \dots\dots(2)$$

$$C_{xb} = \Delta C_b + (G_{xb}/G_s)C_{sg} \quad \dots\dots(3)$$

With an 'unknown' admittance connected to A, the components are given by the relations

$$G_{xa} = -\omega^2(C_1 C_2/C_3)R_s \cdot \Delta C_b \quad \dots\dots(4)$$

$$C_{xa} = \Delta C_a - (G_{xa}/G_s)C_{sg} \quad \dots\dots(5)$$

The value of  $C_{sg}$  can be found by measuring the capacitance of a resistor at A and at B at a low frequency at which the d.c. values of  $G_s$  and  $G_x$  can be assumed to hold with reasonable accuracy. In this case, equations (3) and (5) can be equated, giving

$$C_{sg} = (G_s/2G_x)(\Delta C_a - \Delta C_b) \quad \dots\dots(6)$$

The value of  $G_s$  at any high frequency can be determined by measuring a resistor at A and at B. Equating (2) and (4) then gives

$$G_s = \omega(C_1 C_2/C_3)(-\Delta C_b/\Delta C_a)^{\frac{1}{2}} \times (1 + \omega^2 C_{sg}^2/G_s^2)^{-\frac{1}{2}} \quad \dots\dots(7)$$

In this way the bridge can be used to measure its own standard conductance in terms of capacitance and frequency.

The foregoing description is only an outline. Although the design of the bridge is such that the self and mutual earth junction residual impedances are substantially self-compensating, there are residual impedances between the connecting points of  $L_a$ ,  $C_a$  and the junction between  $C_1$  and  $C_2$  for the A arm (and similarly for the B arm) which have to be determined.<sup>2</sup> Finally, a correction must be determined and applied for the length of conductors between the reference-planes of the connectors and the effective bridge junction points, and allowance must be made for the fringe-fields at the coaxial terminals when in the open-circuit condition.

The following uncertainties have been confirmed by experiment:

At 200 MHz:

$$G: \pm 0.2\% \pm 5 \mu\Omega^{-1}$$

$$C: \pm 0.2\% \pm 0.005 \text{ pF (up to } 10 \text{ m}\Omega^{-1} \text{ shunt conductance)}$$

$$\pm 0.2\% \pm 0.02 \text{ pF (up to } 30 \text{ m}\Omega^{-1} \text{ shunt conductance)}$$

Up to 100 MHz:

$$G: \pm 0.1\% \pm 2 \mu\Omega^{-1}$$

$$C: \pm 0.1\% \pm 0.005 \text{ pF (up to } 10 \text{ m}\Omega^{-1} \text{ shunt conductance)}$$

$$\pm 0.1\% \pm 0.02 \text{ pF (up to } 30 \text{ m}\Omega^{-1} \text{ shunt conductance)}$$

The total range is  $50 \text{ m}\Omega^{-1}$ ,  $\pm 50 \text{ pF}$ .

### 2.2. Coaxial-line Standards of Impedance

Quarter wavelength, air-spaced, rigid coaxial lines with unsupported inner conductors and precisely defined planes of contact at which the ends of both inner and outer conductors are coincident, can be used as standards of impedance equal to the characteristic impedance of the line. The properties of such standards are determined primarily by precise dimensional measurements of the uniform cylinder and tube, but for the highest accuracy certain residuals arising from the finite conductivity of the metal have to be determined electrically.<sup>3</sup> The inner conductor is supported by the two coaxial lines between which the standard line is connected, the two ends of the standard forming 'laboratory precision connectors'. Both the distributed residuals of the line at high-frequency and the high-frequency typical contact impedance of the connections can be determined from a line, similar to a standard line, but an integral multiple of half a wavelength in length, together with two terminations, a 'short-circuit' disk and an 'open-circuit' formed by a

short-circuit at the end of a quarter-wave line. The details of the method of measurement are given in reference 3.

It has already been stated in Section 1 that reflection coefficients are defined relative to a nominal, resistive characteristic impedance  $R_0$ , whereas all actual standard lines, however precise, have a complex characteristic impedance  $Z_0$  which closely approximates to  $R_0$ . To enable corrections to be made in any application where the highest precision is required, the standard line may be regarded as a two-port circuit element defined by the usual voltage scattering coefficients. If  $L_0$  is the inductance per unit length associated with the magnetic flux in the space between the conductors and  $L_{0i}$  is the inductance per unit length associated with current penetration into the conductors, and if  $r_0$  is the r.f. resistance per unit length and  $\delta R_0$  is a small error in the mean geometrical characteristic impedance, then one can define a reflection coefficient

$$\rho = \frac{\delta R_0}{2R_0} + \frac{L_{0i}}{4L_0} - j \frac{r_0}{4\omega L_0} \quad \dots\dots(8)$$

This is very small, and is typically  $|\rho| = 2 \times 10^{-4}$  at 1 GHz. It varies inversely as the square root of the frequency and is usually appreciable only at frequencies below 1 GHz. The scattering coefficients can then be expressed sufficiently accurately by the approximate relations

$$S_{11} = S_{12} = 2|\rho| \sin \beta l e^{j(\phi + \pi/2 - \beta l)} \quad \dots\dots(9)$$

$$S_{21} = S_{12} = e^{-\alpha l} e^{-\beta l} \quad \dots\dots(10)$$

where the attenuation constant

$$\alpha = r_0 / (2\sqrt{L_0/C_0})$$

and the phase-change constant

$$\beta = \omega\sqrt{L_0 C_0}(1 + L_{0i}/2L_0).$$

$\phi$  is the phase angle of  $\rho$  which equals  $-\pi/2$  when

$$\delta R_0 = 0 \text{ and } \omega L_{0i} = R_0 \text{ and}$$

$l$  is the physical length of the line.

2.3. *Special Standing-wave Methods for 0.4 to 3 GHz*

Impedances which nearly match the nominal characteristic impedance of a coaxial line, usually 50 ohms, are of importance in v.h.f. and u.h.f. work and their measurement with a high degree of precision is often required. Such measurements cannot reliably be carried out in a direct manner with a slotted-line and standing wave indicator because the characteristic impedance of the line is seldom accurate enough, there may be reflections from the support at the measuring end of the line and there may be non-uniformity in the probe pick-up as it traverses the slot. Accordingly, a

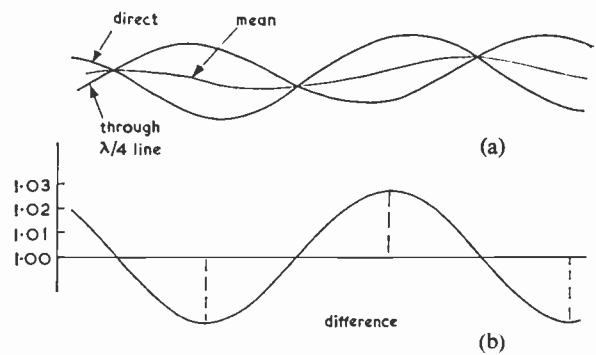


Fig. 3. (a) Typical recorded plots of standing-wave patterns, with and without the standard  $\lambda/4$  line inserted in front of the unknown.

(b) Curve of the difference between the two (a) curves, which gives twice the amplitude of the true standing-wave pattern relative to the standard  $\lambda/4$  line.

method has been devised<sup>4</sup> which refers the impedance to that of a quarter-wave standard line and compensates the effects of probe non-uniformity and of any small reflection from the insulating support for the inner conductor in the slotted-line.

The procedure is simple. First, the apparatus whose reflection coefficient is required is connected directly to the slotted-line and the standing-wave pattern is plotted by a recorder with an expanded scale of amplitude. Secondly, the apparatus is connected to the slotted-line through a standard quarter-wave line and the standing-wave pattern is again plotted with the same position of probe displacement scale as on the first plot. Figure 3 shows a typical pair of plots.

The difference between the two plots is then plotted by hand and the result will be found to be very close to a sine curve. Half the amplitude of this sine curve, divided by the level determined from the mean of the two measured curves relative to the zero level, is equal to the modulus of the reflection coefficient to be measured.

The phase angle of the reflection coefficient may be determined from the position of a minimum of the sine curve obtained, relative to the position of a minimum obtained with a short-circuit at the measurement reference plane.

The mean of the two plotted curves gives the standing-wave pattern that would be obtained if a perfect reflectionless termination, relative to the nominal resistive impedance, were present. This gives information on the state of the slotted-line. The sine-wave component shows how far the actual characteristic impedance departs from the nominal value together with a component which may arise from reflection at the support for the inner conductor. Irregularities and gradual slope can give quantitative

information on the uniformity of probe pick-up along the slot, provided allowance is made for loss in the slotted-line.

Although this method of comparison with a standard is very restricted in range of impedance for an accuracy of  $\pm 0.1$  to  $\pm 0.2\%$  of the major component, the range is a very important one for measurements on nearly-matched laboratory apparatus. Also, it provides means for checking the accuracy, and even for determining certain corrections, of precision slotted lines which can then be used for impedance measurements over a wider range with moderate accuracy ( $\pm 1$  to  $\pm 2\%$ ).

#### 2.4. Precision Reflectometer Methods for Impedance Measurements on Components with Coaxial Connectors

The precision reflectometer method for measuring the modulus of reflection coefficients in waveguide, developed at the National Bureau of Standards<sup>5</sup> has advantages over standing-wave methods. A directional coupler is used with two 'tuners' (actually adjustable impedance transformers) to obtain exceptionally good directivity, absence of unwanted reflections and an

incident wave amplitude that is independent of the reflection coefficient of the component to be measured. The tuners are set-up by connecting in turn at the measurement reference plane:

- (a) a sliding short-circuit in a waveguide of standard cross-section, and
- (b) a sliding lossy termination with a very small reflection coefficient in a waveguide of standard cross-section.

Owing to the difficulty of constructing a satisfactory sliding load for frequencies much below 1 GHz in coaxial line, an alternative solution to the problem has to be found. Also, it is necessary to measure both the magnitude and phase angle of the voltage reflection coefficient if complex impedance values are to be calculated from the results.

A provisional solution to the problem was described by Spinney.<sup>6</sup> The method is to use a nearly-matched load and a quarter-wavelength standard line relative to which the impedances are measured. The general arrangement of an improved proposed method is shown in Fig. 4 in which a detector that can measure amplitude linearly and phase angle relative to a reference phase is required. This 'detector' which comprises an attenuation standard and a phase-change standard as well as auxiliary apparatus, still has to be fully developed and will form the most extensive part of the apparatus, but because it does not enter in detail into the operation of the reflectometer, it will not be discussed here.

The setting-up procedure is as follows:

1. A sliding short circuit in a coaxial line of accurate characteristic impedance (this need be only  $\lambda/4$  long) is connected to the reference plane. Tuner 2 is adjusted so that the amplitude at the detector does not change with position of the slider.
2. A termination with a small reflection coefficient  $\rho_L$  ( $|\rho_L| \leq 0.01$  is suitable) is connected to the reference plane. Tuner 1 is adjusted to obtain a null indication at the detector. This balances the complex reflection coefficient  $\rho_L$  of the termination against the effective reflection coefficient  $\rho_D$  due to the finite directivity and minor reflections of the coupler.
3. The  $\lambda/4$  standard line is inserted between the termination and the reference plane, which reverses  $\rho_L$  to  $-\rho_L$  and produces an amplitude at the detector proportional to  $2|\rho_L|$  if the detector responds linearly to voltage.
4. Tuner 1 is adjusted again to halve the amplitude obtained in operation 3 without changing the phase of the voltage at the detector. This leaves only the effect of  $\rho_L$ ,  $\rho_D$  having now been compensated by the tuner.

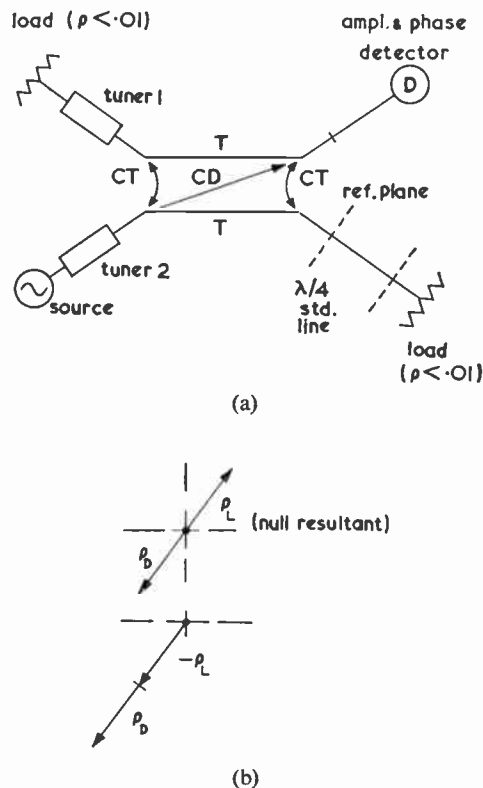


Fig. 4. (a) Basic arrangement of precision reflectometer, using a  $\lambda/4$  line as the standard impedance.

(b) Phasor diagrams of two stages in the setting-up procedure (see text).

5. Re-check operation 1 and repeat 2 to 4 inclusive. The reflectometer is now set up for the chosen frequency. Unity level is established at the detector by placing a short circuit at the reference plane and noting that the phase angle of the resulting reflection is substantially  $-\pi$  radians. For high accuracy, however, corrections both to the level and to the resulting reference phase angle have to be calculated from the properties of the short-circuit disk and from the measured contact impedance between the disk and the conductors of the coaxial line at the reference plane.

A wide range of values of reflection coefficient (or of impedance or admittance) could be measured with a potential accuracy of  $\pm 0.1\%$  of the major component. Because only quarter-wave lines are needed as standards, it should be possible to apply it to frequencies down to 200 MHz. Because the apparatus required is specialized and extensive in amount and because the setting-up requires skill and cannot be done rapidly, the method is suitable only as a basic standard.

In all precise measurements of impedance or equivalent property at a given reference plane, it should be noted that the body of a precision connector is considered as part of the apparatus measured. Furthermore, if half the contact impedance between the connector-pair is also considered as part of the apparatus measured, then provided the contact impedance does not vary excessively between different pairings with the connector, there is no correction to be made on this account. Provided the residuals in the standard line are small, the correction to allow for imperfections in the standard line may be expressed:

$$\rho_L = \rho_{L(\text{meas.})} + \frac{\delta R_0}{2R_0} + \frac{L_{0i}}{4L_0} - j \frac{r_0}{4\omega L_0} \dots\dots(11)$$

where the symbols have the same meanings as in eqn. (8).

### 3. Attenuation

#### 3.1. Definitions

The ratio of the power  $P_{L1}$  absorbed by a load of reflection coefficient  $\rho_L$  to the power absorbed by the same load from the same source of reflection coefficient  $\rho_s$  when a two-port element is inserted is:<sup>7</sup>

$$\frac{P_{L1}}{P_{L2}} = \left| \frac{(1 - \rho_s S_{11})(1 - \rho_L S_{22}) - \rho_s \rho_L S_{21}^2}{1 - \rho_s \rho_L} \right|^2 \frac{1}{|S_{12}|^2} \dots\dots(12)$$

where  $S_{11}$ ,  $S_{22}$  and  $S_{21}$  are the scattering coefficients of the two-port element which is assumed to be reciprocal, i.e.  $S_{21} = S_{12}$ . This equation shows that when a fixed attenuator is inserted between a 'source' and a 'load', the loss is not wholly dependent on the attenuator but depends also on  $\rho_s$  and  $\rho_L$ . Attenuation

may be usefully defined as the insertion loss when  $\rho_s = \rho_L = 0$  (i.e. with nominally matched source and load), so that it depends only on the attenuator. Then the total attenuation is

$$A_{\text{total}} = 10 \log_{10}(1/|S_{21}|^2) \dots\dots(13)$$

The total attenuation may be regarded as the sum of the reflective attenuation and the dissipative attenuation where

$$A_{\text{refl.}} = 10 \log_{10}[1/(1 - |S_{11}|^2)] \dots\dots(14)$$

and

$$A_{\text{diss.}} = 10 \log_{10}[(1 - |S_{11}|^2)/|S_{21}|^2] \dots\dots(15)$$

Thus when the attenuation of a two-port element (such as a fixed attenuator) is measured, the source and load ports attached to it must have zero reflection coefficients.

When a switched or otherwise variable attenuator is measured, each step in the measurement is equivalent to the substitution of one two-port element for another. The 'substitution loss'<sup>8</sup> expressed in decibels is then:

$$A_{\text{subst.}} = 10 \log_{10} \left| \frac{S'_{21}[(1 - S_{11}\rho_s)(1 - S_{22}\rho_L) - S_{21}^2\rho_s\rho_L]}{S_{21}[(1 - S'_{11}\rho_s)(1 - S'_{22}\rho_L) - S_{21}^2\rho_s\rho_L]} \right|^2 \dots\dots(16)$$

where  $S_{nm}$  refer to the final connection and  $S'_{nm}$  refer to the initial connection. Again, it is seen that unless the parts switched in or out are relatively isolated from the two ports of the attenuator so that  $S_{11} \approx S'_{11}$ ,  $S_{22} \approx S'_{22}$  and  $S_{21}, S'_{21}$  are small, then the change in the loss brought about by the switching depends on  $\rho_s$  and  $\rho_L$ . Therefore the source and load should have zero reflection coefficients when measuring this form of switched attenuator.

Often, only the moduli of the voltage reflection coefficients and scattering coefficients are measured, and from these values an uncertainty can be quoted for the effects of small mismatches. Thus from eqn. (12):

$$\Delta A \approx \pm 8.7 \{ |\rho_s| |S_{11}| + |\rho_L| |S_{22}| + |\rho_s| |\rho_L| (1 + |S_{21}|^2) \} \dots\dots(17)$$

for a simple insertion loss measurement.

It is not possible to quote a meaningful approximate uncertainty for the substitution loss (eqn. (16)) in terms of the moduli of the scattering coefficients. The best would be

$$\Delta A \approx \pm 8.7 \{ |\rho_s| |S'_{11} - S_{11}| + |\rho_L| |S'_{22} - S_{22}| + |\rho_s| |\rho_L| |S'_{21} - S_{21}| \} \dots\dots(18)$$

but to use this it would be necessary to know the scattering coefficients in modulus and phase angle. Note that in eqns. (17) and (18), the factor 8.7 arises

from the conversion of nepers to decibels and equals  $20 \log_{10} e$ .

### 3.2. Attenuation Standards

The most accurately realizable attenuators for radio frequencies that are calculable are the 'piston' or 'beyond cut-off waveguide' attenuators in which the variable relative attenuation is determined by measuring the displacement of a pick-up conductor housed in a movable piston. The attenuation difference is a calculable function of the uniform diameter of the metal cylinder in which the piston moves, with a smaller dependence on frequency and on the conductivity of the cylinder wall. Within the operating range, the attenuation is directly proportional to the piston displacement to a high degree of accuracy. The important factor that must be known with precision is the 'rate' of the attenuator  $dA/dl$  expressed in dB/m. For convenience of the scale, it is usual to fix this value (say, 20 dB/inch or 10 dB/cm) and to calculate the radius of the bore of the cylinder  $r$  (m). This is given by a cubic equation, applicable to the  $H_{11}$  evanescent mode in the cylinder, with the approximate solution

$$r = [k^{-1}(1 - k^{\frac{1}{2}}(\pi\mu\sigma f)^{-\frac{1}{2}})]^{\frac{1}{2}}$$

where

$$k = \left(\frac{dA/dl}{15.9923}\right)^2 + \left(\frac{2\pi f}{1.8412V}\right)^2 \quad \dots\dots(19)$$

where  $f$  is frequency (Hz),  $V$  is velocity of propagation in air ( $= 2.997 \times 10^8$  m/s),  $\mu = 4\pi \times 10^{-7}$  (H/m) and  $\sigma$  is conductivity of the cylinder wall ( $\Omega^{-1}\text{m}^{-1}$ ) ( $\approx 1.5 \times 10^7 \Omega^{-1}\text{m}^{-1}$  for brass to BS 249). The rigorous theory on which this formula is based was worked out many years ago<sup>9</sup> and has been applied to the design of standard piston attenuators several times.<sup>10-12</sup>

The two well-known major sources of error in piston attenuators are the excitation of unwanted modes and the interaction between the launching current and current in the pick-up conductor when the two are in close proximity. The first can be reduced by suitable design of the excitation system and the provision of a mode filter in front of the launching conductor(s). A suitable arrangement consists of a single conductor across a diameter of the cylinder to form the launching system, with a mode filter consisting of a parallel-strip metal grid (with the strips at right angles to the launching conductor) mounted a short distance in front of the launching conductor. The use of three or more launching conductors, shaped to follow the natural electric lines of force in the  $H_{11}$  mode, can make an improvement in the purity of the mode launched<sup>10</sup> but the single conductor across a diameter is not unsatisfactory. The second source of error can be reduced considerably simply by stabilizing the current in the launching conductors. By these

means a high accuracy can be obtained without having a very large ( $> 30$  dB) minimum insertion loss resulting from the pick-up conductor not having to approach closer than a distance equal to one diameter to the launching conductor.

The accuracy of the piston attenuator in use at present is about  $\pm 0.005$  dB per 10 dB, giving  $\pm 0.01$  up to 20 dB and  $\pm 0.05$  dB at 100 dB. It is hoped to achieve  $\pm 0.01$  dB over 100 dB with future development.

### 3.3. Comparison of Attenuation

Piston attenuators of the highest precision can operate only at frequencies below 100 MHz, usually at 60 MHz or 30 MHz. Consequently, for the calibration of attenuators at other frequencies a frequency changer has to be used which is linear for a range of levels of at least 100 dB. The problems involved in developing such a comparator are dealt with in another paper<sup>13</sup> and will not be discussed further here.

## 4. Power

### 4.1. Definitions

The power absorbed by a load from a radio-frequency source depends on the impedances of the source and load. Because it is usually inconvenient to measure the impedances when measuring output power, the power must be defined in such a way that the quantity measured is independent of the source impedance. Two ways of doing this have been used. The first is to insert a variable impedance transformer in front of the absorption wattmeter and adjust the transformer to obtain the maximum indication. This operation produces a conjugate impedance match and, apart from any loss in the transformer, gives the available power of the source ( $P_{av.}$ ). The second way is to define output power as the power absorbed by a purely resistive load of resistance equal to the nominal characteristic impedance of the transmission line carrying the power. Any impedance transformation is carried out in the source unit. This definition of output power is used whenever a broadband absorption wattmeter with a fixed load resistance is employed. Again, if the power flowing in one direction along a coaxial transmission line is required, this is best achieved by inserting a calibrated directional coupler in the line and measuring the power from the secondary arm of the coupler by means of a low-level absorption wattmeter.

The ratio of the power  $P_0$  that would be absorbed by a truly nominal resistive load ( $R_0$ ) to the power  $P_L$  actually absorbed, if the wattmeter has a reflection coefficient  $\rho_L$ , is:

$$\frac{P_L}{P_0} = \frac{1 - |\rho_L|^2}{|1 - \rho_s \rho_L|^2} \quad \dots\dots(20)$$

where  $\rho_s$  is the effective reflection coefficient of the source, measured from the reference plane of the power measurement. The ratio of the power absorbed to the available power of the source ( $P_{av.}$ ) is:

$$\frac{P_L}{P_{av.}} = \frac{(1 - |\rho_s|^2)(1 - |\rho_L|^2)}{|1 - \rho_s \rho_L|^2} \quad \dots\dots(21)$$

It is evident from eqn. (20) that if the absorption wattmeter has the commonly met value of v.s.w.r. of 1.2 ( $|\rho_L| = 0.1$ ) and if the source v.s.w.r. is typically 2, ( $|\rho_s| = 0.33$ ) then the uncertainty on this account is as much as  $\pm 6.5\%$ . This shows that absorption wattmeters should have better v.s.w.r. values than has often been the case hitherto. For standards work, eqn. (20) always has to be taken into account.

4.2. Means for Referring R.F. Power to D.C. Power

Radio frequency power is at present best measured by the employment of some form of dissipative element in which the equivalence of the heating effects of d.c. power and r.f. power is established. Under suitable conditions, the d.c. power dissipated in a resistor can be measured with a high degree of certainty, so that if the r.f. to d.c. equivalents can be established with certainty, standards of r.f. power can be established. The chief departure from equivalence of r.f. and d.c. heating arises from the differences between r.f. and d.c. distributions of current and resistance in the element. This problem is most acute when the two forms of power are applied to different parts of the element.

One method of solving these problems has been used in what has been termed a coaxial film bolometer.<sup>14</sup> Here, both forms of power are applied to the same element, a uniform metal film on a thin glass cylinder, housed in a tractorial coaxial outer conductor which ensures a uniform distribution of current and resistance for r.f. and d.c. An arrangement of aligned, thin slits in the film and in the outer sheath, the two halves of the latter being separated by thin insulating material, together with two half flanges separated by a mica ring from a flange on the outer inlet conductor to form a mica d.c. blocking capacitor, enable d.c. to be fed through the two halves of the film resistor in series. Originally,<sup>14</sup> gold was used for the film resistor, but to obtain better stability platinum has been found more suitable, having a temperature coefficient of  $+0.0011$  per degC. The great advantage of employing an accurately electro-formed tractorial outer conductor in conjunction with a uniform cylindrical film resistor is that if a v.s.w.r. close to unity is obtained, equality of r.f. and d.c. distributions of heating is assured. The best of a number of platinum film elements made resulted in a v.s.w.r. within 1.000 to 1.005 up to 1 GHz, with 100 mW of total heating. The element is used with a self-balancing bridge and

the voltage across the whole Wheatstone bridge is measured by a five-digit digital voltmeter. A substitution method is used, the substituted r.f. power being given by:

$$\Delta P = \frac{V\Delta V}{2R} \left[ 1 - \frac{\Delta V}{2V} \right] \quad \dots\dots(22)$$

where  $R$  is the d.c. resistance of one arm of the equi-arm bridge,  $V$  is the applied voltage to achieve balance with no r.f. power applied, and  $\Delta V$  is the decrease in voltage resulting from the application of the r.f. power. When used as a standard, the r.f. power, which should be stabilized in level to about  $\pm 0.1\%$ , is switched on and off for periods of about 2 minutes each to ensure consistency in the state of thermal equilibrium. The overall accuracy is estimated to be about  $\pm 1\%$  at 2 mW and well within this up to a maximum of about 80 mW. The frequency range for full accuracy is from about 200 MHz to beyond 3 GHz.

The disadvantages of the foregoing method are the low sensitivity of the element to temperature changes requiring a chopper and high gain amplifier to obtain adequate response, and the need to operate the instrument in a controlled ambient temperature ( $20^\circ\text{C}$ ) to maintain adequate power range.

A new form of dry load calorimeter thermal power standard is under construction in which a uniform metal film resistor of very low temperature coefficient of resistance is mounted in a tractorial outer conductor to obtain equality of r.f. and d.c. heating, but with a carefully designed thermal 'circuit' and an extremely sensitive temperature measuring device. The form of construction is shown in Fig. 5. The resistor consists of a metal film on a substrate formed by a thin tube of beryllia which has low-loss dielectric properties but a high thermal conductivity. The tractorial outer conductor is electroformed from copper, but is very thin (0.01 inch) to minimize its thermal capacity. Both inner and outer conductors feeding the r.f. to the resistor have a length of thermal isolation from the inlet connector with its insulating support for the inner conductor. This thermal isolation consists of

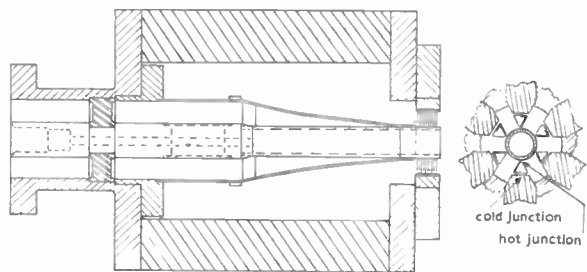


Fig. 5. Axial section of dry-load calorimeter and cross-section through the multiple thermocouple elements.

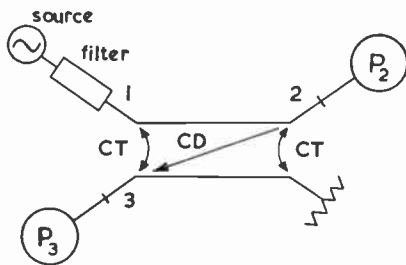


Fig. 6. Arrangement for the comparison of a high-level wattmeter ( $P_2$ ) with a low level wattmeter ( $P_3$ ), using a calibrated directional coupler.

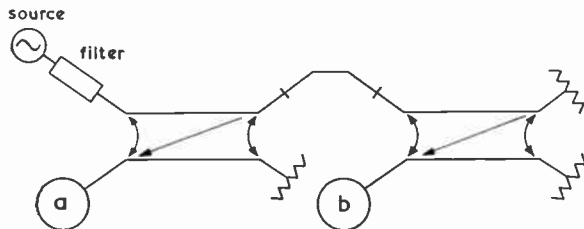


Fig. 7. Arrangement for comparing two wattmeters, a and b, of similar ranges of level, using two similar directional couplers.

thin tubes of steel, each electroplated on one side to form good conducting surfaces for r.f. The beryllia tube protrudes from the short-circuited end of the resistor to conduct heat to the hot junctions of the thermopile. The heat-sink for the cold junctions of the thermopile is formed by a heavy brass ring attached to the end of a thick brass tube which in turn is attached to a heavy brass flange integral with the outer conductor of the inlet. The thermocouples are of the electroplated type<sup>15</sup> in which constantan wire about 0.051 mm (0.002 in) thick is wound on a soluble triangular section former and is plated with a thin layer of copper around half the perimeter of the former. In this way, six groups of 20 thermocouples each, all electrically in series, can be distributed around the protruding end of the beryllia tube. The resulting sensitivity is estimated to be about 48 mV/W. It is expected to be possible to double this in later models when experience has been gained in making electroplated thermocouples.

Allowance has to be made for the small loss in the inlet conductors and the insulating support. This amounts to about one part in  $10^3$  at 1 GHz.

The frequency range is from audio frequencies up to about 5 GHz and the predicted accuracy is about 0.2%. The power range is from 40 mW to 4 W. This dry-load calorimeter can be used singly under controlled conditions, or a pair of them can be used differentially in the usual manner. The time-constant of the dry-load calorimeter is expected to be much less than the 2.5 minutes of the instrument described by Jurkus.<sup>16</sup>

#### 4.3. Methods for the Accurate Comparison of Wattmeters

In comparing the power absorbed by two wattmeters the method must be designed to minimize the effect of multiple reflections when the reflection coefficient of either wattmeter is not negligible. There is every advantage in having both wattmeters connected in circuit simultaneously because this avoids sudden thermal changes at the inlet connectors of each wattmeter and ensures that any small drift in power level from the source affects both wattmeters equally. If the standard wattmeter has a long time-constant, it is essential to employ a power source stabilized to about  $\pm 0.1\%$ . A low-pass filter should be used to ensure that only one frequency, free from harmonics, is present.

If the standard and the unknown wattmeters are at least 10 dB different in power level, a calibrated directional coupler can be used to make the comparison.

The arrangement is shown in Fig. 6, where  $T$  is the voltage transmission coefficient from 1 to 2,  $C$  is the voltage coupling coefficient which compares the voltage at 3 with that at 2 and  $D$  is the directivity, all expressed as voltage ratios less than unity. The ratio of the powers absorbed by the two wattmeters is given by:

$$\frac{P_3}{P_2} = |C|^2 \left| \frac{1 - \rho_2 \Gamma_2}{1 - \rho_3 \Gamma_3} \right|^2 \frac{1 - |\rho_3|^2}{1 - |\rho_2|^2} \quad \dots (23)$$

where  $\Gamma_2$  and  $\Gamma_3$  are the effective source reflection coefficients given in terms of the scattering coefficients of the coupler by

$$\Gamma_2 = S_{22} - S_{12} S_{23} / S_{13} \quad \text{and} \quad \Gamma_3 = S_{33} - S_{13} S_{23} / S_{12}$$

$\Gamma_2$  can be measured directly<sup>17</sup> with a source at 2, detector at 3 and load with 'tuner' at 1. The tuner is adjusted for a null, the source is removed, and  $\Gamma_2$  is the reflection coefficient measured at 2. Likewise,  $\Gamma_3$  can be measured by adjusting the tuner for a null with the source at 3 and the detector at 2, then measuring  $\Gamma_3$  at 3. The determination of  $|C|$ , a voltage ratio less than unity, requires great care. Basically, it is determined from an insertion-loss measurement with nominally matched source and load impedances at 2 and 3, but special precautions have to be taken to account for the effects of the scattering coefficients  $S_{11}$ ,  $S_{22}$  and  $S_{33}$  of the coupler as well as the small reflection coefficients of the source and load used. An accuracy of  $\pm 0.02$  dB is needed for an uncertainty of  $\pm 0.5\%$  in the power ratio.

If both wattmeters are of similar power range and are of low level (e.g. < 100 mW), the arrangement shown in Fig. 7 can be used in which both couplers are similar. The two levels at 'a' and 'b' will differ,

but if the standard is first placed at 'a' (reading  $\theta_{a1}$ ) with the unknown at 'b' (reading  $\theta_{b1}$ ) and then (when the power from the source need not be precisely the same as before) the two wattmeters are exchanged, reading  $\theta_{a2}$  at 'a' and  $\theta_{b2}$  at 'b'. Then, apart from small corrections depending on scattering coefficients and the reflection coefficients of the wattmeters, the 'true' power in the unknown is given in terms of the power defined by the standard as:

$$P_{\text{true}} = \left( \frac{\theta_{a1} \theta_{b2}}{\theta_{b1} \theta_{a2}} \right)^{\frac{1}{2}} \cdot P_{\text{ind.}} \quad \dots\dots(24)$$

When two wattmeters of similar high power are to be compared, one has to be connected after the other to a source. The best method here is to use a 'stabilized' source of very small source reflection coefficient (refer to Fig. 6). The wattmeters are connected in turn at 2, while at 3 a sensitive detector is used to maintain a constant level there. Alternatively, d.c. from the detector at 3 can be used to control the generator power level.<sup>17</sup> In either case, the effective source reflection coefficient is  $\Gamma_2$ .

The directional couplers used in making power level comparisons must have exceptionally good inherent v.s.w.r. (i.e. small  $S_{11}$ ,  $S_{22}$ ,  $S_{33}$ ) and very good directivity. Specially developed couplers for this purpose have been described.<sup>18, 19</sup>

### 5. Conclusions

A set of radio frequency standards has been described in outline, covering frequency ranges within 5 MHz to 3 GHz. The accuracies achieved are, for impedance:  $\pm 0.1\%$  to  $\pm 0.2\%$  up to 200 MHz and  $\pm 0.1\%$  to  $0.2\%$  for the range 47 to 53 ohms from 0.5 GHz to 3 GHz; for attenuation:  $\pm 0.01$  dB up to 20 dB and  $\pm 0.05$  dB at 100 dB for frequencies between 5 MHz and 1 GHz; and for power,  $\pm 1\%$  between 2 mW and 80 mW for frequencies up to 3 GHz.

Developments in progress aim at extending the range of impedance standardization for frequencies between 200 MHz and 3 GHz with an improved accuracy of  $\pm 0.1\%$ , and to improve the basic accuracy of power standards to  $\pm 0.2\%$  for frequencies up to 3 GHz. Also, the development of a new piston attenuator is proposed to achieve an accuracy of  $\pm 0.01$  dB in 100 dB, which would enable the comparator to be used to its full potential accuracy.

### 6. Acknowledgments

Acknowledgments are made to Mr. D. Woods who originally developed the admittance bridge (Section 2.1); to Mr. R. E. Spinney who devised the special methods for measuring reflection coefficients (Section 2.3 and 2.4); and to Mr. E. J. Griffin who is developing

the dry-load calorimeter (Section 4.2) in conjunction with the author.

### 7. References

1. I. A. Harris, 'Mode of use and assessment of precision coaxial connectors', *Proc. Instn Elect. Engrs*, **112**, pp. 2025-32, 1965.
2. D. Woods, 'A precision dual bridge for the standardization of admittance at very high frequencies', *Proc. I.E.E.*, **104C**, pp. 506-21, 1957.
3. I. A. Harris and R. E. Spinney, 'The realization of high-frequency impedance standards using air-spaced coaxial lines', *Trans. Inst. Elect. Electronics Engrs on Instrumentation*, **IM-13**, No. 4, pp. 265-62, 1964.
4. R. E. Spinney, 'The measurement of small reflection coefficients of components with coaxial connectors', *Proc. I.E.E.*, **110**, p. 396, 1963.
5. G. F. Engen and R. W. Beatty, 'Microwave reflectometer techniques', *Trans. Inst. Radio Engrs on Microwave Theory and Techniques*, **MTT-7**, pp. 351-5, 1959.
6. R. E. Spinney, 'A precision reflectometer method for measurements on coaxial components at ultra high frequencies', *Proc. I.E.E.*, **110**, pp. 521-2, 1963.
7. R. W. Beatty, 'Mismatch errors in the measurement of ultra high frequency and microwave variable attenuators', *J. Res. Nat. Bur. Stand.*, **52**, pp. 7-9, 1954.
8. R. W. Beatty, 'Insertion loss concepts', *Proc. I.E.E.E.*, **52**, pp. 663-71, 1964.
9. J. Brown, 'Corrections to the attenuation constants of piston attenuators', *Proc. I.E.E.*, **96**, Part 3, pp. 491-5, 1949.
10. C. M. Allred and C. C. Cook, 'A precision r.f. attenuation calibration system', *Trans. I.E.E.E.*, **I-9**, No. 4, pp. 268-74, 1960.
11. D. L. Hollway and F. P. Kelly, 'A standard attenuator and the precise measurement of attenuation', *Trans. I.E.E.E.*, **IM-13**, pp. 33-44, 1964.
12. B. O. Weinschel and G. U. Sorger, 'Waveguide below cut-off attenuation standard', *Acta IMEKO (Stockholm)*, pp. 407-24, 1964.
13. R. W. A. Siddle and I. A. Harris, 'A c.w. comparator for precision r.f. attenuators', *The Radio and Electronic Engineer*, **35**, No. 3, pp. 175-81, March 1968.
14. I. A. Harris, 'A coaxial film bolometer for the measurement of power in the u.h.f. band', *Proc. I.E.E.*, **107B**, pp. 67-72, 1960.
15. F. J. Wilkins, T. A. Deacon and R. S. Becker, 'Multijunction thermal convertor. An accurate d.c./a.c. transfer instrument', *Proc. I.E.E.*, **112**, pp. 794-805, 1965.
16. A. Jurkus, 'A coaxial radio-frequency power standard', *Trans. I.E.E.E.*, **IM-15**, pp. 338-42, 1966.
17. G. F. Engen, 'Amplitude stabilization of microwave signal source', *Trans. I.R.E.*, **MTT-6**, pp. 202-6, 1958.
18. P. A. Hudson, 'A high directivity, broadband coaxial coupler', *Trans. I.E.E.E.*, **MTT-14**, pp. 293-4, 1966.
19. I. A. Harris, 'Coaxial directional couplers with exceptional directivity and v.s.w.r. over wide frequency bands', *Electronics Letters*, **2**, pp. 100-101, 1966.

Manuscript received by the Institution on 29th August 1967. (Paper No. 1179.)

© The Institution of Electronic and Radio Engineers, 1968

## The Physics Exhibition 1968

The 1968 Physics Exhibition was held at Alexandra Palace, London, from 11th–14th March. The exhibitors showed a general increase in their number and were from three main classes: commercial organizations, government or semi-government laboratories, and university and college physics or electrical and electronic engineering departments. A large number of exhibits had applications in the electronics industry and in general, they came under the following principal groups: instruments, components and systems. Production items, based on prototypes, exhibited in the last three years, were included for the first time. The following are some of the many items which were of interest to electronic engineers.

### Instruments

Philips Research Laboratories of Eindhoven demonstrated a segmentator for sound analysis. This equipment demonstrates the possibility to cut, out of a recorded word, a slice of variable length at any place and make this audible without introducing audible transients as would arise from sharp cutting. The segmentator, of which two varieties, analogue and digital, were shown, is used in research on the phonetic consequences of variations in the time parameters of speech sounds. It also finds application in dialect studies, language instruction and in the treatments for speech impediments. In the demonstration, the audible effects were brought out by loudspeakers and a visual display was made of the time function.

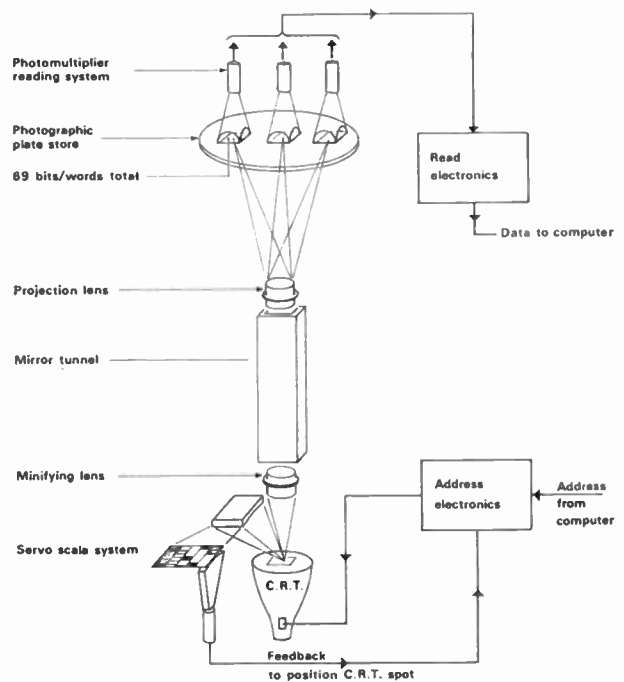
The first British 50 mW helium-neon laser was shown by Ferranti Valve Department of Dundee. This laser is designed to deliver a minimum power of 50 mW in TEM<sub>00</sub> mode at 6328 Å (632.8 nm), and has applications in fields where high powers are called for, particularly in holography and Raman spectroscopy. To obtain such power in a structure whose length is only 2 metres, it is necessary to suppress the preferred emission at 3.39 nm. This has been achieved by the novel method of using an absorption cell. The laser consists of two d.c. excited discharge tubes colinearly mounted, with the absorption cell mounted between the discharge tubes. This form of construction has advantages in that the manufacture of the tubes is eased, as is the power supply problem. The housing consists of a rigid box structure to which the adjustable mirror-mounts are attached; this type of structure offers maximum resistance to microphony.

Two automatic instruments, developed by the Electronic and Applied Physics Division of U.K. Atomic Energy Authority, Harwell, employing ultrasonics and having particular value in non-destructive testing were on show. The instruments use a well-established technique for measuring the wall thickness of a metal tube. A beam of ultrasound is focused on the wall of the tube and the frequency is varied until the energy of reflection is a minimum; this occurs when the half wavelength is equal to the wall thickness.

One of the instruments employs a single probe which both produces the ultrasound and receives the reflected

energy. As the transmitter frequency is swept over the range of interest the resonance absorption peak is detected and the transmitter frequency at this instant measured by digital counting methods. The second instrument uses separate probes which provide continuous transmission and reception. The system locks the mean transmitter frequency to a position near the resonance and the tube can be quickly scanned; the output can be used to give a pictorial record of the thickness variation over the tubing.

To meet the growing demand in data processing systems for fast random access to stored information, International Computers and Tabulators Ltd. has designed an optical fixed store which uses a photographic plate as the storage medium. Information can be read from the store in parallel with a word length up to 69 bits. Addressing is by an electro-optic access system using a cathode-ray tube light source. The store capacity is 65 536 words. The time between successive accesses is less than 3 μs. It is intended that plates shall be interchangeable between stores. A rigid and unstressed tetrahedral type framework has been designed to accurately support the optical components of the system.



I.C.T. optical fixed store.

A portable, compact x-ray camera which, when operated in conjunction with a Polaroid Land camera, can be used to produce instant radiographs, was one of the exhibits from the National Research and Development Corporation. Applications of the unit are both industrial and medical. Bone fractures can be quickly observed because

of the very short exposure time. In the industrial field the equipment has been used for a production check on encapsulated electronic components. It is expected that it would also find use in investigations into high-speed phenomena such as rotating machinery, explosive studies, projectile penetration, and ballistic phenomena of all types.

### Systems

Standard Telecommunication Laboratories, Harlow, showed a single-channel companding p.c.m. codec (coder-decoder) which can be made small enough, by the large scale integration of the logic, to be incorporated in a telephone subset. Another S.T.L. exhibit, a p.c.m. music terminal, was a four-channel equipment providing a means of transmitting high-quality music in digital form. Sampling at 32 kHz and having 11 bits per sample yields 352 kbit per channel. Coding and decoding utilizes counting technique. Transmission rate of 1536 kbit/s is compatible with that used in 24-channel telephone system.

The new production model of their x-band solar radiometer to measure and record the radiation emitted by the Sun was shown by Decca Radar Ltd. The antenna is aimed at the Sun and automatically follows its course during the day. Equipment using a low-power gas laser to measure the velocity of a moving surface by photo-mixing the light back-scattered from the target (with a reference signal derived from the transmitting beam) was another exhibit from Decca. Doppler tracking techniques are used to establish the speed of the target.

An experimental, x-band, solid-state racon (radar beacon) was exhibited by the Admiralty Surface Weapons Establishment. A variety of marine applications are possible and the racon is already used as an aid to navigation in identifying lighthouses. Hitherto, in radar sets magnetrons and klystrons were being used but the present model uses only solid-state components. The power output is therefore low and consequently the equipment has short range, but owing to its small size and low power requirements it could be mounted on a light buoy.

E.M.I. Electronics showed a pulsed television system, which demonstrated the ability of a new intensifier-vidicon tube to operate in a high-speed pulsed mode. The intensifier section of the camera tube is gated 'on' for a period of 25 microseconds every 20 milliseconds. The information stored during the gated period is then scanned off as in a conventional vidicon. This is demonstrated by projecting a pulsed light, synchronized with the gated period of the camera tube, on to a constantly illuminated scene. The camera records the two images in proportion to their peak illumination levels and the pulsed sources is clearly visible on the monitor. An observer, viewing the scene directly, is only able to compare mean illumination levels and the pulsed light source is not visible to him.

Mullard Research Laboratories demonstrated a new optical communication system which makes use of Faraday rotation in yttrium iron garnet (y.i.g.). The optical Faraday effect in single-crystal yttrium iron garnet is large enough to produce 90° rotation in samples with

low absorption in the infra-red region of 1.1 to 5  $\mu\text{m}$ . This effect is utilized in light modulators and deflectors and is demonstrated by using a crystal of y.i.g. to modulate a beam of infra-red radiation. The modulator has no moving parts and can be used to replace disk choppers in a wide range of applications. The optical communicator is a portable battery-powered instrument which transmits a cone of light of 3° divergence enabling it to be quickly aligned for operational use and is insensitive to normal vibrations. The maximum range is 2 km. The bandwidth of the equipment can be extended for multi-channel telephony.

### Components

Working demonstrations of beam lead technology and of the latest complex m.o.s.t. devices were shown in this country for the first time by Elliott-Automation Micro-electronics. The beam lead exhibit featured a circuit composed of three beam-leaded chips connected as a half-adder circuit in a single, dual in-line package. Elliott has pioneered this new connection technology in this country, and is currently working on production equipment to extend its use to m.o.s.t. circuits. Beam leads provide a very much more reliable method of connecting integrated circuits to their outside terminal wires and, when the technique is extended to m.o.s.t. circuits, should provide answers to many of the problems created by the very much higher density and complexity of circuit elements on each single chip. The other display consisted of a dual, 20-bit shift register, using 308 m.o.s.t. elements on a single silicon chip.

A fibre waveguide, completely flexible and which can be handled in the same way as a coaxial cable, suitable for optical communication systems, was shown by Standard Telecommunications Laboratories, who also presented an interesting exhibit of a metal-insulator-metal thin film device which acts as a cold-cathode emitter. Its current-voltage characteristic is similar for both positive and negative bias potentials and shows a low-resistance region, a voltage-controlled negative resistance region and a high-resistance region. With the top metal electrode biased positively, electrons are emitted and accelerated on to the phosphor screen maintained at high potential. This, in conjunction with an array of cathodes, forms the basis of an alpha-numeric optical display panel.

The Research Laboratories of E.M.I. Electronics showed an exhibit using a fast detector for operation in the sub-millimetre wavelength region. The detector is a point-contact diode using gallium arsenide as the semiconductor material. It has been tested at 900 GHz. In the demonstration a cyanide laser was used to generate a beam of radiation at a wavelength of 0.337 mm. The GaAs diode is mounted within a specially constructed cavity, designed to permit a simple assembly technique. The cavity is fed by a waveguide equipped with a horn and is tunable by a short-circuit plunger with a micrometer adjustment. A lens is used to focus the radiation from the laser onto the aperture of the horn. The diode is said to be capable of handling power up to 5 mW.

# Digital Analysis of Current Noise at Very Low Frequencies

By

I. R. M. MANSOUR,  
B.Sc., M.Sc.†

R. J. HAWKINS, B.Sc.†

AND

G. G. BLOODWORTH,  
M.A., D.U.S., C.Eng., M.I.E.R.E.†

**Summary:** Three methods of digital spectral analysis are compared, and their application to the investigation of current noise at very low frequencies is described. In each case periodic sampling of filtered noise voltages is followed by digital computation. Particular attention is given to the errors caused by aliasing in the determination of a power spectrum with the  $1/f$  form characteristic of current noise.

## List of Symbols

Throughout this paper a continuous function is denoted thus:  $R(\tau)$ , and a discrete function thus:  $V_n$ . The addition of a caret, as, for example, in  $\hat{R}_r$ , denotes that the variable is an estimate, and subject to statistical variability.

$A$	class interval width
$B$	bandwidth of sampled data
$B_e$	equivalent resolution bandwidth
$D_{ir}$	lag, or data, window coefficient
$f$	frequency
$f_c$	critical, folding, or Nyquist frequency
$G(f)$	true power spectrum
$G_a(f)$	aliased power spectrum
$\hat{G}_h$	raw, discrete, estimate of $G(f)$
$\hat{G}_{ih}$	$\hat{G}_h$ smoothed by use of lag window
$h$	harmonic number
$I$	current
$J_i(f)$	Fourier transform of $D_{ir}$
$K$	number of class intervals
$m$	maximum lag number
$n$	data-point number ( $t = n\Delta t$ )
$N$	total number of data points ( $T = N\Delta t$ )
$Q_{ih}(f)$	power transfer function of $D_{ir}$
$R(\tau)$	true autocorrelation function
$\hat{R}_r$	discrete estimate of $R(\tau)$
$\hat{R}_{ir}$	$\hat{R}_r$ modified by $D_{ir}$
$T$	record length
$T_h$	required digital filter voltage transfer coefficient
$T(p)$	continuous approximation to $T_h$

$U_n$	data-point after digital pre-whitening
$v_n$	stationary random component of $V_n$
$\bar{V}$	mean value of $V_n$
$V_n$	broad data-point
$\check{V}$	linear trend coefficient
$W_n$	data-point after band-pass digital filtering

## 1. Introduction

The measurement of electrical noise at frequencies higher than 1 Hz is usually carried out by analogue methods, using band-pass filtering with subsequent squaring and averaging. Below 1 Hz such methods encounter severe limitations. Bloodworth and Nesbitt<sup>1</sup> have described active filters operating down to  $10^{-3}$  Hz, but it is not easy to build a range of narrow pass-band filters operating at these frequencies. However, as Bell<sup>2</sup> has pointed out, the very low frequency application of analogue techniques is limited primarily by the necessity to average each measurement over a long period of time, which requires circuits with much larger time-constants than those involved in the active filters. Sutcliffe<sup>3</sup> has described an analogue technique which overcomes this difficulty to some extent, and which he has used at frequencies down to 1 Hz. Martin<sup>4</sup> *et al.* have used variable bandwidth filters with a thermal square-law detector for measurements down to  $10^{-2}$  Hz.

Noise measurements at very low frequencies have also been made using analogue techniques which avoid the need for low frequency filters. The methods used by Rollin and Templeton,<sup>5</sup> and by Firlie and Winston,<sup>6</sup> consisted essentially of low-speed continuous recording followed by high-speed play-back and conventional spectral analysis at audio frequencies. The former workers employed magnetic tape as their recording medium and attained a frequency of  $2.5 \times 10^{-4}$  Hz. Firlie and Winston,<sup>6</sup> who used photographic film, gave results down to  $5 \times 10^{-5}$  Hz obtained by recording data over 6 hours. In the

† Department of Electronics, University of Southampton.

experimental work<sup>7</sup> by the present authors an integration time of 11 days has been used to determine the spectrum down to the same frequency, and it will be shown that this time is needed to achieve reasonable accuracy.

Digital methods of spectral analysis have been applied in a variety of fields, including oceanography,<sup>8</sup> physiology,<sup>9</sup> and sound and vibration research, but have received relatively little attention from workers making measurements of electrical noise at low frequencies. Firlie and Winston,<sup>6</sup> and Baker,<sup>10</sup> investigated digital methods but the recording and computing equipment available to them was limited. The advent of reliable sampling and recording systems and high-speed computers has now made digital methods much more powerful and attractive for low-frequency analysis. Noise voltages can be sampled periodically by a digital voltmeter with the aid of a timing device and recorded on paper tape or, for higher speeds, on a magnetic tape. The data are then analysed in a digital computer. This process avoids both speeding up the data and analogue averaging over long periods of time. The computer programs used to analyse the data are essentially the same for all frequencies and sampling rates, and combine accuracy with flexibility. Recent advances in digital spectral analysis originate in the theoretical work of Rice,<sup>11</sup> Blackman and Tukey,<sup>12</sup> and Bendat<sup>13</sup> and the work described here is largely an application of their theory.

In the indirect method of analysis, the power spectrum is obtained by Fourier transformation of the autocorrelation function. This method has been widely applied to both continuous and discrete data records, and is treated in detail elsewhere.<sup>12</sup> The autocorrelation function can also be used to separate any periodic components which may be present in random phenomena, quite apart from the transformation giving the power spectrum. In the next section a description of the indirect method is given, together with some general aspects of digital spectral analysis including aliasing and pre-whitening.

Two alternative methods of analysis which have recently become practicable are described in Section 3. The first is a digital simulation of the simple analogue technique normally used at higher frequencies, and the second involves direct Fourier analysis of the sampled noise. Neither of these requires the calculation of the autocorrelation function, and they are therefore called direct methods.

The objects of this paper are to compare these three methods, and to show how they can be applied to the measurement of current noise at frequencies below 1 Hz. This noise, which is observed in almost all semiconductor devices, has a power spectral density function  $G(f)$  given approximately by

$$G(f) \approx A \frac{I^\beta}{f^\alpha} \dots\dots(1)$$

where  $I$  is the direct current flowing and  $f$  is the frequency. The indices  $\alpha$  and  $\beta$  are found to be approximately 1 and 2 respectively and the coefficient  $A$  is a weak function of temperature. In this paper particular consideration is given to the errors arising from aliasing in the measurement of a power spectrum of this form and a method of correction is described. An example of the practical application of this theory is given elsewhere.<sup>7</sup>

The computer programs are not included in the paper, but the authors will be pleased to provide full details to those intending to make similar measurements.

## 2. Indirect Method of Analysis

### 2.1. Fourier Transformation of the Autocorrelation Function

The autocorrelation function  $R(\tau)$  of a variable  $v(t)$  is given by the time average of the product of values separated by the time lag  $\tau$ . For a stationary random variable,  $R(\tau)$  is independent of time  $t$ , and is an even function of  $\tau$ . Thus

$$R(\tau) = \{v(t) \cdot v(t + \tau)\}$$

The analysis makes use of the Wiener-Khintchine relations between  $R(\tau)$  and the power spectral density function  $G(f)$ :

$$R(\tau) = \int_0^\infty G(f) \cos 2\pi f\tau \, df$$

$$G(f) = 4 \int_0^\infty R(\tau) \cos 2\pi f\tau \, d\tau$$

where  $f$  is the (positive) frequency.

The digital method forms discrete estimates  $\hat{R}_r$ ,  $\hat{G}_h$ , of the continuous variables  $R(\tau)$ ,  $G(f)$  by considering a finite number  $N$  of data points  $v_n$ . The suffix  $r$  is the lag number and the estimates  $\hat{R}_r$  are formed at equal intervals  $\Delta\tau$ . Thus:

$$\hat{R}_r = \frac{1}{N-r} \sum_{n=1}^{N-r} v_n v_{n+r} \dots\dots(2)$$

where  $r = 0, 1, \dots, m$

and  $\tau = r\Delta\tau$ .

Spectral estimates are computed at integral multiples of the frequency spacing  $1/2m\Delta\tau$ , and the harmonic number is denoted by  $h$  in the following expression:

$$\hat{G}_h = 4\Delta\tau \left[ \frac{\hat{R}_0}{2} + \sum_{r=1}^{m-1} \hat{R}_r \cos \frac{\pi rh}{m} + (-1)^h \frac{\hat{R}_m}{2} \right] \quad (3)$$

where  $h = 0, 1, \dots, m$ . The frequency  $f$  at which  $G(f)$  is estimated is given by  $h/2m\Delta\tau$ .

The choice of  $N$  and  $m$  to yield sufficient accuracy and resolution is discussed in the following sections.

2.2. Lag Windows and Smoothing

For a stationary random process the autocorrelation function decays rapidly for large values of the delay  $\tau$  and little useful information is lost by truncating  $\hat{R}_r$ . The truncation is achieved by choosing a maximum value  $m$  of  $r$ , and this limitation of the possible values of  $r$  determines the amount of computation required.

In the simplest case  $\hat{R}_r$  is multiplied by a weighting function, or lag window,  $D_{0r}$ , to form a truncated estimate  $\hat{R}_{0r}$  of  $R(\tau)$ :

$$\hat{R}_{0r} = D_{0r}\hat{R}_r$$

where, as shown in Fig. 1(a),

$$D_{0r} = \begin{cases} 1, & 0 \leq r < m \\ \frac{1}{2}, & r = m \\ 0, & r > m \end{cases}$$

Since  $R(\tau)$  is an even function, the lag window may also be expressed as an even function centred on  $\tau = 0$ , for mathematical convenience. Similarly  $G(f)$  is often expressed as an even function existing at both positive and negative frequencies.

The Fourier transform of  $D_{0r}$  is given by the continuous function

$$J_0(f) = 2m\Delta\tau \frac{\sin 2\pi fm\Delta\tau}{2\pi fm\Delta\tau}$$

In effect, this represents a filter of bandwidth  $B_e = 1/2m\Delta\tau$  centred on zero frequency as shown in Fig. 1(b).

When estimates  $\hat{G}_{0h}$  are calculated from  $\hat{R}_{0r}$ , using eqn. (3), the centre frequency of this filter is shifted to  $h/2m\Delta\tau$ . The power is estimated at this frequency from the continuous spectrum within the bandwidth  $B_e$ . The small error due to side-lobes from the image window centred at  $-h/2m\Delta\tau$  is neglected. This process is expressed by the power transfer function

$$Q_{0h}(f) = m\Delta\tau \frac{\sin\pi(2fm\Delta\tau - h)}{\pi(2fm\Delta\tau - h)}$$

which is given by the convolution of  $J_0(f)$  with  $\hat{G}_h$ .

As shown in Fig. 1(b), the filter  $J_0(f)$  has large side-lobes, which give undesirable errors. The side-lobes can be reduced by choosing a lag window which truncates  $R(\tau)$  less abruptly. For example, in the process known as 'hanning' the shape of the lag window is given by

$$D_{2r} = \begin{cases} \frac{1}{2}[1 + \cos(\pi r/m)], & 0 \leq r \leq m \\ 0, & r > m \end{cases}$$

as shown in Fig. 1(c).

The corresponding power transfer function, which has very small side-lobes (Fig. 1(d)), and equivalent bandwidth  $B_e \approx 1/m\Delta\tau$ , is given by:

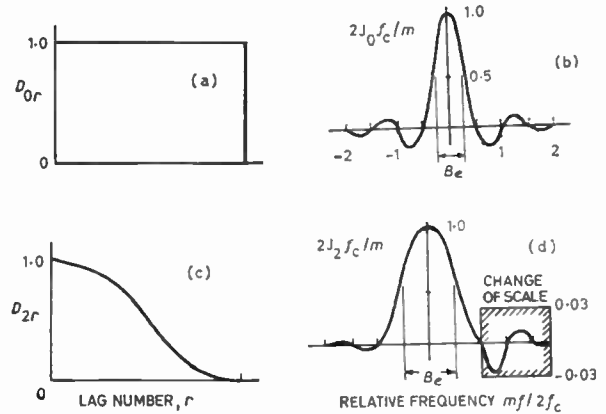


Fig. 1. Examples of lag windows.

- (a) Rectangular lag window  $D_{0r}$ .
- (b) Spectral window  $J_0(f)$  (Fourier transform of  $D_{0r}$ ).
- (c) Hanning lag window  $D_{2r}$ .
- (d) Spectral window  $J_2(f)$  (Fourier transform of  $D_{2r}$ ).

$$Q_{2h}(f) = \frac{1}{2}Q_{0h}(f) + \frac{1}{4}Q_{0h}\left(f + \frac{1}{m\Delta\tau}\right) + \frac{1}{4}Q_{0h}\left(f - \frac{1}{m\Delta\tau}\right) \dots (4)$$

The spectral estimates  $\hat{G}_{0h}$  obtained by the Fourier transformation of  $\hat{R}_{0r}$  are related to  $G(f)$  by the expression:

$$\hat{G}_{0h} = \int_0^{\infty} Q_{0h}(f)G(f)df, \quad h = 0, 1, \dots, m \dots (5)$$

Similarly, the estimates  $\hat{G}_{2h}$  which would be obtained from  $\hat{R}_{2r}$ , by multiplying  $\hat{R}_r$  by the 'hanning' lag window  $D_{2r}$  before transformation, are given by

$$\hat{G}_{2h} = \int_0^{\infty} Q_{2h}(f)G(f)df$$

Substituting for  $Q_{2h}(f)$  in terms of  $Q_{0h}(f)$  using eqn. (4), and eliminating the integrals by means of eqn. (5), the estimates  $\hat{G}_{2h}$  are given by:

$$\hat{G}_{2h} = \frac{1}{2}\hat{G}_{0h} + \frac{1}{4}\hat{G}_{0(h-1)} + \frac{1}{4}\hat{G}_{0(h+1)}, \quad \text{for } 1 \leq h \leq m-1 \dots (6a)$$

and in the special cases  $h = 0$  or  $m$  by:

$$\begin{aligned} \hat{G}_{20} &= \frac{1}{2}\hat{G}_{00} + \frac{1}{2}\hat{G}_{01} \\ \hat{G}_{2m} &= \frac{1}{2}\hat{G}_{0(m-1)} + \frac{1}{2}\hat{G}_{0m} \end{aligned} \dots (6b)$$

As the auto-correlation function is calculated at a limited number of points,  $m$ , the rectangular lag window  $D_{0r}$  is automatically applied. Without applying the window  $D_{2r}$  to  $\hat{R}_{0r}$  the Fourier transform is taken and 'raw' spectral estimates  $\hat{G}_{0h}$  are calculated. The window  $D_{2r}$  is then effectively applied in the frequency domain by means of the relations (6). This process is termed smoothing.

2.3. Accuracy, Stability, and Integration Time

At each computed point in the power spectrum there is an error in the estimate due to the finite measurement time,  $T$ . The standard deviation, normalized by dividing by the true value of  $G(f)$ , is given by<sup>12,15</sup>

$$\epsilon \simeq \frac{1}{\sqrt{(B_e T)}} \dots\dots(7)$$

for any system, analogue or digital, if the noise being measured has a flat spectrum (white noise) and has a normal (Gaussian) amplitude distribution. It may be noted that if the bandwidth  $B_e$  is reduced, giving better frequency resolution, there is greater error in the amplitudes of the estimates unless the integration time  $T$  is increased.

With these assumptions (that the noise being measured is both Gaussian and white) the power spectral density estimates are  $\chi^2$  variables<sup>13</sup> with  $2/\epsilon^2$  degrees of freedom. If, for example,  $\epsilon = 0.1$ , the number of degrees of freedom is large, and therefore the  $\chi^2$  estimates have distributions closely approaching Gaussian. Consequently, it can be shown that there is 95% confidence that a spectral estimate will be within  $\pm 2\epsilon$  of its true value. For this value of  $\epsilon$ , the relation between the required values of the bandwidth and the integration time is given by

$$B_e T = 1/\epsilon^2 = 100$$

In the simplest case,  $N$  samples of the noise are taken at equal intervals  $\Delta t$ , and the lag interval  $\Delta \tau$  between autocorrelation estimates is made equal to  $\Delta t$ . Then  $B_e = 1/m\Delta \tau$ ,  $T = N\Delta t$ , and for the error of  $\epsilon = 0.1$ ,

$$N = 100m$$

The standard errors for the other noise parameters computed are given by similar expressions.<sup>15</sup> The variance  $\sigma^2$  has error given by  $1/\sqrt{BT}$ ; the mean  $\bar{V}$  has error given by  $\sigma/\bar{V}\sqrt{2BT}$ ; and the autocorrelation function  $\hat{R}_c$  an error  $\sqrt{\{(1 + \hat{R}_0^2/\hat{R}_c^2)/2BT\}}$ . In these expressions,  $B$  is the bandwidth of the whole record, after any filtering operations on the data.

A numerical example shows the difficulty of making measurements. A wave analyser with a constant bandwidth of 4 Hz will require an integration time of 25 seconds, irrespective of the centre frequency. For very low frequency measurements  $B_e$  might be  $10^{-4}$  Hz, and the required integration time becomes  $10^6$  s. (12 days).

2.4. Pre-whitening

The estimation of error given above is correct only if the noise being measured is white, i.e.  $G(f)$  is independent of  $f$ . If  $G(f)$  is a strong function of  $f$ , the accuracy of the spectral estimates is no longer

given by these simple relations. It will be appreciated that there is additional error and complexity if the power density varies significantly within the resolution bandwidth, and therefore it is desirable to make the noise spectrum as flat as possible prior to analysis. This is called pre-whitening. It will be shown in Section 2.5 that analogue filtering before sampling is necessary, and some pre-whitening can be included in this filtering.

Almost any required transfer function can be obtained by using a digital (transversal) filter after the noise is sampled. This computational program sub-routine acts on the data points  $V_n$  to produce filtered points  $U_n$  given by

$$U_n = \sum_{j=-F}^F a_j V_{n+j} + \sum_{i=1}^E b_i U_{n-i} \dots\dots(8)$$

A filtered point is thus produced at the centre of a span of  $(2F+1)$  original data-points. If the  $b_i$  are non-zero, the filter is termed recursive (i.e. with feedback) because the  $E$  previously filtered points are also used in computing  $U_n$ . The transfer function of a non-recursive filter has no poles.

In general, the digital filter has the following transfer function, which is a polynomial in

$$q \equiv \exp(-p\Delta t).$$

Here  $p$  is the complex frequency and  $\Delta t$  is the time interval between data points.

$$T(p) = \frac{\sum_{j=-F}^F a_j q^{j+F}}{1 - \sum_{i=1}^E b_i q^i} \dots\dots(9)$$

Noise processes can usually be pre-whitened satisfactorily by a non-recursive filter. As the coefficients  $b_i$  are then zero eqn. (9) shows that the voltage transfer function  $T(p)$  is a polynomial of degree  $2F+1$  in  $q$ . Like  $G(f)$ ,  $|T(p)|$  is taken as an even function of frequency. The continuous function  $|T(p)|$  is specified only at the frequencies  $hf_c/F$  ( $h = 0, 1, \dots F$ ) and these discrete values are denoted by  $T_h$ .

The data coefficients  $a_i$  are derived by an inverse Fourier transformation of the desired amplitude transfer coefficients  $T_h$ , following the method given by Hamming and Tukey.<sup>17</sup> In practice  $T_h$  is specified at  $F+1$  points, equally spaced in the frequency range 0 to  $f_c$ . Since  $T(p)$  is symmetrical about  $h = 0$ , this effectively determines  $T_h$  at  $2F+1$  points, and thus completely specifies  $T(p)$  as a polynomial of degree  $2F+1$ . The data coefficients are given by

$$a_i = \frac{C_i}{F} D_{3i} \left[ \frac{T_0}{2} + \sum_{h=-1}^{F-1} T_h \cos \frac{hi\pi}{F} + (-1)^i \frac{T_F}{2} \right]$$

for  $i = -F \dots F$

where  $C_i = \begin{cases} 0.5, & i = F, -F, \\ 1 & \text{otherwise} \end{cases}$

and  $D_{3i} = \left(0.54 + 0.46 \cos \frac{i\pi}{F}\right)$

It may be noted that  $a_i = a_{-i}$  for all values of  $i$ .

The function  $D_{3i}$  is known as the Hamming window,<sup>12,16</sup> and is similar in shape and effect to the 'hanning' window,  $D_{2r}$ , discussed in Section 2.2. One of these two windows is included so that the power transfer function  $|T(p)|^2$  varies in a smooth way between the points at which  $T_h$  is specified. The bandwidth of the Fourier transform of the window determines the maximum resolution of which the filter is capable. A filter of this type is also used with a narrow bandpass characteristic in an alternative method of spectral analysis discussed later.

2.5. Aliasing and the Choice of Sampling Rate

Nyquist's sampling theory<sup>18,19</sup> shows that from equi-spaced data points it is possible to reconstruct a band-limited function, provided the sampling rate is at least twice the upper frequency limit. For complete reconstruction the sampling must extend over infinite time, but the accuracy is good if the sampling time greatly exceeds the reciprocal of the lowest frequency of interest. Thus if  $\Delta t \equiv 1/2f_c$ ,  $G(f)$  must be zero for  $f > f_c$ . Any power at frequencies above  $f_c$  appears at frequencies below, and is superimposed upon the desired spectrum. This is termed aliasing.

Consider a simple example: if a cosine wave  $\cos 2\pi ft$  is sampled at times  $t = 0, 1/2f_c$ , the values obtained are 1 and  $\cos \pi f/f_c$ . Now

$$\cos \frac{\pi f}{f_c} = \cos \left(2n\pi \pm \frac{\pi f}{f_c}\right) = \cos \frac{\pi}{f_c}(2nf_c \pm f)$$

where  $n$  is any integer. Therefore power at all of the frequencies  $2nf_c \pm f$  becomes indistinguishable from power at the frequency of interest  $f (< f_c)$ . This argument can be extended to more than two samples, and any power at frequencies above  $f_c$  gives a contribution below and causes an error in the spectral estimates.

The apparent (aliased) power spectrum  $G_a(f)$  is given by:

$$G_a(f) = G(f) + \sum_{n=1}^{\infty} \{G(2nf_c + f) + G(2nf_c - f)\} \quad (10)$$

To avoid aliasing, the analogue data must be filtered before sampling; no digital analysis can remove the error once aliasing has occurred.

As analogue filtering cannot provide a sharp high frequency cut-off it is not possible to eliminate aliasing in practice if the original spectrum included power above  $f_c$ , which is the normal situation for electrical noise.

If  $G(f)$  is essentially zero for  $f > f_0$  and  $f_c < f_0 < 2f_c$ , aliasing is confined to the frequency

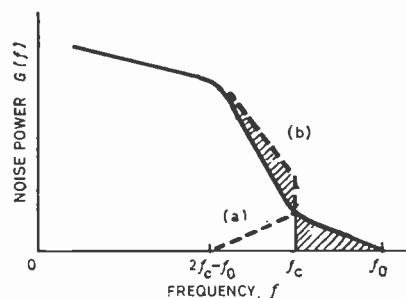


Fig. 2. Aliasing.

Curve (a) shows the power reflected from above to below  $f_c$  (half the sampling rate).

Curve (b) shows the total power measured.

range  $2f_c - f_0 < f < f_c$  as shown in Fig. 2. In this figure the true power spectrum after low-pass analogue filtering is shown by the full line. The broken line (a) shows the power between  $f_c$  and  $f_0$  'reflected' at  $f_c$  and the broken line (b) shows the total power measured. The shaded portion of the curve below  $f_c$ , which represents the aliased power, has the same area as the shaded part above  $f_c$ . The most serious error occurs at  $f_c$  where the apparent power is doubled, and there is no error below  $2f_c - f_0$ . The critical frequency  $f_c$  of the sampled data is given by  $1/2\Delta t$ , but the critical frequency of the computed spectrum equals  $1/2\Delta \tau$ , where  $\Delta \tau$  is the time spacing of the data used to calculate the auto-correlation function  $\hat{R}_r$ . The aliased part of the spectrum can be removed by a low-pass digital filter which rejects all power above  $2f_c - f_0$ , and thus  $\Delta \tau$  can be increased to  $1/2(2f_c - f_0)$  without further aliasing although the critical frequency is thereby reduced. This increase in the sample time spacing is achieved by omitting data points at intervals throughout the record after digital filtering. This process of decimation reduces the amount of computation required to obtain  $\hat{R}_r$ .

2.6. Corrections for Mean and Trend

If a band-pass filter has been used before sampling, the mean (i.e. d.c.) and very low frequency components should be small. However, it is possible that there are both a d.c. component  $\bar{V}$ , and a trend which to a first approximation can be treated as linear with slope  $\dot{V}$ .

The expressions for  $R(\tau)$  and  $\hat{R}_r$  given in Section 2.1 are correct if  $v(t)$  and  $v_n$  are stationary random processes with zero mean. More generally, however, the sampled points  $V_n$  may be expressed as

$$V_n = \bar{V} + \dot{V}\Delta t(n - N/2) + v_n \quad \dots\dots(11)$$

where  $v_n$  is a stationary random process with zero mean, as before.

It can be shown<sup>16</sup> by substituting eqn. (11) in eqn. (2) and manipulating, that the auto-correlation function  $\hat{R}_r$  of  $v_n$  is given by:

$$\hat{R}_r = \frac{1}{N-r} \sum_{n=1}^{N-r} V_n V_{n+r} - \bar{V}^2 - \frac{(\dot{V}N\Delta t)^2}{12}$$

The slope of the linear trend,  $\dot{V}$ , can be found from the difference between the means  $\bar{V}_1$  and  $\bar{V}_3$  of the first and last thirds of the data points, and  $\bar{V}$  is of course given by the mean of all the data. Thus,  $\dot{V}$  is given by

$$\dot{V} = \frac{3(\bar{V}_1 - \bar{V}_3)}{2N\Delta t}$$

A similar correction is necessary to obtain the true variance,  $\bar{v}^2$ , from the variance of the sampled points  $V_n$ . Substituting  $r = 0$  in eqn. (2) shows that  $\hat{R}_0 = \bar{v}^2$ , and therefore

$$\bar{v}^2 = \frac{1}{N} \sum_{n=1}^N V_n^2 - \bar{V}^2 - \frac{3}{16}(\bar{V}_1 - \bar{V}_3)^2$$

The normalized auto-correlation function  $\hat{\theta}_r$  is then given by

$$\hat{\theta}_r = \hat{R}_r / \hat{R}_0 = \hat{R}_r / \bar{v}^2$$

### 3. Direct Methods of Analysis

This section is concerned with two methods of digital spectral analysis which do not require the calculation of the auto-correlation function. The first of these we shall term the analogue simulation method, since by using narrow band-pass digital filters with subsequent squaring and averaging it resembles the analogue methods normally used at frequencies above about 20 Hz. The final method is, perhaps, the most basic of the three since it involves direct Fourier analysis of the sampled noise. The direct methods involve most of the contents of Section 2, particularly Sections 2.3, 2.4, and 2.5. The flexibility and computational requirements of the direct and indirect methods are compared at the end of this section.

#### 3.1. The Analogue Simulation Method

The sampled noise is first pre-whitened by analogue and digital filtering. A second digital filter with the required pass-band and centre frequency is then applied to a span of data points  $U_n$ , to produce each of the filtered points  $W_n$  given by

$$W_n = \sum_{i=-F}^F a_{hi} U_{n+i}, \quad \text{for } F+1 \leq n \leq N-F$$

The amplitudes of these  $N-2F$  points are then squared and averaged to give the noise power in the chosen bandwidth  $B_c$ . The spectral estimate  $\hat{G}_h$ , at the frequency  $hf_c/F$  is given by

$$\hat{G}_h = \frac{1}{B_c(N-2F)} \sum_{n=F+1}^{N-F} W_n^2$$

The bandwidth and centre frequency are defined by the band-pass digital filter, the data coefficients being derived as shown in Section 2.4. An advantage of this, and of the other direct method, is that a different bandwidth may be chosen for each spectral estimate.

The maximum resolution of the digital filter is determined by the number of equi-spaced frequencies at which the desired transfer function is specified, and hence by the number of data weighting coefficients. Following the notation of Section 2.4, if the transfer function is given by

$$T_h = \delta_{hk} = \begin{cases} 1 & \text{for } h = k \\ 0 & \text{otherwise} \end{cases} \quad \dots\dots(12)$$

a narrow band-pass filter is obtained, centred on a frequency  $kf_c/F$ . The data coefficients are given by

$$a_i = \frac{C_i}{F} D_{3i} \cos \frac{ki\pi}{F}$$

The frequency response of this filter, and in particular the bandwidth, are determined by the Hamming window  $D_{3i}$ . The equivalent bandwidth is  $f_c/F$ , and therefore high resolution requires a large number of data coefficients. The bandwidth required to give reasonable resolution at the lower frequencies in the range of interest may give unnecessary detail at the higher frequencies. If a larger bandwidth is employed, fewer independent spectral estimates can be obtained, but from eqn. (7) they are more accurate. A wider pass-band can be obtained in two ways. At all points except one,  $T_h$  may be set at zero as in eqn. (12), and  $F$  may be reduced, or  $F$  may be left unaltered, and  $T_h$  made non-zero at several adjacent points.

If the first method is adopted, the bandwidth of the transfer function is increased, but the shape is unaltered. Figure 3 shows the transfer functions

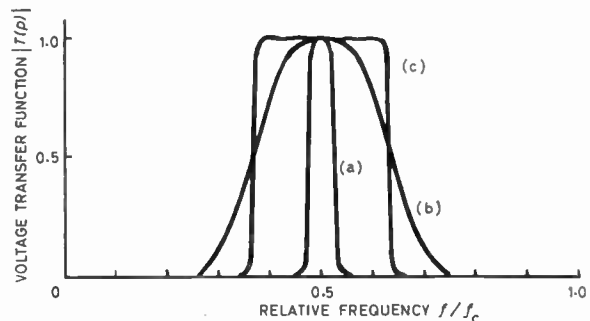


Fig. 3. Three digital filters used in the analogue simulation method.

- (a) Bandwidth  $B_o = f_c/F$ ,  $F = 20$ .
- (b) Bandwidth  $B_o = f_c/F$ ,  $F = 4$ .
- (c) Bandwidth  $B_o = 5f_c/F$ ,  $F = 20$ .

obtained when  $T_h = \delta_{hk}$ , for  $F = 20$  and  $F = 4$  (curves (a) and (b) respectively). The lower value of  $F$  gives a considerable reduction in computation. The second method improves the shape, as shown in curve (c); the steepness of cut-off has been maintained while the bandwidth has been increased. In this example  $F = 20$  and  $T_h$  has been specified by

$$T_h = \sum_{j=k-2}^{k+2} \delta_{hj}$$

### 3.2. The Direct Fourier Analysis Method

The basis of this method has been explained in detail by Akcasu<sup>20</sup> and Welch.<sup>21</sup> A sampled pre-whitened noise record, containing  $M$  data points  $U_n$ , is subjected to discrete Fourier analysis. The coefficients of the sine and cosine terms,  $a_h$  and  $b_h$ , are given by

$$(a_h, b_h) = \frac{1}{M} \left[ \frac{U_1}{2} (\sin, \cos) \frac{2\pi h}{M} + \sum_{n=2}^{M-1} U_n (\sin, \cos) \frac{2\pi hn}{M} + \frac{U_M}{2} (\sin, \cos) 2\pi h \right] \dots (13)$$

Power spectral estimates are produced at harmonics of  $1/M\Delta t$ , and are given by

$$\hat{G}_h = a_h^2 + b_h^2$$

The finite discrete set of data points  $U_n$  may be considered to be derived from a continuous function  $U(t)$  through multiplication by the rectangular window  $D_{0n}$  and by an infinite set of  $\delta$  functions, uniformly spaced at intervals of  $\Delta t$ . This is expressed by

$$U_n = U(t)D_{0n}B(t)$$

where  $D_{0n} = \begin{cases} 1 & \text{for } 0 \leq n \leq M \\ 0 & \text{otherwise} \end{cases}$

and  $B(t) = \frac{1}{M} \sum_{-\infty}^{\infty} \delta(t - n\Delta t)$

The Fourier transform  $J(f)$  of the composite data window  $D_{0n}B(t)$  is given by

$$J(f) = \cos(\pi f \Delta t) \frac{\sin(M\pi f \Delta t)}{M \sin(\pi f \Delta t)}$$

For  $f \ll 1/\pi\Delta t$ , which is the frequency range of interest (since  $f \ll f_c = 1/2\Delta t$ ),  $\cos(\pi f \Delta t) \simeq 1$  and  $\sin(\pi f \Delta t) \simeq \pi f \Delta t$ . Therefore

$$J(f) \simeq \frac{\sin(M\pi f \Delta t)}{M\pi f \Delta t}$$

which is similar to the transform of the window  $D_{0n}$  alone. The effective power transfer function, which we will denote by  $Q_{1h}$ , is given by the square of  $J(f)$  centred on the frequency at which the estimate is required. Thus

$$Q_{1h}(f) = \left[ J\left(f - \frac{h}{M\Delta t}\right) \right]^2$$

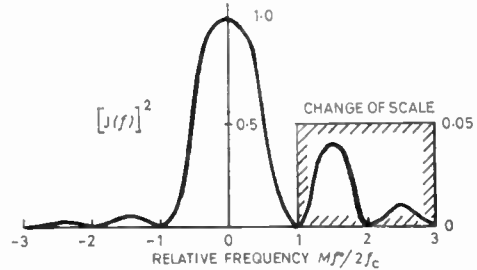


Fig. 4. Spectral window  $(J(f))^2$  for the direct Fourier transform method.

The variation of the function  $[J(f)]^2$  with frequency is shown in Fig. 4. The shape of  $Q_{1h}(f)$  is similar to the hanning spectral window (Fig. 1(d)) but the side-lobes are slightly larger and always positive; it is identical with the spectral window associated with Bartlett smoothing.<sup>22</sup>

The bandwidth of the window  $Q_{1h}(f)$  is  $1/M\Delta t$ ; substituting this value in eqn. (7) gives a standard error of 1 (the estimates have only two degrees of freedom). The accuracy of estimates with a fixed bandwidth is of course improved by increasing the integration time, but in this case the bandwidth is reduced as the data record length increases. The bandwidth may be increased, and hence the error reduced, in two ways as follows. In each case the record has the total number of data points  $N$  necessary for sufficient accuracy in the bandwidth chosen.

In the first method,  $M$  is simply set equal to  $N$ . Spectral estimates may then be calculated with bandwidth  $1/N\Delta t$  at adjacent harmonics of  $1/N\Delta t$ , using eqn. (13). If  $s$  of these adjacent estimates are added, the sum is the power in a bandwidth  $s/N\Delta t$ . Thus the number of degrees of freedom is increased to  $2s$ , and the standard error becomes  $1/\sqrt{s}$ . This method should give a well-defined pass-band with sharp high and low frequency cut-off, but direct Fourier analysis using eqn. (13) requires a considerable amount of computation. However, if  $c$  cycles of the frequency of analysis  $h/M\Delta t$  occupy an integral number of data spacings  $\Delta t$ , that is if  $cM/h$  is an integer, much computation can be saved. Data points separated by a time interval  $cM\Delta t/h$  can then be added before multiplication by the sine or cosine terms, thus reducing the number of multiplications by the factor  $c/h$ . However, the computer program is more complex and for this reason the alternative method given below has been used in our work. Algorithms for this type of fast Fourier transform have been given recently in the literature.<sup>14, 23</sup>

Alternatively, the record may be divided into  $s$  equal pieces, each containing  $M = N/s$  data points. The spectral estimates calculated from each of these

pieces have bandwidth  $s/N\Delta t$ , but are again of low accuracy. However, by taking a mean of the estimates made at the same frequency from the  $s$  pieces, the error is reduced to  $1/\sqrt{s}$  as before. The pass-band obtained by this method has the shape of  $Q_{1b}$ , which is less rectangular than that produced by the first method. Less computation is required, however, and the shape can be improved by multiplying the individual sections of the record by a lag window. Welch<sup>21</sup> has used the 'hanning' window, which gives the power transfer function  $[Q_{2h}(f)]^2$  (see eqn. (4)) having very small side lobes.

### 3.3. Corrections for Mean and Trend

If after sampling and pre-whitening the data includes a non-zero mean and a linear trend, a correction can be made as with the indirect method. In Section 2.6 it was shown that two constant terms subtracted from each point in the correlation function suffice to correct for these unwanted components. However, in the direct methods the mean  $\bar{V}$  and a term  $\bar{V}(n-N/2)\Delta t$  must be subtracted from each data point (using eqn. (11)) to yield the required stationary random variable  $v_n$ .

### 3.4. Comparison of the Indirect and Direct Methods

The three methods which have been described will now be compared for accuracy, flexibility, and computer and data requirements, for the same values of the bandwidth, standard error, and number of spectral estimates. The digital computer requirements are determined by the length of the spectral analysis program, and the amount of data processed; both must be kept within the available computer time and storage limitations.

Several elements in the analysis are common to all three methods. The integration time,  $T$ , is determined by the required accuracy in the narrowest bandwidth used, which in turn depends on the lowest frequency to be analysed. The sampling rate  $2f_c$  depends on the upper frequency limit of the noise, which is usually rather above the highest frequency of interest. From Section 2.3 it follows that for 0.1 standard error the number of data points  $N$  is  $200f_c/B_e$  where  $B_e$  is the narrowest bandwidth required. Thus if the requirements are such that  $f_c$  exceeds  $B_e$  by much more than an order of magnitude the amount of data will be large and computer storage may present a problem.

The direct methods have the advantage that a different bandwidth may be chosen for each spectral estimate. Thus accuracy can be sacrificed in favour of narrow bandwidth in some parts of the spectrum, and unnecessary resolution avoided in other parts.

The most time-consuming of the simple arithmetic operations performed by the digital computer are multiplication and division, and the run-time of a

program is determined primarily by the number of such operations performed. The calculation of sine and cosine requires several arithmetic operations, and in general occupies an order of magnitude more time than simple multiplication.

In order to compare the three methods under similar conditions, it will be assumed that  $m/2$  independent estimates are required, each with a bandwidth of  $2f_c/m$ , equally spaced in the frequency range 0 to  $f_c$ . The digital pre-whitening filter is common to all three methods. If the pre-whitening transfer function is specified at  $m/2$  points, a span of  $m+1$  data points is necessary to produce each filtered point.

As the data coefficients are symmetrical, the pre-whitening operation requires approximately  $mN/2$  multiplications. No additional computer storage is required for the filtered points as they can be stored in the array previously occupied by the raw data points which are no longer required.

To calculate the auto-correlation function in the indirect method requires approximately  $Nm$  multiplications, and the Fourier transformation of  $\hat{R}_r$  requires very little additional time. In some cases it is possible by efficient programming<sup>24</sup> to reduce the number of multiplications required. Each of the  $m/2$  filtering processes in the analogue simulation method requires  $mN/2$  multiplications, giving a total of  $m^2N/4$  operations. This number will be reduced if fewer data coefficients, and hence a wider bandwidth, are used for the higher frequency filters.

The direct Fourier transformation of a record containing  $M$  data points requires  $2M$  multiplications and the calculation of  $2M$  sine and cosine terms. If the record has been divided into  $q$  pieces, computation is reduced by storing the sine and cosine terms, since these are used in the analysis of each piece of the record. Thus this method of computation requires the calculation of  $Nm/q$  sine and cosine terms, and  $Nm$  multiplications. Again this number may be reduced slightly if at higher frequencies the bandwidth is increased and fewer estimates are produced.

Thus for similar conditions the indirect and direct Fourier analysis methods require approximately the same computation time, while the analogue simulation technique takes slightly longer. The direct methods have a distinct advantage, however, if it is not required to compute all  $m/2$  spectral estimates, the computation time being roughly proportional to the number of values of  $\hat{G}_h$  required. If the indirect method is used the complete auto-correlation function must be calculated irrespective of the number of spectral estimates to be computed.

It has been shown in Section 2.3 that  $N = 100m$  for 0.1 standard error in the narrowest bandwidth estimate. In this case the number of multiplications

required by each method is approximately  $100m^2$ , which will be very large if the highest frequency  $f_c$  in the record exceeds the bandwidth by much more than an order of magnitude.

4. Current Noise Measurement

This section is concerned with the digital measurement of  $1/f$  noise, that is noise conforming to eqn. (1), and in particular considers the effect of aliasing and the necessity of analogue filtering.

4.1. Accuracy

When investigating the current noise produced by a semiconductor device, the object of the analysis is to determine the coefficients  $\alpha$  and  $\beta$  in eqn. (1). Many values of  $G(f)$  are required, but for each estimate a high accuracy is unnecessary and a normalized standard error of 0.1 is usually satisfactory.

4.2. Resolution

The power spectrum of a random process such as current noise is expected to be a smoothly-varying function of frequency, and it is therefore unnecessary to have very sharp resolution; to give reasonable detail the bandwidth should be of the same order as the lowest frequency in the range of interest. In the indirect method spectral estimates are produced at harmonics of  $B_c/2$ , but unless pre-whitening has been accurately applied the estimate at  $f = B_c/2$  may not be reliable. A bandwidth equal to the lowest frequency of interest provides a reliable spectral estimate at that frequency.

4.3. Sensitivity of the Measuring System

The required sensitivity of the measuring equipment clearly depends on the total noise power in the frequency range under consideration. For current noise this has a simple form if the approximation  $\alpha = 1$  is made in eqn. (1): then integration between limits  $f_1$  and  $f_2$  yields the following result:

$$\int_{f_1}^{f_2} G(f) df = AI^\beta \ln \frac{f_2}{f_1}$$

Thus the current noise power in any frequency range depends only on the ratio of the limiting frequencies. If the resolution bandwidth  $B_c$  is made a constant fraction of the frequency at which the noise is being measured, the required sensitivity of the system will be the same for all frequencies. A disadvantage of the indirect method is that  $B_c$  is a constant for a given value of maximum lag and hence throughout the frequency range being analysed. This is quite acceptable, however, if each frequency range is not large—say one decade—and the bandwidth is of the order of the lowest frequency. Also, as shown in Section 3.4, the frequency range recorded and analysed must be limited to reduce the amount of computation and computer storage required, and 10

is a suitable value for the ratio of the frequency range to the bandwidth for each spectral estimate.

4.4. Aliasing and Analogue Filtering

It has been shown in Section 2.5 that if discrete data points have been sampled at time intervals  $\Delta t = 1/2f_c$ , the computed (aliased) power spectral density function  $G_a(f)$  is given by

$$G_a(f) = G(f) + \sum_{n=1}^{\infty} \{G(2nf_c + f) + G(2nf_c - f)\}$$

If

$$G(f) = g/f$$

where  $g$  is constant, which is approximately correct for current noise, then

$$G_a(f) = \frac{g}{f} + g \sum_{n=1}^{\infty} \left[ \frac{1}{(2nf_c + f)} + \frac{1}{(2nf_c - f)} \right] \quad (14)$$

As  $G(f)$  is decreasing with increasing  $f$ , it may appear at first sight that analogue filtering before sampling is unnecessary and that aliasing will cause only a small error. For large  $n$ ,  $2nf_c \gg f$  and the terms in brackets in eqn. (14) become independent of  $f$ ; the effect of aliasing is then to produce an apparent white noise component in the frequency range  $0 < f \leq f_c$ . The total noise power is given approximately by

$$G_a(f) = \frac{g}{f} + g \sum_{n=1}^{\infty} \frac{1}{nf_c}$$

which does not converge. Some analogue filtering must therefore be used to prevent, or at least limit aliasing.

For large  $n$ , the summation in eqn. (14) can be approximated by an integral, and the aliased power from the frequency range  $n_1f_c$  to  $n_2f_c$  is then given by  $g \cdot \ln(n_2/n_1)$ . As this depends on the ratio  $n_2/n_1$ , the aliased power from each frequency decade is the same.

For simplicity, suppose an ideal low-pass filter with a sharp cut-off at a frequency  $f_0$  is introduced before sampling, so that

$$G(f) = \begin{cases} g/f, & 0 < f < f_0 \\ 0, & f_0 \leq f \end{cases}$$

The effects of aliasing on a spectrum of this form for various values of  $f_0$  have been computed from eqn. (14) and are shown in Fig. 5. Each curve is labelled with the frequency  $f_0$  at which it is assumed that the filter cuts off. If  $f_0 = f_c$  there is no error and the true  $1/f$  spectrum is obtained. If  $f_0 = 3f_c/2$ , error is introduced between  $f_c/2$  and  $f_c$ , as explained in Section 2.5. If  $f_0$  is raised to  $2f_c$  (the sampling frequency) error is introduced at all frequencies below  $f_c$ , and this error increases progressively as  $f_0$  is further increased. Above  $10f_c$  the effect is essentially to add white noise, increasing in proportion to the number of frequency decades thereafter.

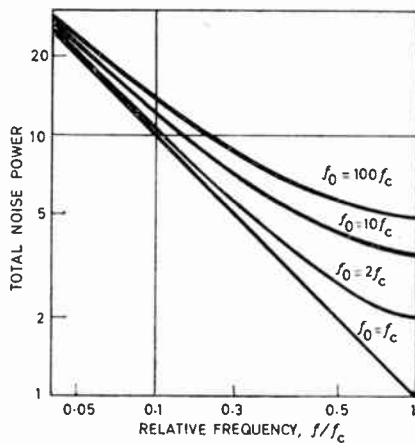


Fig. 5. Apparent power spectrum for various values of  $f_0$  (the cut-off frequency of the idealized low-pass analogue filter), showing the effect of aliasing on '1/f' noise.

The error in the frequency decade of interest is small, particularly at the lower frequencies, if a low-pass analogue filter is available with a cut-off not much greater than  $f_c$ . This error is even less significant if  $f_c$  is chosen such that frequencies just below it are of little interest.

For very low frequencies (below about  $10^{-2}$  Hz) the construction and testing of analogue filters involve considerable difficulties, and so aliasing may be unavoidable. However, the required correction can be calculated using eqn. (10), if the power spectrum has been found previously for frequencies above the current range of interest. The cut-off frequency of the low-pass filter should, of course, be made as low as possible to minimize the magnitude of the correction.

#### 4.5. Pre-whitening

As shown in Section 2.4, it is desirable that the computed spectrum should be flat, and pre-whitening may be obtained by both analogue and digital filtering. A simple pre-whitening analogue filter is provided by a single R-C high-pass section. This has a transfer function which increases linearly with frequency near  $f = 1/2\pi CR$ , and thus provides approximate pre-whitening for 1/f noise.

A low-pass analogue filter is necessary to limit aliasing, and it is convenient to add an R-C high-pass section which removes any d.c. component which may be present and also gives approximate pre-whitening. A further advantage is that power from frequencies well below the range of interest is severely attenuated, and so greater sensitivity may be employed in the sampling system. If necessary, a digital filter can be added to yield any required pre-whitening characteristic with high accuracy. Any change of transfer function, for example an index of frequency differing from

unity, is made by altering the set of coefficients in eqn. (8). Each set is stored on one data card in the computer program.

A power transfer function capable of pre-whitening a noise spectrum is normally realizable by a non-recursive filter. The indirect method of analysis produces  $m/2$  independent spectral estimates between 0 and  $f_c$ , and if the power transfer function  $T_h^2$  of the digital filter is to be specified at each of these points it must be represented by a polynomial of degree  $m + 1$ . Therefore in eqn. (8)  $F = m/2$ , and each filtered point is produced from a span of  $m + 1$  data points.

If  $m$  is small, or if the voltage transfer function  $T_h$  is not to be specified at every point, it may be possible to fit a polynomial of the form shown in Section 2.4. In general, however, the Fourier transformation procedure given in that section has to be used, and in most cases it is quicker and simpler. To correct for the pre-whitening produced by the digital filter, the power transfer function  $T_h^2$  must be known wherever  $G(f)$  is estimated. It is therefore convenient to specify  $T_h$  at every point; if this is not done the values which have not been specified must be obtained by Fourier transformation of the data coefficients  $a_i$  or by interpolation.

#### 4.6. Amplitude Probability Distribution

When calculating the accuracy of the spectral analysis in Section 2.3 it was assumed that the noise being measured has a Gaussian distribution of amplitudes, and hence that the spectral estimates have  $\chi^2$  distributions. A Gaussian (normal) distribution is expected for noise in electron devices, which arises from a large number of independent noise generators.

In our measurements<sup>7</sup> the normality of the amplitude distribution of current noise data in the very low frequency range has been tested by computation.

The program is essentially a sorting procedure: the standard deviation  $\sigma$  of the sampled data is first calculated, and an amplitude range of  $6\sigma$  centred on the mean value is divided into  $K$  class intervals each of width  $A$ . The number of data points in each class interval is then counted, giving the probability density function  $\hat{p}(V)$ .

The optimum value of  $K$  to give the best overall accuracy and resolution is given by the empirical formula:<sup>25</sup>

$$K = 1.87(N - 1)^{0.4}$$

for  $N > 2000$ , and a level of significance of 0.05. The standard error in  $\hat{p}(V)$  is approximately  $1/\sqrt{NA\hat{p}(V)}$ , where  $A = 6\sigma/K$ .

The estimates  $\hat{p}(V)$  have been compared with the theoretical function  $p(V)$  which would be obtained

if the distribution were Gaussian with the same mean and standard deviation. The discrepancy can be compared with that expected statistically from a  $\chi^2$  distribution with  $K-3$  degrees of freedom. The normality was confirmed by this method for a representative set of records, and therefore the theoretical errors quoted in this paper should be justified.

### 5. Conclusions

Electrical noise can be analysed down to very low frequencies by sampling and storage followed by digital computation, with greater efficiency and accuracy than by analogue methods. Three methods of digital spectral analysis have been described, and it has been shown that they have similar computational requirements. The two direct methods have greater flexibility than the more conventional auto-correlation technique, and require less computation if relatively few spectral estimates are required. The indirect method generates the whole spectrum, and also gives the auto-correlation function which itself provides information about the physical process being investigated. In general, a judicious combination of the various methods gives an efficient and powerful technique for analysis.

Errors are produced by aliasing unless sampling is preceded by analogue low-pass filtering. This is difficult to achieve accurately at very low frequencies, and a method of correction for aliasing errors has been given in this paper. An example of the application of this technique occurs in noise measurements down to  $5 \times 10^{-5}$  Hz reported in an accompanying paper.<sup>7</sup>

### 6. Acknowledgments

The work described in this paper is part of a programme of research supported by the Atomic Energy Establishment at Winfrith Heath, and the authors are grateful to Messrs. D. Harrison and E. P. Fowler of this establishment for valuable discussions. Two of the authors (R.J.H. and I.R.M.M.) are indebted respectively to the Science Research Council and the United Arab Republic Atomic Energy Establishment for financial support.

### 7. References

1. G. G. Bloodworth and N. R. S. Nesbitt, 'Active filters operating below 1 Hz', *Trans. Inst. Elect. Electronics Engrs on Instrumentation and Measurement*, IM-16, pp. 115-120, 1967.
2. D. A. Bell, 'Electrical Noise' (Van Nostrand, New York, 1960).
3. H. Sutcliffe, 'Noise-spectrum measurement at subaudio frequencies', *Proc. Instn Elect. Engrs*, 112, pp. 301-309, 1965.
4. J. C. Martin, F. X. Mateu-Perez and F. Serra-Mestres, 'Mesures de bruit de fond des transistors plans aux très basses fréquences', *Electronics Letters*, 2, pp. 343-345, 1966.
5. B. V. Rollin and I. M. Templeton, 'Noise in semiconductors at very low frequencies', *Proc. Phys. Soc.*, B, 66, pp. 259-261, 1953.
6. T. E. Firlie and H. Winston, 'Noise measurements in semiconductors at very low frequencies', *J. Appl. Phys.*, 26, pp. 716-18, 1955.
7. I. R. M. Mansour, R. J. Hawkins and G. G. Bloodworth, 'Measurement of current noise in m.o.s. transistors from  $5 \times 10^{-5}$  to 1 Hz', *The Radio and Electronic Engineer*, 35, No. 4, pp. 212-6, April 1968.
8. R. D. Gaul and N. L. Brown, 'A free-floating wave meter', *Proc. I.E.R.E. Conference on Electronic Engineering in Oceanography*, Southampton, 1966. (I.E.R.E. Conference Proceedings No. 8 and Paper No. 8.)
9. D. M. A. Mercer, 'Analytical methods for the study of periodic phenomena obscured by random fluctuations', *Cold Spring Harbor Symposia on Quantitative Biology*, 25, pp. 73-85, 1960.
10. D. K. Baker, 'Flicker noise in germanium rectifiers at very low- and audio-frequencies', *J. Appl. Phys.*, 25, pp. 922-24, 1954.
11. S. O. Rice, 'Mathematical analysis of random noise', *Bell Syst. Tech. J.*, 23, pp. 282-332, 1944, and 24, pp. 46-156, 1945.
12. R. B. Blackman and J. W. Tukey, 'The measurement of power spectra from the point of view of communications engineering', *Bell Syst. Tech. J.*, 37, pp. 185-282 and 485-569, 1958. Later published in book form (Dover, New York, 1959).
13. J. S. Bendat, 'Principles and Applications of Random Noise Theory' (Wiley, New York, 1958).
14. J. W. Tukey, 'An Introduction to the Calculations of Numerical Spectrum Analysis', 'Advanced Seminar on Spectral Analysis of Time Series, University of Wisconsin, Madison, October 1966 (Wiley, New York, 1967).
15. J. S. Bendat and A. G. Pierson, 'Measurement and Analysis of Random Data' (Wiley, New York, 1966).
16. R. B. Blackman, 'Linear Data-smoothing and Prediction in Theory and Practice' (Addison-Wesley, Reading, Massachusetts, 1965).
17. R. W. Hamming and J. W. Tukey, 'Measuring noise color' (unpublished).
18. H. Nyquist, 'Certain topics in telegraph transmission theory', *Trans. Amer. Inst. Elect. Engrs*, 47, pp. 617-644, 1928.
19. C. E. Shannon, 'A mathematical theory of communication', *Bell Syst. Tech. J.*, 27, pp. 379-423 and 623-656, 1948.
20. A. Z. Akcasu, 'Measurement of noise power spectra by Fourier analysis', *J. Appl. Phys.*, 32, pp. 565-568, 1961.
21. P. D. Welch, 'A direct digital method of power spectrum estimation', *IBM J. Res. Dev.*, 5, pp. 141-156, 1961.
22. M. S. Bartlett, 'Periodogram analysis and continuous spectra', *Biometrika*, 37, pp. 1-16, 1960.
23. 'Guest Editorial' to issue on 'The Fast Fourier Transform', *Trans. I.E.E.E. on Audio and Electroacoustics*, AU-15, No. 2, p. 43, 1967.
24. L. P. Schmid, 'Efficient autocorrelation', *Commun. Association of Computer Manufacturers*, 8, p. 115, 1965.
25. C. A. Williams, Jr., 'On the choice of the number and width of classes for the  $\chi^2$  test of goodness of fit', *J. Amer. Statistical Ass.*, 45, pp. 77-86, 1950.

Manuscript first received by the Institution on 18th December 1967 and in final form on 16th February 1968. (Paper No. 1180/CC2)

© The Institution of Electronic and Radio Engineers, 1968

# Measurement of Current Noise in M.O.S. Transistors from $5 \times 10^{-5}$ to 1 Hz

By

I. R. M. MANSOUR,  
B.Sc., M.Sc.,†

R. J. HAWKINS, B.Sc.†

AND

G. G. BLOODWORTH,  
M.A., D.U.S., C.Eng., M.I.E.R.E.†

**Summary:** Very low frequency electrical noise can be analysed by periodic sampling, followed by digital computation of the statistical parameters. The measurement technique used with m.o.s. transistors is described. The results show that in the frequency range  $5 \times 10^{-5}$  to 1 Hz the power spectral density of the current noise is proportional to  $f^{-\alpha}$  where  $1 < \alpha < 1.2$ .

## 1. Introduction

In almost all semiconductor devices the predominant noise component at low frequencies has a power spectral density  $G(f)$  given approximately by

$$G(f) \simeq A \frac{I^\beta}{f^\alpha} \quad \dots\dots(1)$$

where  $I$  is the direct current flowing and  $f$  is the frequency. The indices  $\alpha$  and  $\beta$  are found to be approximately 1 and 2, and  $A$  is a weak function of temperature. Measurements at very low frequencies are being made because the apparent continuation of the  $1/f$  spectrum without limit is an obstacle to the general acceptance of certain theories for the origin of the noise. The existence of any low-frequency turnover point has not been shown conclusively in the literature, and in our measurements down to  $5 \times 10^{-5}$  Hz on m.o.s. transistors the spectrum continues without deviation.

These measurements have been made using a digital analysis technique. Filtered noise is sampled periodically and stored on paper tape, and then analysed in a digital computer. In addition to the conventional indirect method of spectral analysis involving the autocorrelation function, two direct methods have been used. A description and comparison of the three techniques is given elsewhere,<sup>1</sup> together with definitions of the various symbols used here.

Almost all of our results were obtained originally by the indirect method, and the spectra for a representative sample of the data tapes have been re-computed by one or other of the direct methods. From this work it is concluded that all three methods of analysis are suitable for low frequency electrical noise.

† Department of Electronics, University of Southampton.

## 2. Experimental Arrangement

In this Section, the practical choice of time and frequency parameters is explained and the sampling system described for current noise measurements in the frequency range  $5 \times 10^{-5}$  to 1 Hz.

### 2.1. Time and Frequency Parameters

To limit the amount of data and the computation required, the frequency range was divided into decades which were analysed separately. A bandwidth equal to the lowest frequency in each decade was chosen for all three methods to allow a direct comparison. A standard error of 0.1 in each spectral estimate was chosen, and the required values of the integration time  $T$  are shown in Table 1 for the four decades investigated. Analysis of the lowest decade also yielded an estimate at  $5 \times 10^{-5}$  Hz.

If it were possible to realize low-pass analogue filters with a perfectly sharp cut-off, a sampling rate of, say, 2 per second would have been sufficient for the decade 1–0.1 Hz. Reasonably simple practical filters have a high frequency cut-off which extends roughly over one octave above the top of the required decade, and to avoid aliasing the required sampling rate is of course higher by another octave. Therefore, as shown in Table 1, the sampling rate  $1/\Delta t$  is about 4 times the highest frequency of interest. At the lower frequencies the choice of  $\Delta t$  and hence the bandwidth was determined to some extent by the availability of timing mechanisms.

The transfer functions of the digital pre-whitening filters, and of the band-pass filters used in the analogue simulation method, were specified at the  $m/2$  points at which independent estimates were computed. Thus the span of data points required for each filtered point was  $(m+1)$ .

To obtain the bandwidths given in Table 1, when the direct Fourier analysis method was used, the

**Table 1**  
Time and frequency parameters used

Frequency range analysed (Hz)	Resolution bandwidth, $B_o$ (Hz)	Period of measurement, $T$ (s)	Sampling interval, $\Delta t$ (s)	Number of data points, $N$	Number of resolved bands, $m/2$
$1-10^{-1}$	$10^{-1}$	$10^3$	0.25	4000	20
$10^{-1}-10^{-2}$	$10^{-2}$	$10^4$	2.5	4000	20
$10^{-2}-10^{-3}$	$9.8 \times 10^{-4}$	$10^5$	30	3333	17
$10^{-3}-10^{-4}$	$9.8 \times 10^{-5}$	$10^6$	300	3333	17

total record containing  $N$  data points was divided into approximately 100 sections, each containing  $m$  points. In both direct methods, spectral estimates were calculated only in the frequency range of interest, between 0 and  $f_c/2$ , where the accuracy was not impaired by aliasing or by the attenuation due to the non-ideal analogue filter. The indirect method involved some extra computation because the inaccurate information in the range  $f_c/2$  to  $f_c$  was included in the autocorrelation function.

**2.2. Sampling and Recording System**

A schematic diagram of the experimental system is shown in Fig. 1. A matched pair of m.o.s. transistors was connected in a bridge circuit to minimize spurious fluctuations in output voltage caused by variations in temperature and bias voltages. The mean value of the voltage between the transistor drains was set to zero by adjusting one load resistor. The temperature fluctuations of each transistor in the frequency range of interest were reduced to less than 0.01 degC by mounting them in an aluminium block immersed in an oil bath with temperature control. The drain and gate bias voltages were derived from Mallory cells mounted with the load resistors in an external circuit close to the oil bath. The bridge output was connected to a d.c. amplifier with a voltage gain of  $2 \times 10^4$ . The amplifier chosen<sup>2</sup> used a junction f.e.t. as a chopper, and its contribution to the noise was less than 1% of the  $1/f$  noise from the m.o.s. transistors under test.

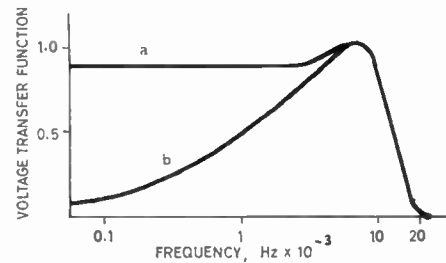


**Fig. 2.** Analogue filter transfer functions used in practice.

Curve a: Typical fourth-order low-pass active filter.

Curve b: Pre-whitening effect of adding a high-pass passive R-C filter section.

To avoid aliasing in the three decades  $1-10^{-3}$  Hz, low-pass active filters were used of the type developed by Bloodworth and Nesbitt.<sup>3</sup> A typical 4th-order filter response is shown in Fig. 2, curve a. Active filters with high-frequency cut-offs at 2, 0.2, and 0.02 Hz were used, together with high-pass RC sections to give approximate pre-whitening Fig. 2, curve b. Although it is possible<sup>3</sup> to construct a low-pass filter with a cut-off at  $2 \times 10^{-3}$  Hz, spectra below  $10^{-3}$  Hz have normally been analysed using a filter cutting off at  $2 \times 10^{-2}$  Hz and applying the correction method derived elsewhere.<sup>1</sup>

The sampling and recording equipment is a commercial data-logging system, which consists essentially

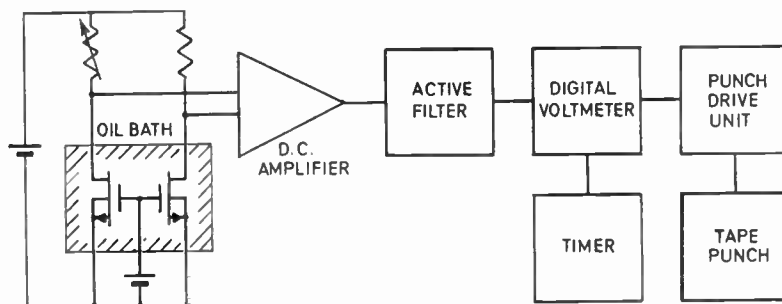
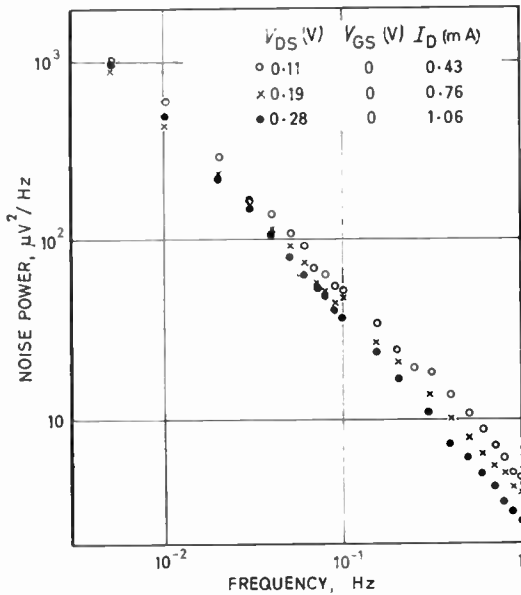
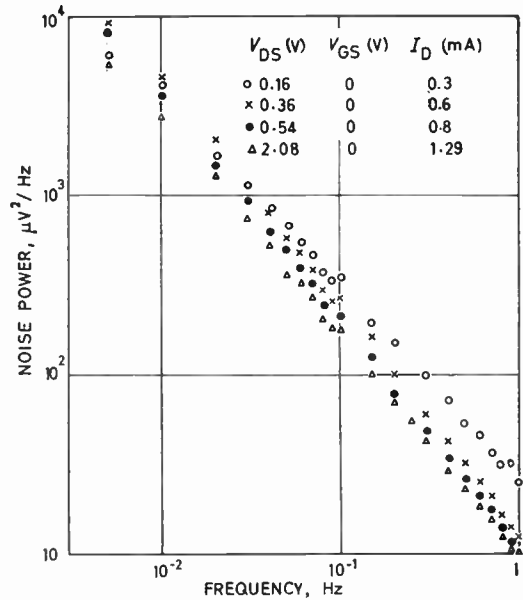


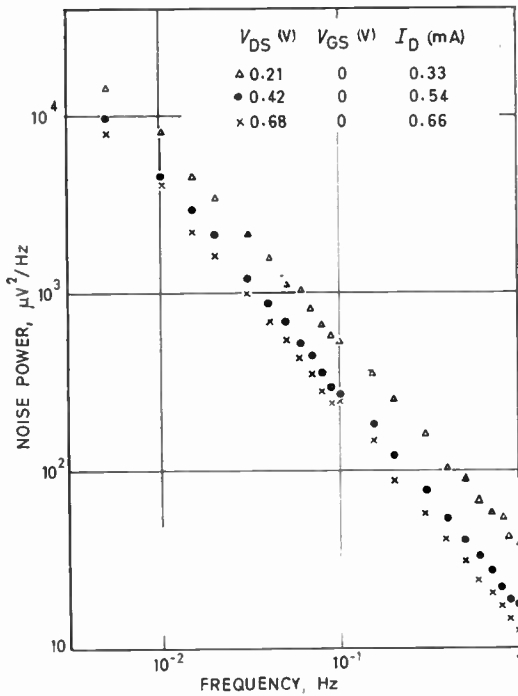
**Fig. 1.** Measurement system used.



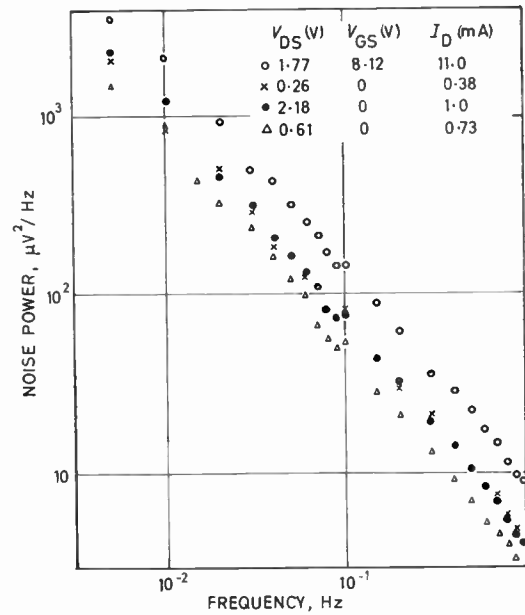
(a) Mullard BFX63, samples M1, M2.  
n-channel depletion type.  $\beta = 1.7 \text{ mA/V}^2$ ,  $V_T = 1.3 \text{ V}$ .



(b) Mullard BFX63, samples M5, M6.  
 $\beta = 2 \text{ mA/V}^2$ ,  $V_T = 1.2 \text{ V}$ .

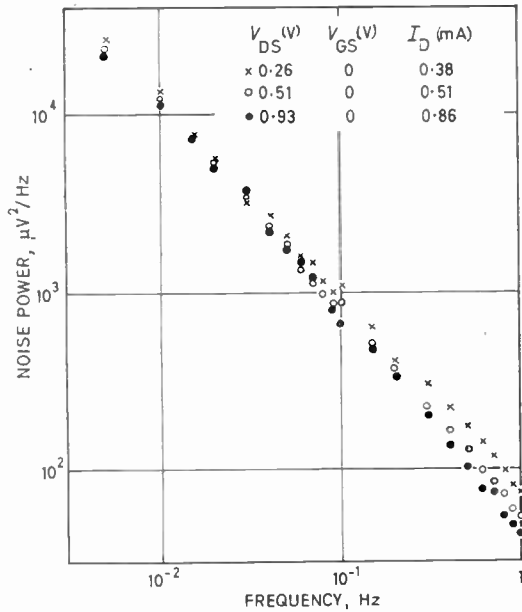


(c) Mullard BFX63, samples M3, M4.  
 $\beta = 1.5 \text{ mA/V}^2$ ,  $V_T = 0.7 \text{ V}$ .

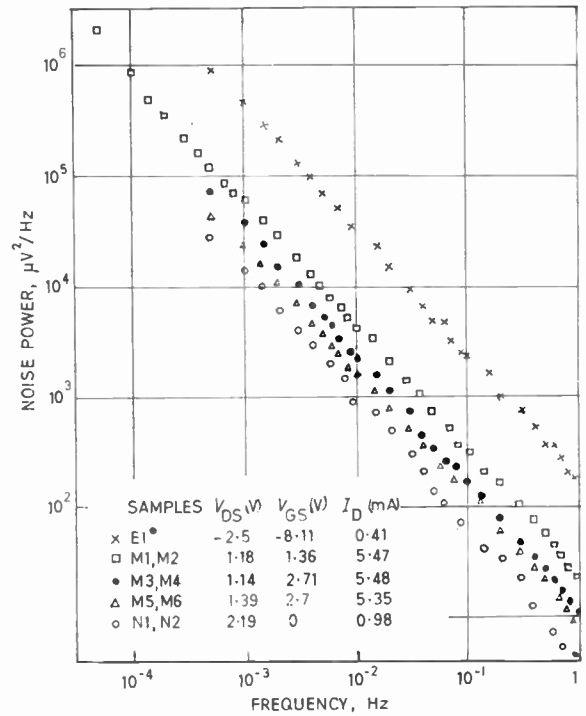


(d) Motorola 2N3796, samples N1, N2, n-channel depletion type.  $\beta = 1.25 \text{ mA/V}^2$ ,  $V_T = 1.0 \text{ V}$ .

Fig. 3(a-g). Noise power spectra obtained for several samples of m.o.s. transistors at various bias conditions and two temperatures.



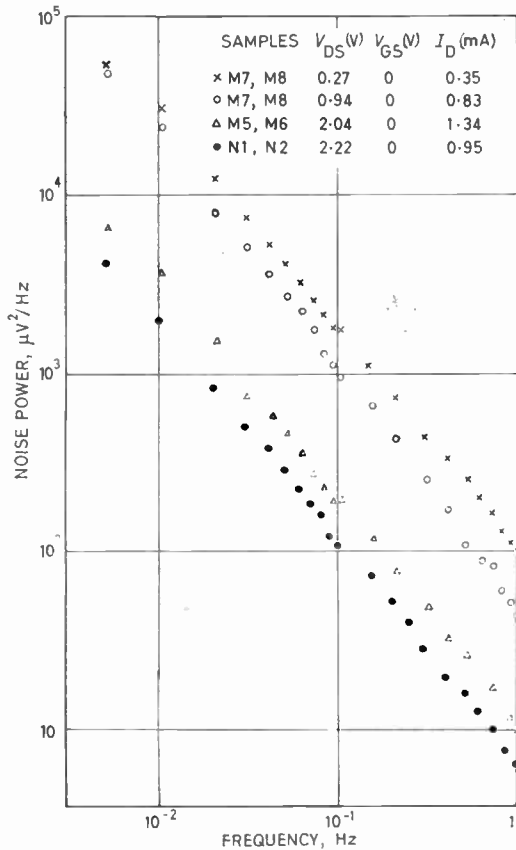
(e) Mullard experimental, samples M7, M8. n-channel depletion type.  $\beta = 0.7 \text{ mA/V}^2$ ,  $V_T = 1.3 \text{ V}$ .



\* ELLIOTT EXPERIMENTAL DUAL P-TYPE ENHANCEMENT M.O.S.

(g)

Fig. 3 (contd.) (e-g).



(f)

of the remaining four units shown in Fig. 1. The digital voltmeter is triggered periodically and the output recorded on paper tape. Each sample requires six characters in the format in use, and therefore a punch speed of 24 characters per second gives 4 samples per second and permits analysis of the spectrum up to 1 Hz.

### 3. Experimental Results

In this Section some results of current noise analyses for six matched pairs of m.o.s. transistors in the frequency range  $5 \times 10^{-5}$  to 1 Hz are presented.

Before each measurement the transistors were held at the required temperature and bias conditions for longer than the proposed integration time. In this way, drifts in the bridge output voltage during the measurements were reduced considerably from those experienced immediately after the application of bias. The remaining drift gave essentially a linear trend which was removed in the computation. The transistors were operated with zero resistance in the gate circuit, as shown in Fig. 1. The noise can then be represented by a single voltage generator in series with the gate of each transistor. It has been shown by Flinn *et al.*<sup>4</sup> that for low frequencies the value of this generator is independent of the external resistance

in the gate circuit, unless this exceeds about  $10^{10} \Omega$ . In other words, the equivalent noise current generator in parallel with the gate can be ignored, except in applications involving extremely high source resistances, and has not been measured in this work.

The results shown in Fig. 3 are given in terms of the square of the equivalent noise voltage at the gate for each transistor, calculated from one half of the noise power output measured for a pair of similar transistors. In every case the estimate of noise power has a standard error of 10%. The operating temperature of the transistors was 100°C for Fig. 3(f), and 40°C for the rest of the figures. A comparison of the spectra obtained at the two temperatures with similar bias conditions shows that within the accuracy of measurement the current noise exhibits no temperature dependence.

#### 4. Conclusions

The values plotted in the figures represent about one-tenth of the results we have obtained for m.o.s. transistors and we also have some results for junction field-effect transistors. Without exception the spectra obtained have been consistent with eqn. (1) throughout the frequency range investigated. The values of the frequency index  $\alpha$  obtained are invariably near to but greater than unity, with the majority between 1 and 1.2. The results are consistent with those obtained by other workers at higher frequencies.<sup>4-6</sup> A physical model will be proposed<sup>7</sup> to account for the variation from unity of the frequency index for m.o.s. transistors.

#### 5. Acknowledgments

The work described in this paper is part of a programme of research supported by the Atomic Energy Establishment at Winfrith Heath, and the

authors are grateful to Messrs. D. Harrison and E. P. Fowler of this Establishment for valuable discussions. Two of the authors (R.J.H. and I.R.M.M.) are indebted respectively to the Science Research Council and the United Arab Republic Atomic Energy Establishment for financial support.

Particular acknowledgment is due to Mr. M. Harknett who first made measurements of this type at Southampton University, and whose work<sup>8</sup> has since been developed by the present authors.

#### 6. References

1. I. R. M. Mansour, R. J. Hawkins and G. G. Bloodworth, 'Digital analysis of current noise at very low frequencies', *The Radio and Electronic Engineer*, **35**, No. 4, pp. 201-11, April 1968.
2. K. Barton, 'The f.e.t. used as a low level chopper', *Electronic Engng*, **37**, pp. 80-3, 1965.
3. G. G. Bloodworth and N. R. S. Nesbitt, 'Active filters operating below 1 Hz', *Trans. Inst. Elect. Electronics Engrs on Instrumentation and Measurement*, **IM-16**, pp. 115-20, 1967.
4. I. Flinn, G. Bew and F. Berz, 'Low frequency noise in m.o.s. field effect transistors', *Solid State Electronics*, **10**, pp. 833-45, 1967.
5. S. M. Bozic, 'Noise in the metal-oxide-semiconductor transistor', *Electronic Engng*, **38**, pp. 40-41, 1966.
6. M. Decker, L. Gonsov and D. Rigaud, 'Noise measurements in metal-oxide-semiconductor transistors below saturation', *Electronics Letters*, **3**, pp. 565-66, 1968.
7. I. R. M. Mansour, R. J. Hawkins and G. G. Bloodworth, 'Physical model for the current noise spectrum of m.o.s. transistors' (To be published.)
8. M. R. Harknett, 'The Measurement of Very Low Frequency Electrical Noise', M.Sc. Thesis, University of Southampton, 1966.

*Manuscript first received by the Institution on 18th December 1967 and in final form on 16th February 1968. (Paper No. 1181/CC3.)*

© The Institution of Electronic and Radio Engineers, 1968

# Measurements on Microcircuits in the range 100–1000 MHz

By

H. A. KEMHADJIAN,  
M.Sc.(Eng.), C.Eng., M.I.E.E.†

A. NEGANDHI, M.Sc., D.U.S.,†

AND

B. J. LEWIS, B.Sc.†

*Reprinted from the Proceedings of the Joint I.E.R.E.-I.E.E. Conference on 'R.F. Measurements and Standards' held at the National Physical Laboratory, Teddington, on 14th–16th November 1967.*

**Summary:** The paper outlines the problems associated with the measurement of microcircuit components, in the range 100–1000 MHz. Two experimental arrangements are described suitable for thin-film and integrated circuit components with an estimate of accuracy on typical components.

## 1. Introduction

The paper deals with methods of measurement of thin film and monolithic microcircuit components, at frequencies up to 1000 MHz. The results are to be used for microcircuit design and the accuracy aimed at is therefore of the order of component tolerances, say, 1–5%.

Table 1 gives typical dimensions of components in thin film and silicon monolithic form.

**Table 1**  
Typical dimensions of components in thin film and silicon monolithic circuits

Component	Thin film $\mu\text{m}$	Monolithic $\mu\text{m}$
2 k $\Omega$ resistor	250 × 250 × 0.1	500 × 25 × 5
100 pF capacitor	1000 × 1000 × 0.2	250 × 375 × 3
High-frequency transistor	—	100–200 between pads
Typical circuit area	20 000 × 30 000	1250 × 1250

The small size of the components highlights the principal difficulty, another one being that components are not manufactured individually but in circuit. In general, therefore, test pieces are needed, manufactured at the same time as a circuit, but with more accessible connections than would normally be available in circuit. Some transition is then needed from the small components to the size of normal sockets and connectors on measuring instruments.

Because of the frequency range of the measurements, transmission line methods of measurement seemed most appropriate and the specific instruments designed for were the two forms of Thurston Bridge<sup>1</sup> manufactured by General Radio (GR): the admittance meter Type 1602-B and transfer function bridge Type 1607-A. Admittance/impedance measurements

† Department of Electronics, University of Southampton.

can also be made using the General Radio Type 874-LBA slotted line which uses the same connectors. This extends the frequency range to 5000 MHz and provides a useful check at frequencies below 1000 MHz. It is of course not direct reading in admittance and so is less convenient to use.

Because of the small size of the components, microstrip lines seemed an obvious construction for the transition between components and the coaxial air line of the bridges.

Slightly different approaches were adopted for the thin film and monolithic circuit measurements, though in retrospect either might be adapted for the other measurement

## 2. Thin Film Circuits

The following three properties distinguish thin film circuits from integrated circuits:

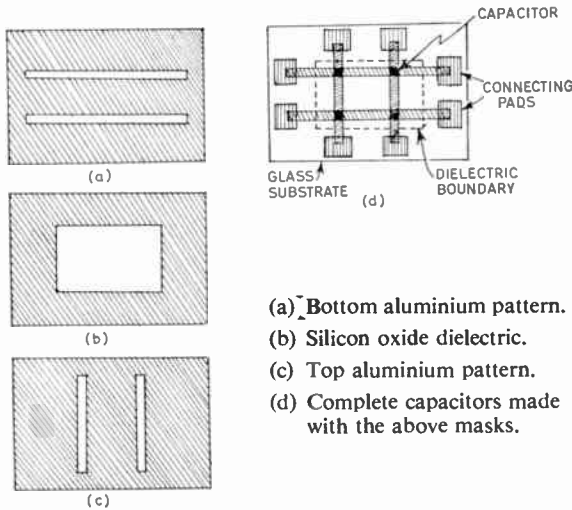
- (i) They are essentially two dimensional as opposed to three dimensional, the area always being much greater than the thickness.
- (ii) The overall circuit is usually many times larger.
- (iii) At the moment active devices have not reached a practical stage.

Passive components can have their properties accurately predicted from a knowledge of the capacitance or resistance per square and their dimensions. Thus, for example, the making of a suitable test piece for measurement is not restricted by the need for accurate non-linear scaling in three dimensions to preserve edge effects. This is not the case for integrated circuits which are discussed later. Hence, for thin film circuits the measurements required are of capacitance and resistance per unit area.

### 2.1. Measurement of Capacitance per Unit Area

A thin film capacitor is made by evaporating in turn a bottom electrode, a dielectric layer and a top

electrode. The most accurate construction for defining the area of the capacitor is to make the top and bottom electrodes in the form of strips of well defined width, crossing at right angles. The dielectric in between is made to overlap both strips so that the capacitor is then defined by the electrode widths and registration problems are avoided completely. Figure 1 shows such a capacitor. The strips also link the capacitors to suitable connecting pads.



(a) Bottom aluminium pattern.  
 (b) Silicon oxide dielectric.  
 (c) Top aluminium pattern.  
 (d) Complete capacitors made with the above masks.

Fig. 1. Molybdenum masks for capacitors.

For accurate measurements, lead inductance has to be eliminated or at least reduced to the point where resonance with the capacitor being measured is removed outside the frequency range of interest.

For a single connecting wire the inductance can be calculated from the formula:<sup>3</sup>

$$L_s = 2l \left( \ln \frac{4l}{d} - 1 \right) \text{ nH} \quad \dots\dots(1)$$

where  $l$  is length in cm  
 $d$  is diameter in cm

For  $l = 1$  and  $d = 0.0286$ ,  
 $L_s = 3.8 \text{ nH}$

In addition to this, there will be a minimum length of thin film electrode, for which:

$$L_s = 2l \left( \ln \frac{2l}{w+t} + 0.5 + 0.2235 \frac{w+t}{l} \right) \text{ nH} \dots\dots(2)$$

where  $w$  is the strip width in cm  
 and  $t$  is the strip thickness in cm  
 For  $l = 1$ ,  $w = 0.1$  and  $t = 3000 \text{ \AA}$ ,

$$L_s = 5.8 \text{ nH}$$

giving a total lead inductance of about 10 nH.

The aim of the measurements described is to investigate capacitors with dielectrics giving values of capacitance of 15–100 pF/mm<sup>2</sup>. Also 1 mm<sup>2</sup> was the smallest area which could be accurately reproduced with the available facilities, so that the range of capacitance to be measured is 15–100 pF.

The lead inductance of about 10 nH derived above will resonate with a 100 pF capacitor at about 160 MHz which is in the middle of the frequency range of interest. The apparent variation in capacitance and loss, produced by a lead inductance of 9.6 nH is shown in Fig. 2, and to avoid these effects it was decided to move the self-resonant frequency to well above 1 GHz.

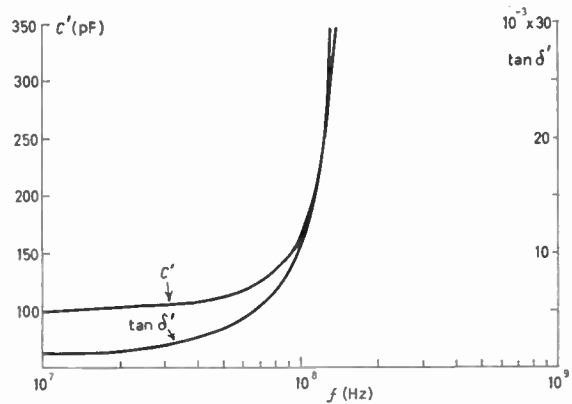


Fig. 2. Apparent capacitance and loss of 100 pF with a series inductance of 9.6 nH.

Since the capacitance range is fixed, a lower value of inductance was obtained by using the symmetrical arrangement shown in Fig. 3. The electrodes are now made up of a central disk and an outer annulus with the smallest possible overlap between them. Four breaks occur in the outer annulus because of the need to support the centre of the out-of-contact mask used to produce the capacitor. The set of masks is also shown in Fig. 3.

This arrangement also minimizes the series resistance, and fixes the electrical position of the component in the line very accurately, which is essential for the type of measurements being considered.

Assuming a dominant TEM mode in the coaxial line we can calculate the series inductance and resistance per unit area from the following formula:<sup>4</sup>

$$Z = R + j\omega L = (1 + j) \frac{\cosh xt}{\sinh xt} \quad \dots\dots(3)$$

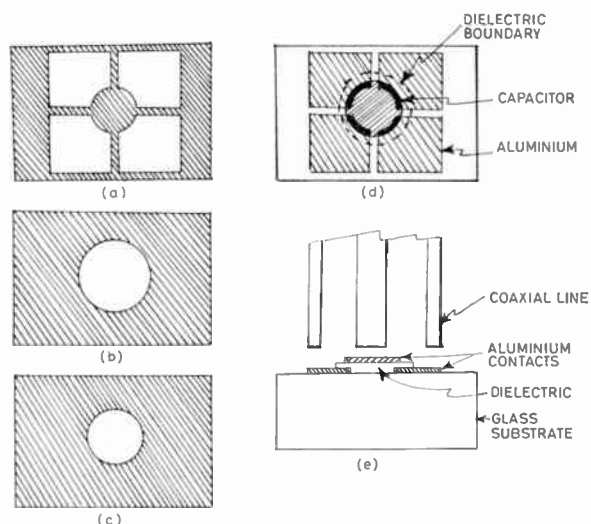


Fig. 3. Molybdenum masks for capacitor with reduced lead inductance and series resistance.

- (a) Bottom aluminium.
- (b) Silicon oxide.
- (c) Top aluminium.
- (d) Complete capacitor.
- (e) Cross-section through (d) showing contact with line.

where  $t$  = film thickness,

$\sigma$  = conductivity of the film,

$\mu$  = permeability of the film,

$f$  = frequency =  $\omega/2\pi$  and

$$x = (1+j)\sqrt{\pi f \mu \sigma} \quad \dots\dots(4)$$

All the above quantities are expressed in m.k.s. units.

Writing

$$\delta = \frac{1}{\sqrt{\pi f \mu \sigma}} = \text{skin depth}$$

we have resistance per square

$$R = \frac{1}{\sigma \delta} \frac{\sinh 2t/\delta + \sin 2t/\delta}{\cosh 2t/\delta - \cos 2t/\delta} \quad \dots\dots(5)$$

and reactance per square

$$\omega L = \frac{1}{\sigma \delta} \frac{\sinh 2t/\delta - \sin 2t/\delta}{\cosh 2t/\delta - \cos 2t/\delta} \quad \dots\dots(6)$$

For the coaxial geometry used we can determine the resistance of an annulus to be

$$R_s = \frac{1}{2\pi \sigma t} \ln \frac{R_2}{R_1} \quad \dots\dots(7)$$

where  $R_1, R_2$  represent respectively the radii of inner and outer conducting surfaces of the coaxial system. Also the characteristic impedance of a coaxial line is given by:

$$Z_o = \frac{\sqrt{\frac{\mu}{\epsilon}}}{2\pi} \ln \frac{R_2}{R_1} \quad \dots\dots(8)$$

and for an air dielectric line

$$\sqrt{\frac{\mu}{\epsilon}} = \sqrt{\frac{\mu_0}{\epsilon_0}} = 377$$

From eqns. (7) and (8) and by writing  $R$  for  $1/\sigma t$  = sheet resistance, we get

$$R_s = \frac{Z_o}{377} \times R \quad \dots\dots(9)$$

For the aluminium film used

$$\sigma = 3.72 \times 10^7 \Omega^{-1} \text{m}^{-1}$$

$$t = 3000 \text{ \AA}$$

$$R_s = 0.012 \text{ ohm}$$

and

$$L_s = 0.2 \text{ pH}$$

in the frequency range of interest.

Curves of calculated  $R_s$  and  $\omega L_s$  are shown in Fig. 4 with the reactance of 10 and 100 pF capacitors included for comparison. With 100 pF, resonance occurs first at  $3.8 \times 10^{10}$  Hz which satisfies the requirement for a high resonant frequency.

$R_s$  is seen to be constant at its low-frequency value up to about  $10^{11}$  Hz when skin effect becomes noticeable.

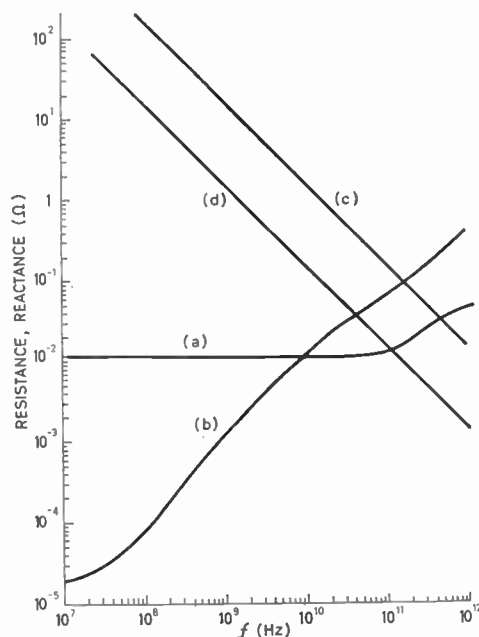


Fig. 4. Series resistance (a) and series reactance (b) of an aluminium annulus 3000 Å (300 nm) thick. (c) shows the reactance of 10 pF for comparison and (d) the reactance of 100 pF.

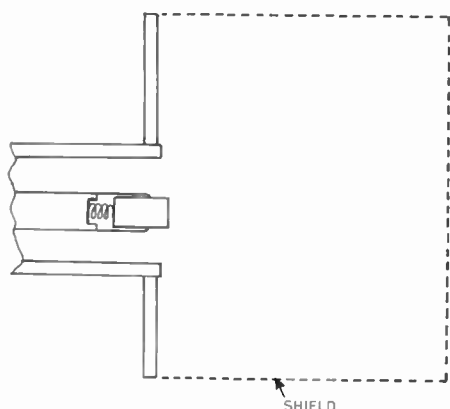


Fig. 5. Cross-section of modified General Radio component mount 874-ML.

Contact to the line is made via a spring-loaded centre conductor in an otherwise standard component mount. Figure 5 shows the arrangement diagrammatically. Adequate sliding contact is maintained between the plunger and the centre conductor.

The only disadvantage with the arrangement shown in Fig. 3(d) is that the capacitor area (in black) can no longer be easily determined. This is done by simultaneously fabricating a standard type capacitor of accurately known area and comparing the low-frequency (10 kHz, say) capacitance of the two structures.

Using the slotted line, the quality of the connections was tested. A short circuit was made by evaporating a continuous 3000 Å (300 nm) aluminium film over a slide and mounting it in the jig described. This was compared with a standard GR short-circuit and showed no significant difference. A further test was made by using the quadrant geometry shown in Fig. 3 (without dielectric), and a difference in series resistance of 0.065 Ω was measured compared to a GR short-circuit. A time domain reflectometer measurement gave a value of 0.05 ± 0.025 Ω. These values compare favourably with a d.c. value of 0.04 Ω.

### 2.2. Resistors

Film resistance can be measured in much the same arrangement except that in this case the outer annulus just fails to overlap the centre disk. The arrangement is shown in Fig. 6.

The resistor inter-electrode capacitance and substrate-loss were measured using an admittance meter, and Fig. 7 shows the results. The capacitance is negligible but the substrate-loss should be subtracted from measured values of high resistance films.

The geometry shown in Fig. 6 provides a 15.5 : 1 step-down in resistance value from the 'ohms/square'

value thus making possible the study of high resistivity cermet films with resistance up to 300 kΩ/square. Equation (7) shows that by making the inner and outer radii of the resistive annulus more nearly equal, greater step-down ratios from the ohms/square value can be obtained. This is only limited by the accuracy to which the aluminium electrodes can be kept concentric.

### 3. Measurement Accuracy

Since the essential characteristic being evaluated is usually the *Q*-factor or 'time-constant' of a component, for good components this implies a high ratio of reactance to resistance, or vice versa.

Special precautions are thus needed with the instruments being used—these are described in the appropriate instrument manuals provided by General Radio<sup>5</sup> and it will suffice merely to note the method being used. The comments relate to the measurements on a capacitor but obviously apply, in an analogous manner, to resistors.

#### 3.1. Admittance Measurement on GR Admittance Meter λ/2, λ/4 Line-lengths

The losses in capacitors made with standard dielectrics are usually small in the range of frequencies being considered. This means that with a typical value of capacitance, of 30 pF say, a much higher susceptance than conductance has to be measured. A special multiplier plate is therefore used which increases the coupling on the reactance loop compared to that for the resistance and multiplier loops. Impedance is measured up to 5 Ω (200 mΩ<sup>-1</sup>) and beyond that admittance measurement gives better accuracy—the procedure is outlined in the instrument manual.

If the straightforward procedure is used for measurement, the leakage between the resistance and

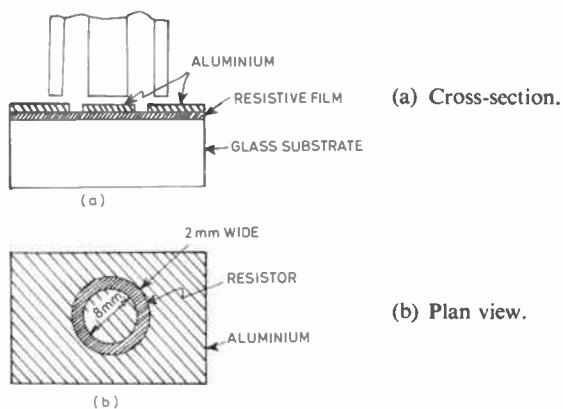


Fig. 6. Annular thin-film resistor.

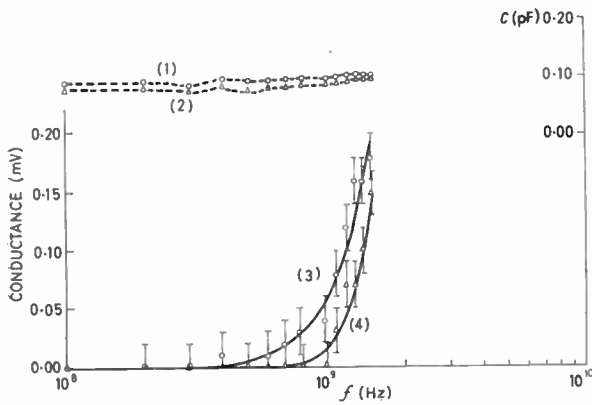


Fig. 7. Stray impedance across resistor electrodes.

- (1) Capacitance for 705a glass substrate.
- (2) Capacitance for quartz substrate.
- (3) Resistance for 705a glass.
- (4) Resistance for quartz.

reactance coupling loops is not negligible compared to the reduced coupling to the resistance loop.

The modified procedure outlined in the handbook is therefore used which involves:

- (a) balancing the line with the unknown ( $g + jb$ );
- (b) replacing the unknown with an open-circuit and a length of air line to give a balance, with the susceptance scale untouched, but varying the conductance scale ( $g' + jb$ ).

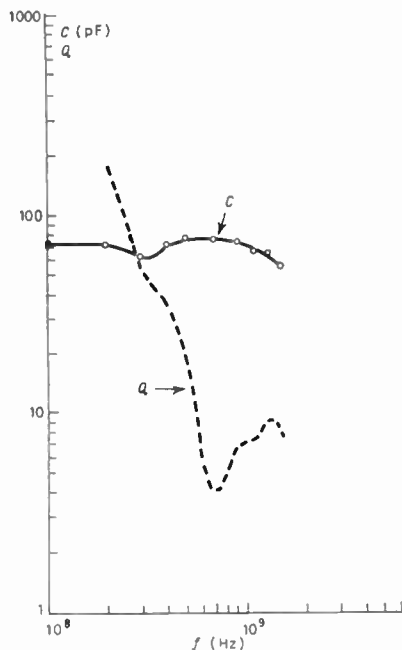


Fig. 8. Typical thin-film capacitor measured on admittance meter.

The true conductance is now  $g - g'$ . Typical values of  $g$  and  $g'$  for the capacitors described are  $5.6$  and  $4.6 \text{ m}\Omega^{-1} \pm 0.1 \text{ m}\Omega^{-1}$  with a susceptance of about  $j200 \text{ m}\Omega^{-1}$  at  $1000 \text{ MHz}$ . With the accuracy of  $\pm 0.1 \text{ m}\Omega^{-1}$  on each measurement we are limited to an accuracy of  $\pm 2\%$  for a susceptance/conductance ratio of  $200$ .

This effectively sets the limit of accuracy of a component of given  $Q$ -factor. A typical measurement on a capacitor is shown in Fig. 8.

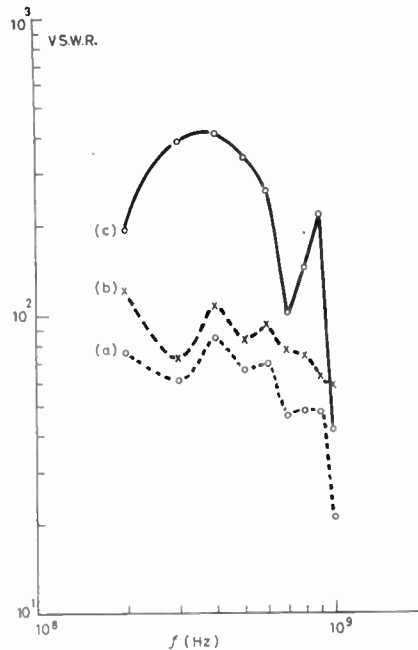


Fig. 9. Resistor v.s.w.r. measured on slotted line.

- (a) Resistor as measured.
- (b) Open-circuited line.
- (c) Corrected curve from (a) and (b).

### 3.2. Slotted Line

This provides accurate two-terminal measurements over a wide frequency range.

The method adopted was the standard one for high v.s.w.r. using the 3 dB up from minimum method.<sup>6,7</sup> A GR Type DNT detector was used on the probe. The arrangement is fully described in the GR instrument manual and in the literature.

Two precautions were found necessary:

- (a) For capacitor measurements the full expression involving line losses must be used. The v.s.w.r. of the line with a standard GR open circuit is shown in Fig. 9. Results of measurements on short-circuited and open-circuited lines at  $1 \text{ GHz}$ , are also given in Tables 2 and 3 for slotted line and admittance bridge measure-

ments. The effect of taking this into account in determining overall v.s.w.r. is shown in Fig. 9. For capacitor loss measurements,  $0.1 \text{ m}\Omega^{-1}$  can be subtracted from the conductance value measured.

- (b) For resistance measurements it is desirable to compare the v.s.w.r. of the unknown with that of a standard high quality  $50 \Omega$  load. This smooths out effects of residual line v.s.w.r. due to connectors and other minor discontinuities. Figure 10 shows a plot of corrected resistance readings against frequency.

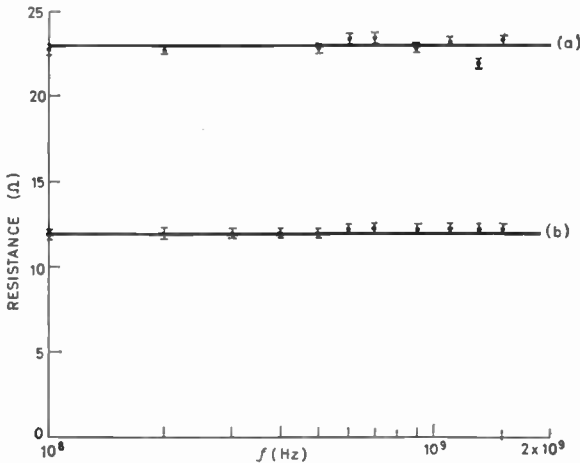


Fig. 10. Typical cermet resistors measured on admittance meter. Solid lines show d.c. values. (a), (b) correspond to different chromium/silicon-oxide ratios.

For admittances near  $20 \text{ m}\Omega^{-1}$  therefore the Thurston bridge<sup>1</sup> is preferable to the slotted line, whereas the slotted line is useful for measuring large values of v.s.w.r. and generally for measurements at frequencies beyond 1 GHz.

#### 4. Silicon Monolithic Circuits

The particular problem with these components is their three-dimensional nature. Transistors are now being made with lateral dimensions of the same order of magnitude as the depth of diffusion. This makes scaling virtually impossible, as the boundaries of the device in the silicon do not have a simple geometry.

A second problem arises in the measurement of transfer parameters, where two accurate  $50 \Omega$  lines have to be brought down to an area of about  $0.25 \text{ mm} \times 0.25 \text{ mm}$  and kept well shielded from each other. This gives rise to a number of mechanical problems, some of which can only be solved by compromising electrical characteristics.

The jig described here was designed to provide a transition between a silicon chip and the GR transfer-function bridge 1607-A while allowing the full facilities of the bridge to be used.

Standard encapsulations for monolithic circuits, either flat-pack type or TO-5 cans, have a number of ill-defined discontinuities between external leads and components:

- (i) at the glass to metal seal where, apart from variable geometry, discontinuities occur in plating applied to the leads;

Table 2  
Line with GR open-circuit,  $f = 1 \text{ GHz}$

GR bead	$G_x$ u.h.f. bridge	$B_x$ u.h.f. bridge	$G_x$ slotted line	$E_{\text{max}}/E_{\text{min}}$	v.s.w.r. 3 dB method
P.T.F.E.	$0.16 \pm 0.01$	0.00	$0.0914 \pm 0.005$	$219 \pm 10$	$238 \pm 12$
Polystyrene: Opaque	$0.10 \pm 0.01$	0.16	$0.0904 \pm 0.005$	$221 \pm 10$	$238 \pm 12$
Transparent	$0.10 \pm 0.01$	0.16	$0.0924 \pm 0.005$	$216 \pm 10$	$233 \pm 12$

Table 3  
Line with GR short-circuit,  $f = 1 \text{ GHz}$

GR bead	$R_x$ u.h.f. bridge	$X_x$ u.h.f. bridge	$R_x$ slotted line	$E_{\text{max}}/E_{\text{min}}$	v.s.w.r. 3 dB method
P.T.F.E.	$0.12 \pm 0.01$	0.00 standard	$0.151 \pm 0.005$	$331 \pm 20$	$318 \pm 20$
Polystyrene: Opaque	$0.11 \pm 0.01$	$0.09 \pm 0.01$	$0.160 \pm 0.005$	$313 \pm 20$	$298 \pm 20$
Transparent	$0.11 \pm 0.01$	$0.13 \pm 0.01$	$0.157 \pm 0.005$	$319 \pm 20$	$298 \pm 20$

- (ii) at the junction between the connecting 'post' and the fine wire used to connect to the component pad.

In general, no provision is made for connections to individual components. This means that test chips are practically essential for component investigations and these need to be specially produced (though at the same time as a normal production run).

In view of the above points it was decided to design the jig assuming that test chips could be connected to special blanks, and wire connection to the lines could then be made with the chip mounted on the jig. This requires the use of a chip bonder and wire-bonder but the measurement problem is greatly simplified.

#### 4.1. Design of Line

Micro-stripline seemed the obvious choice for the transition to the connectors of the measuring bridge. Because of the size problem the following characteristics were thought desirable:

- (i) low losses in thin sheet form,
- (ii) mechanical strength,
- (iii) dimensional stability and
- (iv) resistance to heat because of the need to bond wires to the end of the line.

'Kapton' Polyimide film was obtained which met most of the above requirements and is available in thicknesses 0.025 mm, 0.050 mm, 0.075 mm and 0.125 mm (0.001, 0.002, 0.003 and 0.005 in).

The electrical properties, shown in Fig. 11, were obtained by making a sample capacitor to fit on the thin film component jig described in the previous section. The dielectric constant is seen to be reasonably constant over the range of frequencies and the loss factor is just beginning to become significant at the higher frequencies.

A jig was then designed to connect the two lines on the transfer bridge to the chip, with striplines

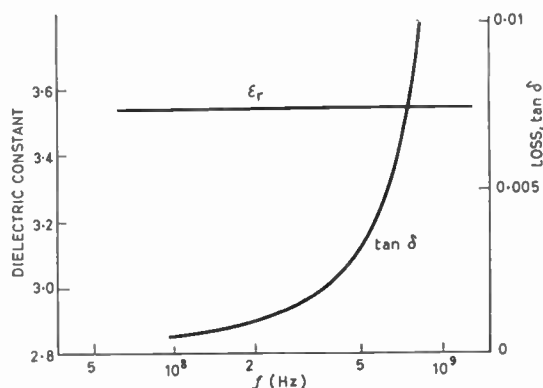


Fig. 11. Properties of polyimide film.

separated along their length by an earth plane. Figure 12 shows the layout of the jig.

The width of the centre strip for a triplate microstrip line—with 0.125 mm dielectric was found from standard charts<sup>8</sup> to be approximately 0.175 mm;

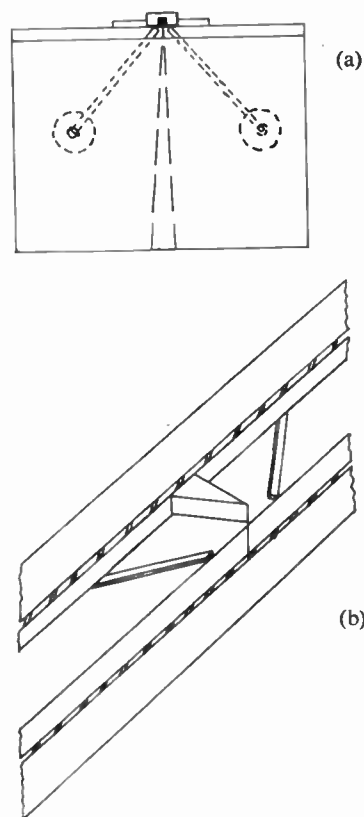


Fig. 12.

- (a) Plan view of jig, showing the two striplines, and their coaxial feed and isolation centre earth plane.
- (b) Close-up of stripline ends for connection to integrated circuits.

the thickness of the strip is 0.025 mm. The line was formed by laying a gold ribbon of appropriate dimensions between the two layers of dielectric sheet and clamping the arrangement between thick brass plates. Transition from microstrip to coaxial line was arranged by means of miniature 'Sealectro' plugs type no. 50-056-2211 making a pressure contact on the line. A appropriate adaptor is then used to connect to standard 874 type connectors.

The equivalent electrical length of each line was 6.1 cm and the line impedance was found by measuring the open- and short-circuit impedance using the formula:

$$Z_0 = \sqrt{Z_{oc} \times Z_{sc}}$$

Thus  $Z_0$  was 53.5 ohms.

End effects on the line were negligible because of the small dimensions and shielded construction, so that either an open-circuit or short-circuit reference condition can be reliably set up at the end of the line.

4.2. Connection to Chip

The test chips are bonded to either a specially prepared blank or a standard flat-pack with the leads on one side removed. Annealed gold wire is then used to make thermo-compression connections between component pads and lines. Taking a typical length of connecting wire of 1.5 mm the self inductance can be calculated from eqn. (1) giving

$$L_s = 1.37 \text{ nH for } 0.025 \text{ mm (0.001 in) diameter wire}$$

or

$$0.9 \text{ nH for } 0.125 \text{ mm (0.005 in) diameter wire}$$

This is a relatively high value for the measurements being considered and lengths of wire were therefore measured to see how reproducible the inductance was. Figure 13 shows a curve of inductance against length of 0.025 mm diameter wire measured at 900 MHz. The vertical bars indicate the spread on individual values for measurements using the slotted line.

Figure 14 shows curves for a nominal 100 Ω resistor as measured and with the correction for lead-length.

A slight improvement in the series inductance can be obtained if the gold ribbon forming the centre conductor is brought out over the chip and used to make the connection. Assuming the 50 Ω line ends at the same place as before the series inductance is calculated from eqn. (2). For 1.5 mm of 0.175 mm × 0.025 mm ribbon, the self-inductance  $L_s$  is 1 nH.

Calculations to correct for lead inductance are very tedious except in the case of high- $Q$  components.

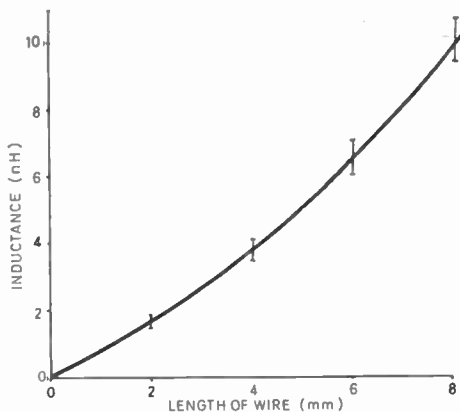


Fig. 13. Inductance of 0.025 mm (0.001 in) diameter gold wire. ( $f = 900 \text{ MHz}$ .)

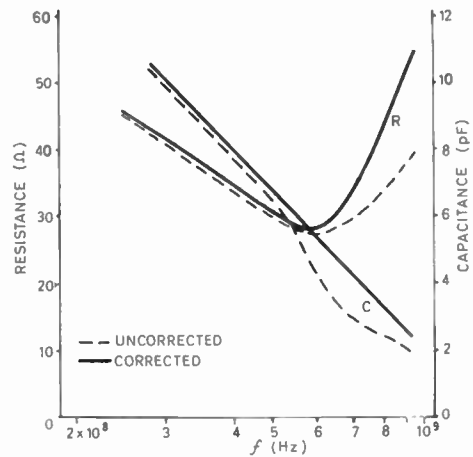


Fig. 14. The behaviour of an integrated circuit resistor at u.h.f. (nominally 100 Ω).

This is further aggravated by the fact that semiconductor components are themselves ‘distributed’ and therefore frequency sensitive.

The Appendix shows the relationship between measured susceptance and resistance, as modified by series inductance, and the true values. Figures 15 and 16 show the way in which the error varies with susceptance/resistance ratio and measuring/self resonant frequency. The self-resonant frequency is defined as:

$$f_r = \frac{1}{2\pi\sqrt{L_s C}}$$

where  $C$  is the capacitance to be measured.

4.3. Improvements to Above System

The above results show that it is desirable to reduce the series inductance by at least an order of magnitude. A way of doing this is shown in Fig. 17 using a uniline construction. The line dimensions can again be obtained from charts,<sup>9,10</sup> and for a 50 Ω line with 0.075 mm dielectric the line-width is about 0.25 mm. Pressure contact is made to the pads of the component and the length of the strip is now accurately defined by the length of the component. For a typical strip length of 0.25 mm with a 0.25 mm × 0.025 mm strip we have a value of  $L_s = 0.124 \text{ nH}$  which is an improvement by a factor of 8.

For even greater improvements it would be necessary to evaporate a uniline directly on the silicon to make connection to the component. This is described by Hylltin<sup>11</sup> together with suitable transition to go from stripline to coaxial system.

5. Acknowledgments

Part of the work described in this contribution was financed by a Ministry of Technology contract. The

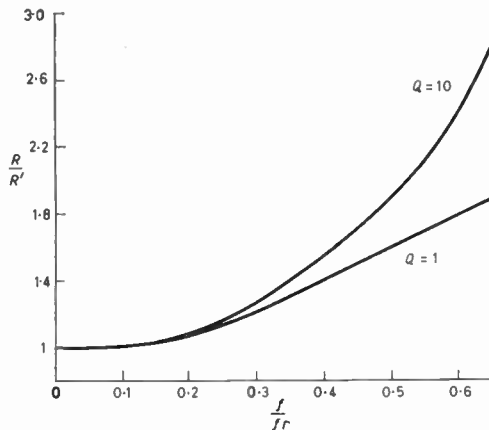


Fig. 15. Variation of measured and corrected resistances with frequency and Q factor.

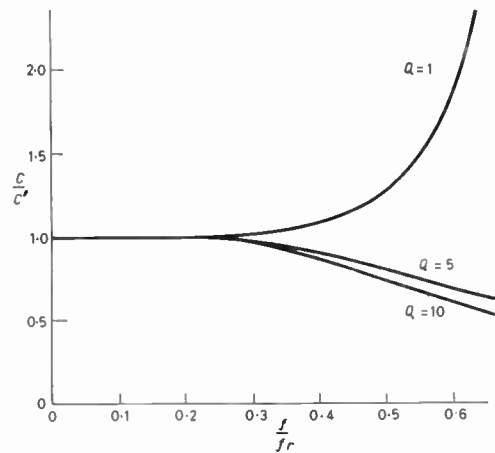


Fig. 16. Variation of measured and corrected capacitances with frequency and Q factor.

help received in this connection from members of A.S.W.E. is gratefully acknowledged, as is the direction of this part of the work by our colleague Mr. G. G. Bloodworth. Two of the authors (H.A.K. and B.J.L.) gratefully acknowledge the financial support of the Science Research Council for the work on monolithic circuits. They would also like to thank their colleague Mr. R. D. Stewart for many useful discussions.

6. References

1. W. R. Thurston, 'A direct-reading impedance measuring instrument for the v.h.f. range', *General Radio Experimenter*, 24, No. 12, May 1950.
2. R. A. Soderman, 'Improved accuracy and convenience with type 1602-B admittance meter in v.h.f. and u.h.f. bands', *General Radio Experimenter*, 28, No. 3, August 1953.
3. A. Hund, 'High Frequency Measurements', p. 233, (McGraw Hill, New York, 1933).
4. S. Ramo, J. R. Whinnery and Theodore van Duzer, 'Fields and Waves in Communication Electronics', p. 288 and p. 298, (John Wiley, London, 1965).
5. General Radio Manual for type 1602-B Admittance Meter.
6. E. Ginzton, 'Microwave Measurements', p. 266, (McGraw Hill, New York, 1957).
7. General Radio Manual for type 874-LBA Slotted Line.
8. 'Microwave Engineers' Handbook', (Horizon House, London, 1964).
9. J. Swift, 'Strip transmission lines', *Electronic Engng*, 39, No. 474, pp. 490-3, August 1967.
10. M. Caulton, J. Hughes and H. Sobol, 'Measurements on the properties of microstrip transmission lines for microwave integrated circuits', *RCA Rev.*, 27, No. 3, pp. 377-91, September 1966.
11. T. M. Hyltin, 'Microstrip transmission on semiconductor dielectrics', *Trans. Inst. Elect. Electronics Engrs on Microwave Theory and Techniques*, MTT-13, No. 6, pp. 777-80, November 1965.

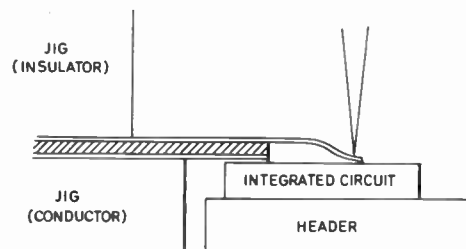


Fig. 17. Uniline jig with evaporated earth plane on polyimide film (shaded) and pressure contact of line to the integrated circuit.

7. Appendix

Referring to Fig. 18,

$$\begin{aligned} \text{measured admittance} &= \frac{1}{R'} + j\omega C' \\ &= \frac{1 + j\omega CR}{R(1 - \omega^2 LC) + j\omega L} \end{aligned}$$

Therefore,

$$\frac{1}{R'} = \frac{R}{R^2(1 - \omega^2 LC)^2 + \omega^2 L^2}$$

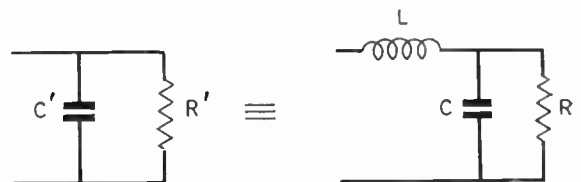


Fig. 18. Equivalent circuit connection of leads to chip.

and

$$\omega C' = \frac{\omega CR^2(1 - \omega^2 CL) - \omega L}{R^2(1 - \omega^2 CL)^2 + \omega^2 L^2}$$

Writing

$$\omega_r^2 = 1/LC, \quad \frac{\omega}{\omega_r} = p, \quad \text{and} \quad \omega CR = Q$$

it can be seen that

$$\frac{R}{R'} = \frac{1}{(1 - p^2)^2 + p^4/Q^2}$$

and

$$\frac{C}{C'} = \frac{(1 - p^2)^2 + p^4/Q^2}{(1 - p^2) - p^2/Q^2}$$

These ratios are plotted against  $p$  in Figs. 15 and 16 for values of  $Q$  of 1 and 10. For  $Q < 1$  it would probably be easier to measure impedance in the first place and then do similar transformations to the parallel combination which exists physically. For  $Q > 10$  the expressions are considerably simpler.

*Manuscript received by the Institution on 18th September 1967. (Paper No. 1182/CC4.)*

© The Institution of Electronic and Radio Engineers, 1968

## World Federation of Engineering Organizations

As reported in the November 1967 issue of *The Radio and Electronic Engineer*, plans for a world-wide Federation of Engineering Organizations are now being realized. An inaugural meeting, with U.N.E.S.C.O. support, was held in Paris from 4th to 7th March.

At this meeting 120 representatives of the engineering profession in 60 countries and of four regional federations of engineering societies agreed unanimously to form a World Federation of Engineering Organizations. This meeting was followed by the First General Assembly of the Federation.

Dr. Eric Choisy, an eminent Swiss engineer, was elected first President. M. R. Gibrat, a Past-President of the Société des Ingénieurs Civils de France, was elected Vice-President; and Dr. G. F. Gainsborough, Secretary of the Institution of Electrical Engineers in the United Kingdom, was appointed Secretary General.

The Federation comprises National Members, representing the engineering profession in the participating countries, and International Members, which

represent existing regional federations of engineering societies. Its aims are to advance engineering as a profession in the interests of the world community; to foster co-operation between engineering organizations throughout the world, and to undertake special projects by co-operation between member organizations and other international bodies.

Decisions were taken at the General Assembly to carry out programmes of work on the qualification and continuing development of professional engineers and of their technical supporting staff; and on the promotion of a world-wide system of information dissemination and retrieval in the engineering field. Arrangements were also made to draw up a world-wide code of professional conduct for engineers. Other matters discussed included the role of professional engineering societies in public affairs, and the role of the engineer in assisting developing countries.

The next General Assembly of the World Federation of Engineering Organizations will be held in Beirut in October 1969.

# Noise Source Calibration in the Decimetre Band

By

G. J. HALFORD†

AND

E. G. ROBUST†

*Reprinted from the Proceedings of the Joint I.E.R.E.-I.E.E. Conference on 'R.F. Measurements and Standards', held at the National Physical Laboratory, Teddington, on 14th-16th November 1967.*

**Summary:** This paper discusses the problems involved in the design of noise comparators and standards for the frequency range 300–3000 MHz. The problems are illustrated by reference to an existing noise comparator built for the frequency range 300–1000 MHz, and to an experimental system for the range 1–2 GHz. Thermal noise standards are considered with reference to an existing 1000°C coaxial design, employed at the lower frequencies. A projected 400°C model, more suitable for the higher frequencies, is also discussed. Experimental results are given for the calibration of various types of broadband coaxial noise sources, demonstrating the need for accurate calibration facilities.

## 1. Introduction

The measurement of noise factor or noise temperature is of prime importance in the design and maintenance of receivers.

Its measurement has brought about the use of three types of noise generators in the range of frequencies to be discussed, namely, 0.3–3.0 GHz.

Temperature limited noise diodes are the most versatile of these. Their noise output varies linearly with current, and can be adjusted over the range from ambient temperature up to at least 6000°K (at 20 mA). However, it is usually necessary to make corrections at frequencies above 300 MHz to account for resonance and transit-time effects. These corrections become increasingly large and uncertain at higher frequencies, and diodes are seldom used above 1.5 GHz.

Gas discharge noise sources, normally employing a helical coaxial line surrounding the plasma, are available throughout the frequency range. They are, in general, less well matched than the diodes and have only two output levels, corresponding to on and off, i.e. ambient temperature and about 11 000°K for argon. The latter figure varies with gas pressure, tube radius, operating current and circuit losses and must be determined by calibration.

Finally, there exist thermal noise sources, i.e. resistive terminations raised or lowered to known temperatures. These can be well matched, but provide only a single level of output. Cold terminations, operated at the boiling point of a liquefied gas, are invaluable for the measurement of very low noise receivers. Hot terminations, with controlled electric heating, are mainly used as calibration standards in the range up to 1000°C. In both cases, temperature gradients caused by connection to apparatus at

ambient temperature involve corrections which are not always adequately known.

There is thus a need to compare and calibrate noise sources of each type throughout the frequency range in order to provide an accurate basis for noise measurements on receivers. It is the object of the present paper to describe noise comparators designed for this purpose, together with the thermal standards involved.

## 2. Noise Comparators

Before discussing the type of comparators adopted it is useful to review the general principles involved.

A comparator for comparing two noise sources is shown in its simplest form, in Fig. 1. It consists of a switch and a receiver with a power output indicator, e.g. a meter measuring the current from a square-law detector.

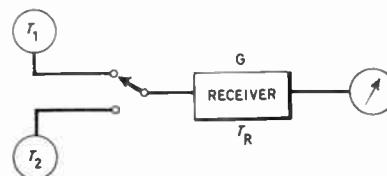


Fig. 1. Simple noise comparator.

If  $O_1$  and  $O_2$  are the output levels corresponding to the switch being connected in turn to sources at temperatures  $T_1$  and  $T_2$ , then

$$\frac{G(T_1 + T_R)}{G(T_2 + T_R)} = \frac{O_1}{O_2}$$

where  $G$  and  $T_R$  are the receiver gain and noise temperature respectively.

It will be noted that this measurement depends on the receiver being linear, and on its gain and noise temperature remaining constant.

† Services Valve Test Laboratory, Haslemere, Surrey.

Furthermore, unless one of the sources is adjustable so that  $O_1$  and  $O_2$  can be equalized, an additional measurement using a third known temperature  $T_3$  is necessary in order to eliminate  $T_R$ .

Because of the nature of noise there will be random fluctuations of the receiver outputs having r.m.s. values corresponding to noise temperatures of

$$\frac{a(T_1 + T_R)}{\sqrt{B\tau}} \quad \text{and} \quad \frac{a(T_2 + T_R)}{\sqrt{B\tau}}$$

respectively, where  $B$  is the receiver input bandwidth,  $\tau$  is the post-detection integration time-constant, and  $a$  is a constant, of value unity in this case.<sup>1</sup> These fluctuations limit the accuracy obtainable to a similar order.

Once  $T_R$  and  $B$  have been fixed by the choice of receiver, increase in  $\tau$  is the only practical means of increasing the accuracy of measurement. However, this increases the time of measurement, so that variations of  $G$  and  $T_R$  become more important and set a limit to the improvement possible.

It was for this reason, coupled with its elimination of  $T_R$  from the calculations, that Dicke<sup>2</sup> introduced the switched radiometer. This system uses a rapidly acting switch to alternate the sources continuously, with a phase sensitive detector for measuring the resulting modulation. The constant  $a$  now has the value 2 or greater<sup>1</sup> since  $T_1$  and  $T_2$  are each viewed for only half the total time. However, for the same total time of measurement, the time-constant  $\tau$  can be twice the value used with the simple receiver viewing first  $T_1$  and then  $T_2$ , so that the Dicke receiver (provided its zero is stable) is not necessarily less sensitive by a factor greater than  $\sqrt{2}$ . Its great advantage is that the time of measurement can now be extended very considerably, to an even greater extent than in most radio astronomy applications.

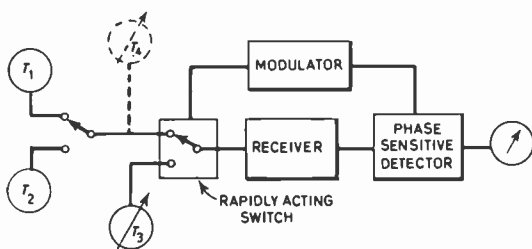


Fig. 2. Switched radiometer-type noise comparator.

A Dicke-type receiver can be made even less sensitive to gain variations if the compared sources are equal,<sup>1,3</sup> so that a null-balance is obtained. This consideration leads to the noise comparator circuit of Fig. 2. Because it is difficult to design a rapidly-acting

switch, either mechanical or electronic, which has equality of v.s.w.r. and insertion loss in the two arms, it is convenient to retain the original switch so that the compared sources ( $T_1$  and  $T_2$ ) operate under the same conditions. This system has the additional advantage that two sources of fixed temperatures  $T_1$  and  $T_2$  can be compared in terms of the corresponding settings of the variable balancing source  $T_3$ .

It will be evident that the temperatures  $T_1$ ,  $T_2$  and  $T_3$  must all be greater, or all less, than ambient. Normally, sources above ambient will be compared. However, by introducing an additional known amount of noise from a compensating noise source  $T_4$ , the output from a cooled termination at temperature  $T_1$  can be raised to ambient temperature or above, and so can be measured with the same system.

Another consideration of importance relates to matching. The accuracy of comparison of two sources is affected by reflection losses, or by any change of receiver noise temperature caused by differing impedances of the two sources.

Preferably, a noise generator should be calibrated in terms of equivalent available power,<sup>4</sup> i.e. the power delivered into a perfectly matched load, so that the comparator receiver should be matched to the nominal impedance of the noise source. On the other hand, a thermal noise source is an absolute standard primarily in terms of available power, so that the receiver should be conjugately matched to it.

The above requirements are conflicting, and the weight given to each must depend on circumstances. Since practical difficulties, plus the bandwidth involved, limit the degree of match obtainable, the uncertainties which depend on the product of noise source and receiver reflection coefficients, are minimized by matching both as closely as possible to their normal impedances. This will result in a noise source being calibrated in terms of available power. However, a single measurement of v.s.w.r. can be made to obtain the equivalent available power. In fact, provided v.s.w.r. is better than 0.95, the two powers are the same to within 0.003 dB.

Obviously, any matching apparatus used for the noise source must not introduce errors due to insertion loss. These can be minimized by using similar units in front of each noise source, and by designing them for low and constant loss.

### 3. Noise Comparator for 0.3-1.0 GHz

Early in 1961 it was decided to build a noise comparator capable of operation over the complete range of 0.3-1.0 GHz.

There was little previous experience available in this frequency band, or on wideband comparators in general. Smith<sup>5</sup> had designed coaxial radiometer

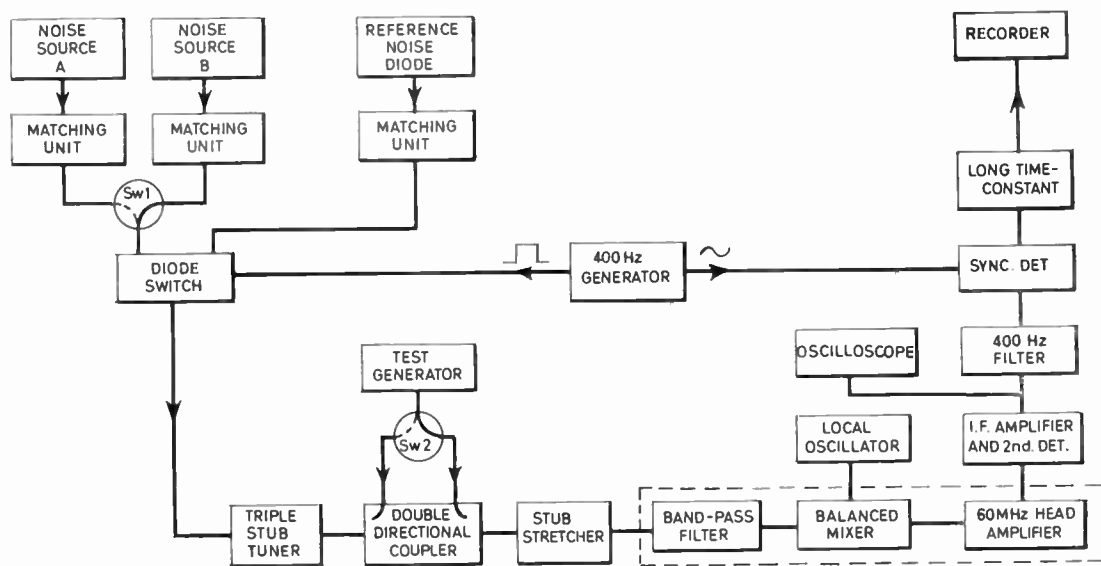


Fig. 3. Noise comparator for 0.3-1.0 GHz.

systems at various discrete frequencies up to 408 MHz. These incorporated narrow-band diode switches, usually in hybrid-ring circuits constructed from lengths of cable. A particularly valuable feature of some of Smith's circuits was that the electronic switching could also be used to match the compared sources to a high degree of accuracy.

At higher frequencies, using waveguides, considerably more work had been done. In particular, at the National Bureau of Standards in America a noise comparator had been built<sup>6</sup> covering the whole of X-band. This employed a radiometer circuit similar to that of Fig. 2, except that a calibrated attenuator was used in the common path of  $T_1$  and  $T_2$  to balance each in turn against the reference temperature  $T_3$ . Switching was performed by two rotary vane attenuators maintained in continuous rotation. Matching problems in this equipment were less severe because of the availability of good broad-band isolators.

At the authors' laboratory a design was being developed for an i.f. switched radiometer which eliminated the need for an r.f. switch.<sup>7</sup> This would not, however, have provided the required facility for accurate matching. Hence the decision was taken to design an r.f. diode-switch capable of operation over the complete frequency band. This could then be used in a system which combined the advantages of other systems mentioned above.

The equipment, as completed in its final form in 1963, is shown diagrammatically in Fig. 3. It basically follows Fig. 2 with the addition of a test generator for matching purposes. The matching problem was

particularly serious because of the non-availability of isolators, together with the necessity for using a crystal mixer receiver. Any unbalance in match between the two compared sources could result in unequal power transfer to the receiver, to modulation of the receiver noise temperature, and to modulation of the local oscillator power level. These first two effects could occur at both signal and image frequencies.

Whilst a filter could be used to provide additional isolation at local oscillator and image frequencies, calculations showed that the two sources had to be identical to  $\pm 0.001$  in reflection coefficient at the signal frequency. Fortunately the radiometer-type receiver was well adapted to doing this as will be explained later.

An associated problem which soon became apparent was that type GR 874 and type N connectors used in this equipment were insufficiently rigid or constant in impedance and insertion loss, even when used with solid coaxial line rather than cable. It was accordingly necessary for the whole of the front end of the equipment, including the diode switch, to embody the precision  $\frac{3}{4}$ -inch line and 50  $\Omega$  coaxial connectors developed by Woods<sup>8</sup> at the Electrical Inspection Department (E.I.D.) of the Ministry of Aviation.

Beyond the diode switch the system was balanced as far as the 400 Hz switching frequency was concerned, and commercially available components with type N connectors and solid coaxial line could be employed.

The diode switch, Fig. 4, was designed to employ an experimental type of p-i-n diode developed by Associated Electrical Industries, Rugby. The use of

diodes in series with the inner conductor provided basically a broadband design. However, the requirements of rigidity and of providing d.c. returns to the diodes led to the addition of  $\lambda/4$  tunable stubs at the input and output terminals of the switch.

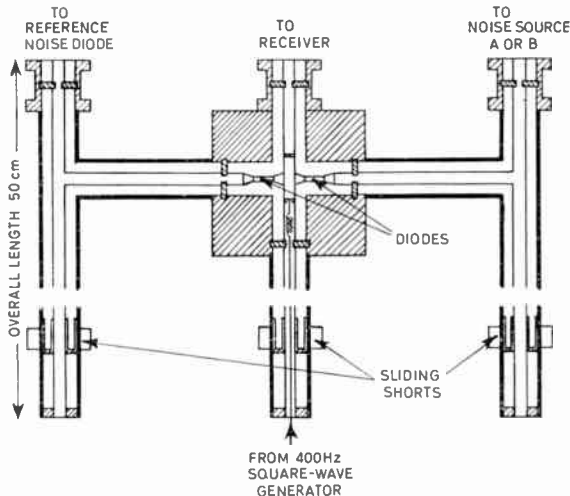


Fig. 4. Diode switch.

These stubs could be set up at each operating frequency, and they improved the overall match of the switch. The common-arm was isolated at the switching frequencies by small capacitors built into the inner conductor. It was fed by a 400 Hz square-wave generator through a large capacitor, thus equalizing the currents through the two diodes.

The manually-operated switch Sw 1 of Fig. 3 should ideally be perfectly matched, and have constant, equal and very low insertion loss in both arms. There was no design of switch available which approached the required standard of performance. However, the E.I.D. connectors themselves possessed the necessary properties. Hence, it was arranged to mount the noise sources and their associated matching sections vertically on opposite sides of a vertical pillar. The pillar could be raised to disengage the connectors, and rotated to bring either noise source in position above the right-hand arm of the diode switch. When lowered, contact pressure between the connector flanges was provided by the weight of the assembly. The arrangement can be seen in Fig. 5. The reference noise diode, of the E.I.D. type<sup>9</sup> is on the extreme left, whilst the two compared sources are a Rohde and Schwarz noise diode, centre, and a prototype 1000°C thermal standard, on the right. The diode switch is mounted below the base-plate: its common arm can be seen tapering to a type N connector and triple-stub-matcher.

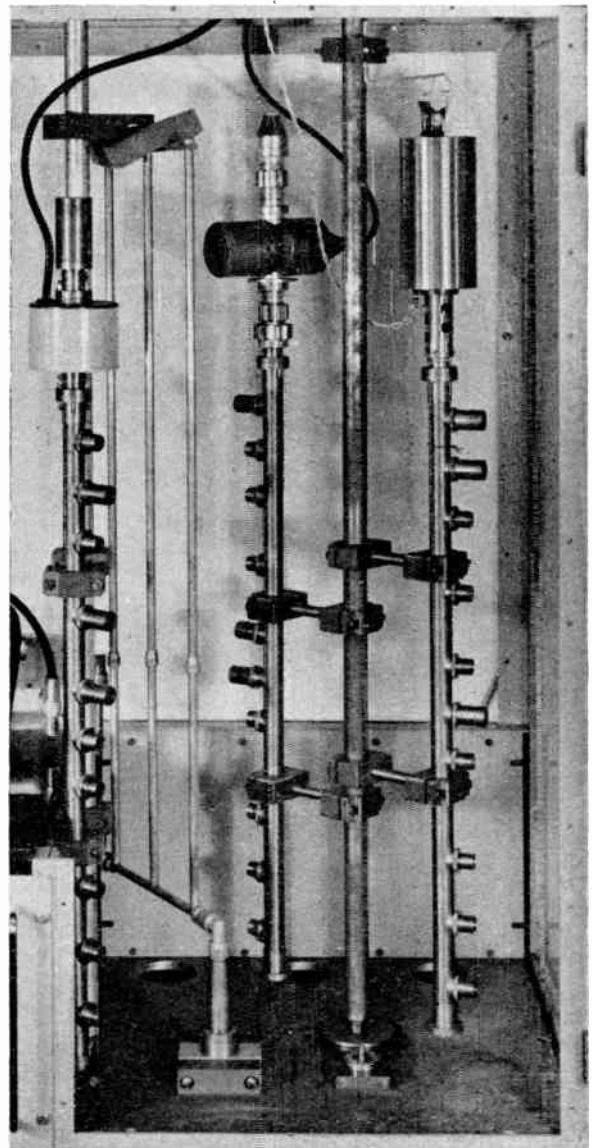


Fig. 5. Noise comparator for 0.3-1.0 GHz-manual switch and matching units.

The long vertical sections of coaxial line constitute the matching units. Quartz rods can be screwed into these lines at ten different positions to provide capacitive mismatches cancelling out the relatively small mismatches of the noise sources. The length of the units is explained by their being designed to operate at frequencies as low as 200 MHz. These units provide low-loss finely-adjustable and stable matching of a standard unobtainable with the conventional stub-tuner.

The remainder of the r.f. system beyond the triple-stub-tuner included a dual directional coupler for inserting matching signals, and a stub-stretcher

providing complete matching adjustments for the following filter and balanced-mixer.

For the signal-frequency filter a series of four-stage fixed tuned filters were obtained, spaced at 100 MHz intervals, and each of 60 MHz bandwidth. Since an intermediate frequency of 60 MHz was used, these provided at least 20 dB and 45 dB of attenuation at local oscillator and image frequency respectively. These filters, and the two balanced mixers of 250–500 and 500–1000 MHz respectively, were the only items of the system not covering the full bandwidth.

All the r.f. components were mounted in a metal framework with perspex sides and doors. An air-stirring fan and heater provided rudimentary temperature control.

The receiver units were mounted in a separate rack. The main i.f. amplifier had switchable bandwidths, giving 7, 12 or 24 MHz overall. An oscilloscope was provided to monitor the detected output; this, with its instantaneous response was employed to indicate balance during the matching procedure. For indication of noise balance, the video signal, after passage through a 400 Hz one-third octave filter, was converted to a d.c. signal in a phase sensitive detector. Further smoothing was performed in a multiple R-C filter of time-constant 1–90 seconds, and the output displayed on a potentiometer strip chart recorder. A particularly valuable feature of the R-C filter was that all the resistance values could be simultaneously switched by a factor of ten. This provided a change of time-constant without altering sensitivity or changing the charge on the capacitors. With the exception of this filter all the above were commercially available items, though the phase-sensitive detector and its associated amplifier had to be modified to reduce temperature coefficient and drift.

An additional rack held the power supplies of the reference noise diode, together with those of the noise diodes or thermal standards under comparison.

The noise-diode power supplies presented considerable difficulties in obtaining the desired degree of stability. Circuits were developed in which the heater voltage was controlled from the anode current of the diodes. Control ranges of 0.2–0.6, 0.6–2.0, 2.0–6.0, 6.0–20.0, and (when possible) 20–60 mA were provided which could be switched simultaneously with the anode current meters—grade I instruments with 6 inch scales.

During switch-on, these controls were overridden by thermal delays allowing heater voltages corresponding to half-scale currents to be initially applied.

Additional fine controls were provided so that anode current could be set with a resolution of the order of one part in five thousand. The stability was such that

maximum changes of anode current did not exceed one part in one thousand over a ten minute period.

Before operation, the system had to be matched at the required frequency. Since the receiver had a relatively wide percentage bandwidth the aim was to match each part of the system—noise sources, diode switch and receiver—independently by means of controls adjacent to them, thus giving minimum frequency sensitivity.

The receiver was first tuned using the stub-stretcher to obtain maximum received signal from the test generator.

The test signal was then fed towards the diode switch which operated at 400 Hz, with its stubs and those of the triple stub matcher set to nominal  $\lambda/4$  values, and a matched 50  $\Omega$  load in place of the compared sources A and B with their matching units.

The matching unit of the reference noise diode was then adjusted for minimum modulation at 400 Hz of the reflected signal reaching the receiver, whilst the centre stub of the diode switch, and finally the triple stubs, were adjusted for minimum mean received signal (i.e. minimum second detector current).

The 50  $\Omega$  load was then replaced by each of the compared noise sources in turn. Their matching units were adjusted to provide minimum modulation of received signal, indicating that they also appeared as 50  $\Omega$ .

During this measurement one stub of the triple stub tuner was moved up and down from its matched position to provide a large reflected signal of variable phase at the receiver. This ensured adequate sensitivity for detecting amplitude and phase unbalances of the compared and reference arms.

After matching the system, the tuning signal was removed and the synchronous detector was switched on. The system was first balanced with the noise sources switched off—i.e. at ambient temperature.

One of the compared sources was then switched on, and the level of the reference source adjusted till the system was again balanced. The system was then switched over to the second compared source which was adjusted to rebalance the radiometer output, usually being set to known values of output which bracketed the value given by the first source.

Alternatively, if both A and B were fixed sources, their ratio could be determined as a ratio of currents of the reference diode required for balance.

In general, the sensitivity of the apparatus was such that 0.01 mA of diode current corresponded to five chart-divisions on the recorder, whilst with the longer time-constants the r.m.s. noise level was of the order of one division. Thus the comparator had a sensitivity somewhat better than 1 degK.

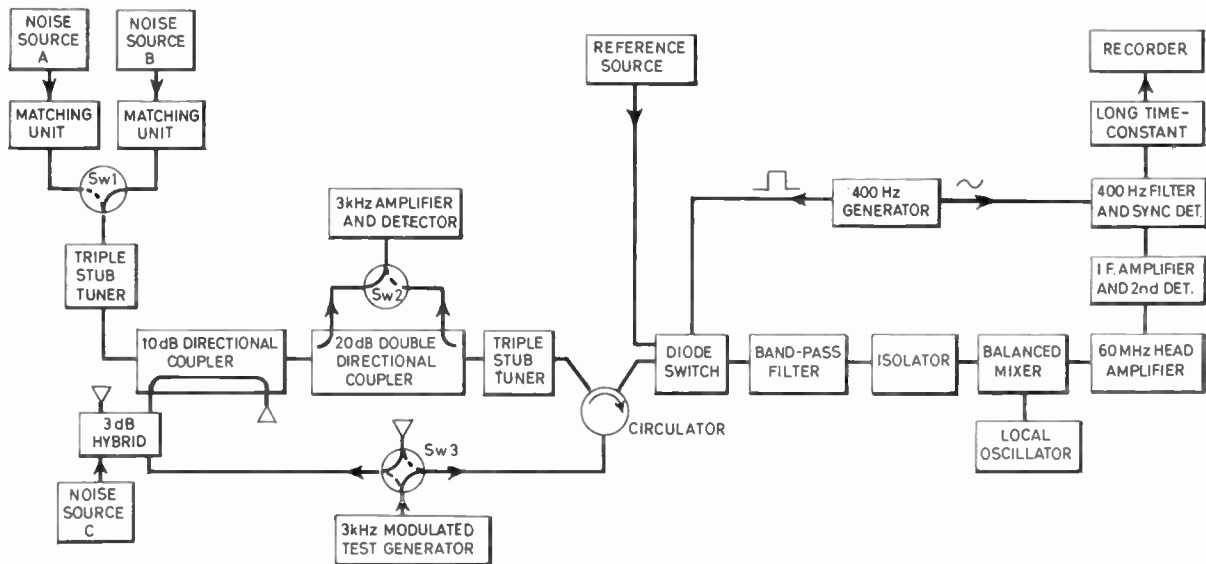


Fig. 6. Noise comparator for 1.0-2.0 GHz.

#### 4. Noise Comparator for 1-2 GHz

An equipment is currently being built to cover the range 1-2 GHz with possible extension to higher frequencies. It provides additionally for measurements on cold sources, and embodies various improvements in components and techniques which have now become available. A block diagram is shown in Fig. 6.

Switch I is a mechanical switch which has been found to provide the necessary degree of performance. In particular, its insertion loss of 0.05 dB has been found repeatable to within  $\pm 0.005$  dB.

With this switch a horizontal layout can be employed which is more suitable for the gas discharge noise sources common in this waveband. Provision will, however, be made for rotation of the switch through 90° so that the compared arms are vertical, as might be more convenient with cooled terminations.

The matching units, which are still under development, are of an improved quartz-rod type. With the incorporation of coplanar inductances, each rod can provide a range of positive or negative reactance, halving the overall length necessary to one-sixth of the longest wavelength.

Due to an isolation from the receiver of over 40 dB provided by a circulator and an isolator, the requirement for matching the sources is reduced to that necessary for accuracy of power transfer. This is accomplished using the test generator and dual directional coupler to match the line in both directions. Experiments have shown that the residual mismatch corresponds to a v.s.w.r. not worse than 0.96. Provided the two sources can be equally matched to within

$\pm 0.01$  in reflection coefficient, errors will not exceed 0.004 dB.

Noise source C is a noise diode capable of providing an additional noise signal of up to 400°C which can be added to A or B. This is sufficient to bring any cooled termination up to ambient or a room temperature termination to the 400°C level of the proposed thermal standard.

For the reference source both a noise diode and a c.w. source with piston attenuator are being considered. The latter has the advantage of providing larger available signals and an accurate decibel scale for comparisons of two widely different noise sources. However, the c.w. sources so far tried have been less stable than the noise diodes, besides introducing severe screening problems.

An r.f. switching system using p-i-n diodes has been retained so that the receiver rack developed for the earlier equipment can be used. Modifications have, however, been made so that the diode switch can be permanently set to either position as required during the matching procedure. The impedance of the switch is less critical in this system, so that a commercially available unit can be employed.

It has also been possible to obtain a tunable band-pass filter with five stages, which covers the whole frequency range with a bandwidth of 5% and a loss of under 0.5 dB. It provides at least 40 dB rejection at the image frequency.

Two circulators are at present used to cover the waveband, but all other items have full-band capability.

The equipment has operated for some months in an

experimental form, with sensitivity very similar to that of the lower frequency version.

## 5. Thermal Standards

### 5.1. 1000°C Coaxial Standard

Since the original aim was the calibration of noise diodes a heated termination was desired as a standard of thermal noise. An operating temperature as high as possible was aimed at as the accuracy achievable with the comparator was at that time unknown.

The work of Zucker *et al.*<sup>10</sup> had demonstrated the feasibility of building a carbon-film coaxial termination operating at 1000°C with a good match up to at least 1 GHz.

This was accordingly adopted as a target for the standards described by Murray in another paper.<sup>11</sup>

These standards were produced in a very compact form comparable in size with the noise diodes. They were operated from stabilized d.c. power supplies which had current limiting facilities, allowing a maximum current of 3 A to pass during the warm-up period. Temperature was found to be stable within one or two degrees.

One disadvantage with this sealed-off form of standard is that it is impossible to make temperature gradient measurements within the thin-walled line, or to check the calibration of the measuring thermocouple at any subsequent time. Thus estimates of the loss of output noise temperature due to losses in the structure, i.e. 3 degC at 300 MHz and 6 degC at 1000 MHz are unlikely to be accurate to better than  $\pm 50\%$ .

Taking all sources of variation into account one would expect these standards to be accurate to  $\pm 10$  degC, i.e.  $\pm 0.04$  dB.

Measurements at 300 and 970 MHz indicate that the actual spread is about twice this figure. However, their mean value at 300 MHz agrees closely with two different types of noise diode, giving confidence that an absolute accuracy within  $\pm 0.1$  dB has been achieved. Comparisons with other sources suggest that this holds up to 1 GHz. Above this there is an increasing spread, whilst even the best sample is about 0.2 dB low in output compared with an S-band thermal standard at 3 GHz.

### 5.2. 400°C Standard for Higher Frequencies

Experience at microwave frequencies<sup>7</sup> suggests that it is much easier to design thermal standards for lower temperatures such as 400°C. There is a much wider choice of materials, and vacuum envelopes can be dispensed with. This makes it much easier to perform temperature gradient measurements, or to remove temperature measuring devices for calibration.

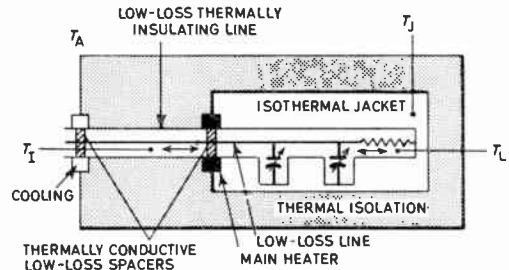


Fig. 7. Suggested design of thermal standard for 1–2 GHz.

The sketch in Fig. 7 shows one suggested form that a thermal standard for 1–2 GHz might take.

The spacers would preferably be made of beryllia which combines low electrical loss with high thermal conductivity. Matching elements might be incorporated within the structure so that any loss connected with them would be at the same elevated temperature, and so introduce no error.

A decision has still to be made as to whether to use a thin-film 50  $\Omega$  resistor as the termination, or the tapered lossy-wedge form used at S-band.<sup>7</sup> The former would have the advantages of smaller size and of use down to much lower frequencies.

## 6. Comparisons of Various Noise Sources

Measurements have been made at frequencies up to 2 GHz, comparing three types of noise source with the present thermal standards. These results are summarized in Fig. 8.

The E.I.D. type of noise source follows a law which can be calculated if the constants of the individual diodes are assumed.<sup>9</sup> Calibration at one or two frequencies might well be sufficient to draw a suitable correction curve up to frequencies of 1250 or 1500 MHz.

The Rohde and Schwarz sources, though flatter at lower frequencies, follow a less well-defined pattern, and are likely to need individual calibration at any frequency of use above 1000 MHz. Voltage standing wave ratios of both diode sources also depart considerably from unity about 1000–1500 MHz.

By contrast the output from a helical-line gas discharge source is flatter, but there is still a change of output of nearly 1 dB between 300 and 2000 MHz. This source has worst v.s.w.r.s in the on and off conditions of 0.86 and 0.5 respectively.

## 7. Conclusions

The noise comparators described indicate clearly the progress which is possible with the increasing availability of broadband components. An adequate sensitivity has been achieved for the comparison of noise diodes or gas discharge sources, with noise standards derived from heated terminations.

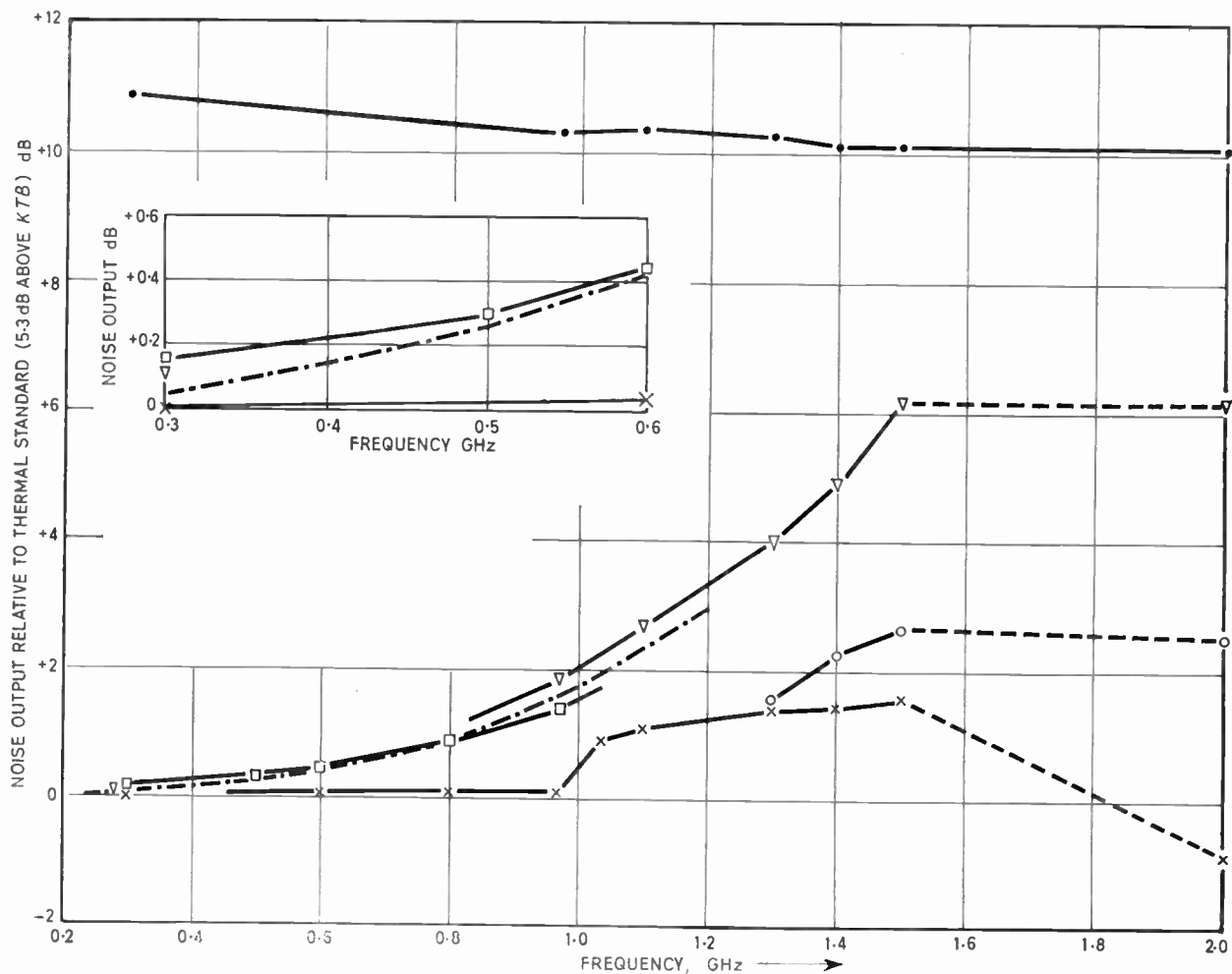


Fig. 8. Calibration of three types of noise source.

--- THEORETICAL E.I.D.      □ E.I.D. NOISE DIODE B      ○ ROHDE AND SCHWARZ DIODE D  
 ▽ E.I.D. NOISE DIODE A      × ROHDE AND SCHWARZ DIODE C      ● HELICAL GAS DISCHARGE NOISE SOURCE

It remains to be seen whether this sensitivity will prove adequate for the comparison of cooled terminations. An obvious possibility would be the introduction of a low-noise amplifier in front of the crystal mixer. Here modern technology offers parametric, tunnel diode or u.h.f. transistor amplifiers of ever-increasing bandwidth.

Requirements have been discussed for heated noise standards. Similar requirements will exist for cooled standards. The availability of liquefied gases makes the maintenance of temperature easier, but against this must be set the necessity to avoid condensation in the cooled parts of the apparatus. In both cases it is necessary to have an accurate knowledge of temperature gradients and the distribution of electrical losses.

The measurements described indicate the magnitude of errors which may arise if present noise generators in this frequency range are not calibrated. With the diode-type sources in particular, calibration at or near the frequency of measurement is essential. There is a particular need, in the range 1-3 GHz, for a well-matched frequency-insensitive coaxial source of either the noise diode or gas discharge type.

8. References

1. M. E. Tiuri, 'Radio astronomy receivers', *Trans. Inst. Elect. Electronics Engrs on Military Electronics*, MIL-8, Nos. 3 and 4, pp. 264-272, July-October 1964.
2. R. H. Dicke, 'The measurement of thermal radiation at microwave frequencies', *Rev. Sci. Instrum.*, 17, pp. 268-275, July 1946.

3. P. D. Strum, 'Considerations in high-sensitivity microwave radiometry', *Proc. Inst. Radio Engrs*, **46**, No. 1, pp. 43-53, January 1958.
4. D. Woods, 'The concept of equivalent source e.m.f. and equivalent available power in signal-generator calibration', *Proc. Instn Elect. Engrs*, **108**, Part B, No. 37, pp. 37-42, January 1961.
5. F. G. Smith, 'R.f. switching circuits and hybrid ring circuits used in radio astronomy', *Proc. I.E.E.*, **108**, Part B, No. 38, pp. 201-204, March 1961.
6. A. J. Estlin, C. L. Trembath, J. S. Wells and W. C. Daywitt, 'Absolute measurement of temperatures of microwave noise sources', *Trans. I.R.E. on Instrumentation*, **1-9**, No. 2, pp. 209-213, September 1960.
7. G. J. Halford, 'Noise comparators and standards for S and X-bands', *Trans. I.E.E.E. on Instrumentation and Measurement*, **IM-15**, No. 4, pp. 310-317, December 1966.
8. D. Woods, 'A coaxial connector system for precision r.f. measuring instruments and standards', *Proc. I.E.E.*, **108**, Part B, No. 38, pp. 205-213, March 1961.
9. I. A. Harris, 'The design of a noise generator for measurements in the frequency range 30-1250 Mc/s', *Proc. I.E.E.*, **108**, Part B, No. 42, pp. 651-658, November 1961.
10. H. Zucker, Y. Baskin, S. I. Cohn, I. Lerner and A. Rosenblum, 'Design and development of a standard white noise generator and noise indicating instrument', *Trans. I.R.E. on Instrumentation*, **1-7**, pp. 279-291, December 1958.
11. R. W. Murray, 'A coaxial primary standard for noise-source calibration', *Proc. Joint I.E.R.E.-I.E.E. Conference on Radio Frequency Measurements and Standards, 1967 (I.E.R.E. Conference Proceedings No. 10)*.  
*Manuscript received by the Institution on 26th July 1967. (Paper No. 1183.)*

© The Institution of Electronic and Radio Engineers, 1968

## STANDARD FREQUENCY TRANSMISSIONS

(Communication from the National Physical Laboratory)

Deviations, in parts in  $10^{10}$ , from nominal frequency for March 1968

March 1968	24-hour mean centred on 0300 U.T.			March 1968	24-hour mean centred on 0300 U.T.		
	GBR 16 kHz	MSF 60 kHz	Droitwich 200 kHz		GBR 16 kHz	MSF 60 kHz	Droitwich 200 kHz
1	-300.0	-0.1	0	16	-300.1	-0.1	0
2	-300.1	0	0	17	-300.1	-0.1	0
3	-300.1	+0.1	0	18	-300.0	0	-0.1
4	-299.9	0	0	19	-300.0	-0.1	0
5	-299.9	0	0	20	-300.1	0	-0.1
6	-300.0	+0.1	0	21	-300.1	0	0
7	-300.1	+0.1	0	22	-300.1	0	0
8	-300.0	0	0	23	-300.0	0	0
9	-300.1	0	0	24	-300.1	0	0
10	-300.0	0	0	25	-299.9	0	+0.1
11	-300.0	0	+0.1	26	-300.0	+0.1	+0.1
12	-300.1	0	+0.1	27	-300.0	0	+0.2
13	-299.9	+0.1	+0.1	28	-299.9	+0.1	+0.1
14	-299.9	0	+0.1	29	—	—	+0.2
15	-299.9	+0.1	0	30	—	—	+0.2
				31	—	—	+0.2

Nominal frequency corresponds to a value of 9 192 631 770.0 Hz for the caesium F<sub>m</sub>(4,0)-F<sub>m</sub>(3,0) transition at zero field.

Notes: (1) All measurements were made in terms of H.P. Caesium Standard No. 134 which agrees with the NPL Caesium Standard to 1 part in  $10^{11}$ .

(2) The offset value for 1968 will be -300 parts in  $10^{10}$  from nominal frequency.

## I.F.I.P. CONGRESS 1968

The 1968 Congress of the International Federation for Information Processing is to be held in Edinburgh from 5th to 10th August 1968. The Conference aims to present a review of the current state of data processing and to discuss the most important developments and significant advances that have occurred in this field since the previous Congress, held in New York in 1965.

The inaugural speech of the Congress will be given by Earl Mountbatten of Burma on the morning of Monday, 5th August, and the closing speech will be delivered by Sir Paul Chambers on Saturday morning, 10th August.

During the intervening five days more than 250 papers on computers, computing and the information sciences will be given to an audience expected to number 4000 delegates drawn from more than forty countries. The following are some of the invited papers.

- 'Numerical integration of ordinary differential equations'—T. E. Hull (Canada).
- 'Error bounds and computer arithmetic'—K. Nickel (Germany).
- 'Numerical stability in mathematical analysis'—I. Babuska (Czechoslovakia).
- 'Rigorous computation and the zeros of the Riemann zeta-function'—L. Schoenfeld (United States).
- 'Stability in linear algebra problems'—V. N. Faddeeva (U.S.S.R.).
- 'Achievements and problems in formula manipulation'—M. Engeli (United States).
- 'A survey of some results in the field of discrete mathematics'—S. V. Yablonskiy (U.S.S.R.).
- 'How to succeed in software'—S. Michaelson (United Kingdom).
- 'Representation of geometrical notions in programming languages'—S. S. Lavrov (U.S.S.R.).
- 'Compiler building'—W. L. Van der Poel (Netherlands).
- 'Data structures in two level storage'—C. A. R. Hoare (United Kingdom).
- 'Introduction of real-time concepts in simulation languages'—K. Nygaard and O. J. Dahl (Norway).
- 'Some considerations in supervisor program design for multiplexed computer systems'—F. J. Corbató and J. H. Saltzer (United States).
- 'Trends in computer system organization'—T. Kilburn (United Kingdom).
- 'Advances in circuit technology and their impact on computing systems'—E. Bloch and R. A. Henle (United States).
- 'Computer graphics communication systems'—G. A. Rose (Australia).
- 'Memory systems'—E. Goto (Japan).
- 'The changing role of analog and hybrid computer systems'—W. J. Karplus (United States).
- 'Communication networks to serve rapid-response computers'—D. W. Davies (United Kingdom).
- 'Real time computer systems'—A. A. Borsei and A. C. Bos (United States).
- 'Development automation'—G. T. Artamonov (U.S.S.R.).
- 'Artificial intelligence: themes in the second decade'—E. A. Feigenbaum (United States).
- 'A survey of formal grammars and algorithms for recognition and transformation in mechanical translation'—B. Vauquois (France).
- 'Automatic picture processing for pattern recognition'—H. Kazmierczak (Germany).
- 'On formula manipulation connected with computer design'—S. Waligorski (Poland).
- 'Search and retrieval experiments in real-time information retrieval'—G. Salton (United States).
- 'Experimental data processing systems'—A. D. Smirnov (Australia).
- 'New directions in mechanical theorem proving'—J. A. Robinson (United States).
- 'Computer science and education'—G. E. Forsyth (United States).
- 'Computer applications to urban planning and analysis—examples and prospects'—E. Horwood (United States).
- 'Computer assisted education'—P. Suppes (United States).
- 'Operations research and computers: which should be servant of which?'—H. Le Boulanger (France).
- 'The computer in literary studies'—A. Q. Morton (United Kingdom).
- 'A generalized medical information facility'—J. J. Baruch (United States).
- 'On the analysis and design of a management data processing system based on information system theory'—P. Bagge (Switzerland).

Applications for Registration forms and all enquiries should be addressed to the I.F.I.P. Congress Office, 23 Dorset Square, London, N.W.1.

# The Service of Broadcasting:

## Some Technical Requirements for the Reception of Sound Broadcasting including Transmission from Earth Satellites

By

R. A. ROWDEN,

B.Sc.(Eng.), D.I.C., C.Eng., F.I.E.E.†

*Presented at a Conference on 'Radio Receiver Systems' organized by the University College of Swansea, with the support of the Institution, on 11th–14th September 1967.*

**Summary:** A satisfactory service of sound broadcasting is achieved over a given area when sufficient field strength is provided to give an acceptable signal/interference ratio and an acceptable quality of reproduction to a high proportion of listeners for a large part of the time. An acceptability of 100% is unlikely to be achieved because of the variability both in time and with location, of the interferences affecting broadcasting and also because subjective judgement of acceptability varies between listeners. Levels of man-made noise, atmospheric noise and interference from other stations vary widely and allowance for these factors is made in planning a sound broadcasting service.

Refinements to the sound broadcasting services, which have become possible and desirable as a means of improving the services, have been the introduction of the f.m. v.h.f. service, the increased use of compression of the range of modulation and more recently a 'compatible' stereophonic service.

If there is a future demand for increased sound broadcasting services other methods may have to be considered and these may become economically more feasible as receiver design progresses. These might include single-sideband and pulse modulation methods to conserve spectrum space. Direct broadcasting from artificial Earth satellites, useful where a single programme is required over a large area, is envisaged as becoming practicable at v.h.f. or s.h.f. within the next ten years.

### 1. Introduction

There are at the present time approximately 500 million sound broadcasting receivers in use in the world, about one to every six of the population: they still outnumber television receivers by about 3 : 1. A restatement of the technical requirements for present and possible future methods of sound broadcasting is therefore still felt to be justified. It should, however, be borne in mind that many of the principles described for sound can also be adapted to television by making due allowance for the different parameters appropriate to the wider bandwidth of television systems.

The technical aim of the sound broadcasting engineer has always been to produce a signal of sufficient intensity as to provide a service of acceptable quality over the whole area to be served. What is acceptable quality to listeners has long been the subject of discussion and subjective listening tests. These tests have shown that the relative importance of the parameters of distortion, fidelity of reproduction and signal/noise ratios varies both with the individual and

with the type of programme being transmitted. However, once the broadcasting engineer has established the basis of acceptability in terms of amplitude distortion, frequency distortion and signal/noise ratio, he can then set about his task of providing a sufficiently high field-strength and ensuring that this is maintained for a sufficient proportion of the time.

### 2. Quality of Reception

If a listener is asked to judge the overall quality of a broadcast programme he will take into account, perhaps unconsciously, one or more of the following effects or he may be conscious of the presence of one over-riding effect:

- (a) Frequency distortion (amplitude-frequency response);
- (b) Harmonic or inter-modulation distortion (amplitude distortion);
- (c) Background noise;
- (d) Interfering programme background or interfering r.f. signal, heterodyne, etc.;
- (e) Volume variations (fading) or signal/noise ratio variations with time.

† Research Department, British Broadcasting Corporation, Kingswood Warren, Tadworth, Surrey.

Broadcast transmission quality, in general, satisfies the requirement that the first two effects are negligible, at least to the standards of a very high proportion of the listening public, and a high proportion of receivers also are satisfactory, perhaps to a slightly lower proportion of the listening public. Conscious deterioration of quality arises from the properties of the propagation medium in producing effects (a), (b) and (e) and from lack of sufficient field strength of the required transmission to overcome (c) and (d), noise and interference, which are of course the old enemies of the radio engineer.

Dealing first with noise, it can be said that broadcasting is affected by:

- (a) receiver noise,
- (b) natural noise (atmospherics),
- (c) man-made noise.

In general, on all the sound broadcasting bands at present in use, the broadcasting engineer does not need to take receiver noise into account when considering the extent of his service areas—most receivers are designed to give an adequate output level and acceptable output signal/noise ratio in areas where the field is strong enough to overcome the other types of noise. An exception to this is the case of some small portable receivers which rely on the availability of relatively strong signals for fully satisfactory operation.

### 3. Limitation of Service by Natural Noise

Natural noise (atmospherics) varies greatly with time, season and location and the broadcasting engineer must plan his service areas to overcome its effect. Such planning nowadays is greatly assisted by the study of noise, on a worldwide scale, conducted over many years by the International Radio Consultative Committee (C.C.I.R.). Figure 1, which has been derived from C.C.I.R. data,<sup>1</sup> shows the required field strength to provide a 40 dB ratio of signal carrier to r.m.s. noise for 90% of the time in winter and summer at a temperate latitude such as N.W. Europe, including S.E. England. It is interesting to note, in passing, that there is a significant difference between the south and north of the British Isles in this respect. The curve for tropical East Africa is added to show how greatly the atmospheric noise, and hence the required field strength to overcome it, varies in different parts of the world.

The curves have not been extended to include the v.h.f. part of the spectrum as here atmospheric noise is of small importance in determining the required field strength. A study of the C.C.I.R. report<sup>1</sup> will show that at v.h.f. galactic noise from outer space assumes a greater importance than atmospheric noise, and the receiver noise can also be of much greater relative importance.

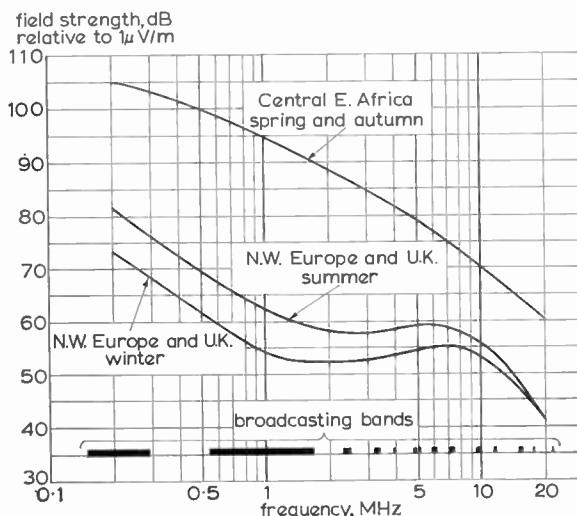


Fig. 1. Field strength required for broadcasting service in presence of radio noise.

To provide a broadcasting service to the standards to which Fig. 1 applies will require the provision of strong signals in the more 'noisy' parts of the world and it may be felt that, at least for medium- and long-wave broadcasting, there is no point in designing highly sensitive receivers of good noise factor for use in such areas. Consider an example of what the curves mean in practical terms. At a frequency of 1 MHz and using a transmitter power of 100 kW, the range of the station over 'good' ground to provide the field strengths indicated in Fig. 1 would be 125 miles in N.W. Europe in winter but only 16 miles in Central East Africa in spring and autumn. In case the curves cause too much alarm, it must be pointed out that they are drawn for the signal/noise standard aimed at for broadcasting (C.C.I.R.) of 40 dB and the values given would provide this standard for 90% of the time. Many broadcast listeners would accept a much lower standard, particularly for news and light entertainment.

### 4. Limitation of Service by Man-made Noise

A definition of the required levels of field strength giving a fully acceptable broadcasting service in the presence of man-made noise of all kinds (and there are many) is not possible owing to the extreme variability of the noise levels. Studies of the intensity of man-made interference, methods for its measurement and proposals for its limitation have been made on an international scale over many years by C.I.S.P.R. (Comité International Spécial des Perturbations Radioélectriques). To understand the problems and methods it is recommended that reference should be made to the classical paper by Gill and Whitehead,<sup>2</sup> to the publications of C.I.S.P.R.,<sup>3</sup> and to the work of the British Post Office Interference Service.<sup>4</sup>

**Table 1**

Desirable levels of field strength for sound broadcasting to overcome man-made interference

Frequency band	Receiver location	Required field strength	Source of information	Remarks
150-300 kHz Long-wave Band	City and factory area	20 mV/m	B.B.C.	Based on observations
	Residential and urban	10 mV/m	B.B.C.	
	Rural	5 mV/m	B.B.C.	
550-1600 kHz Medium-wave Band	City, business and factory area	10-50 mV/m	F.C.C. (U.S.A.) <sup>5</sup>	Based on experience in U.S.A.
	City residential area	2-10 mV/m	F.C.C. (U.S.A.) <sup>5</sup>	
	Rural	0.1-0.5 mV/m	F.C.C. (U.S.A.) <sup>5</sup>	
3-21 MHz Short-wave Band	Urban	0.5-2 mV/m	'Reference Data for Radio Engineers' <sup>6</sup>	Allows 30 dB signal/median of quasi-peak noise
	Suburban	0.2-0.5 mV/m		
88-100 MHz V.H.F. F.M. Band Monophonic	'Principal city'	3-5 mV/m	N.A.B. Handbook <sup>7</sup> U.S.A.	Based on experience in U.S.A.
	City, business and factory area	1 mV/m		
	Rural areas	50 μV/m		
88-100 MHz Monophonic	Large cities	3 mV/m	C.C.I.R. Rec. 412 <sup>8</sup>	Refers to industrial and domestic equipment
	Urban areas	1 mV/m		
	Rural areas	0.25 mV/m		
88-100 MHz Stereophonic	Large cities	5 mV/m	U.K. proposals	To be submitted to C.C.I.R.
	Urban areas	2 mV/m		
	Rural areas	0.5 mV/m		

The broadcasting authorities, with a knowledge of existing interference levels, have tended to establish their own standards for the field strength required to overcome man-made noise. A summary of these standards is shown in Table 1 and it will be seen that, within fairly wide limits, there is some degree of agreement between the various opinions.

**5. Limitation of Service by Interference**

Apart from noise, there is another serious limitation to sound broadcasting service areas caused by the effects of common channel or overlapping channel interference from distant transmissions. The standards of protection for such cases agreed by the C.C.I.R. in their Recommendations<sup>8, 9</sup> No. 412, 448 and 449 are a useful guide here.

Table 2, which is largely based on these C.C.I.R. standards, shows that the extremes of protection required are 60 dB where an audible heterodyne note of approximately 2 kHz is produced and only 6 dB for the case of 'near-synchronized' working with highly compressed common programmes of the 'popular music' type.

Broadcasting station service areas are ideally planned so that at an agreed level of 'minimum field strength to be protected' the protection ratios given in Table 2 are achieved. The agreed levels for instance,

at an international conference, of minimum field strength to be protected generally lie somewhere between the level limited by atmospheric noise and the levels limited by receiver noise in any part of the spectrum where the former normally exceeds the latter. Under present day conditions these standards are seldom achieved by day and night.

**Table 2**

Protection ratios for various conditions of a.m. sound broadcasting

Wanted programme	Interfering programme	Carrier frequency difference	Protection ratio required
Normal speech and music broadcasting	A different (normal) programme	0-50 Hz	40 dB
"	"	2 kHz	60 dB
"	"	5 kHz	40 dB
"	"	9 kHz	12 dB
"	"	18 kHz	-12 dB
"	Common programme with wanted station	1 Hz	10 dB
Music, highly compressed	"	1 Hz	6 dB

## 6. Other Limiting Factors

Finally, among the factors which affect quality of reception is fading. This will be apparent either as a volume variation, with or without distortion, or an audibly varying signal/noise ratio with the noise background becoming obtrusive during the troughs of the fades. Particularly for the planning of long-distance overseas services at h.f., a knowledge of the effects of the ionosphere<sup>10</sup> is essential to the broadcasting engineer who must endeavour to provide an acceptable quality of reception for a large proportion of the time. At l.f. and m.f., fading sets in at a distance from the transmitter even where the ground-wave is still quite strong enough to provide a daylight service, and is due to the interaction between the steady ground-wave and the variable wave reflected from the lower ionosphere. The point at which this occurs can be controlled to some extent by designing the transmitting aerial to limit the skyward radiation. In other cases, and over much greater distances a service at m.f. is maintained using only the ionospheric ray. To allow for the effects of fading in this case and also in the case of h.f. overseas services, sufficient power is required to ensure that the received signal does not fall too low except for a small proportion of the time. At h.f., serious fading is avoided by the choice of a frequency suitable for transmission at a particular time of day and season and the transmissions are sometimes directed to the 'target' area over a more stable path by the use of relay stations.

The broadcasting engineer is always aware that it is the presence of the Earth itself, with its irregular, though roughly spherical, surface, and its surrounding atmosphere, whether ionized or having a non-uniform permittivity, that cause major restrictions to services. He looks forward to the possibility of alleviating these effects by the use of direct satellite broadcasting, which is discussed in some detail in Section 8.

## 7. Future Possible Systems

A significant trend in the development of sound broadcasting over the past 20 years has been the introduction of f.m. systems in the v.h.f. band instead of the more conventional a.m. systems.<sup>11</sup> The choice was made because of the established advantage of f.m. in giving a system with a better signal/noise characteristic than in the case of a.m. The spectrum space available by international agreement (88–100 MHz) could, however, have accommodated a much larger number of a.m. stations but to have provided the same numbers of population with a signal, with a.m. giving a comparable receiver output signal/noise ratio would have required a larger number of a.m. stations and have been on balance less economical.

Other systems might be considered for future sound

broadcasting purposes bearing in mind that the main requirement is additional spectrum space for more services. One proposal<sup>12</sup> is for 'compatible single-sideband broadcasting' (c.s.s.b.) which could be used on a.m. systems. The system has already been tried experimentally in several countries and the major advantage claimed is that it can be received on conventional double-sideband (d.s.b.) apparatus, yet radiates over a restricted bandwidth, thus making possible closer spacing of the channels in a waveband.

The broadcasting engineer has looked towards other improvements in the service, either under the pressure of the requirement for more and more programmes to be simultaneously transmitted or because it was believed that there was a demand for a higher quality of reception with more freedom from radio or noise interference. The use of v.h.f. and f.m. made possible the distribution of more programmes, higher quality and freedom from noise and other interference and now, after many years of tests and discussions, has led to an acceptable stereophonic system.<sup>13, 15</sup> The advantage of either of the stereo systems internationally accepted is that existing receivers can still receive a 'normal' monophonic signal. The range of a stereophonic transmission is a little less than for monophonic transmission but can be restored by conventional means at the receiver, such as by the installation of a higher gain receiving aerial, use of pre-amplifiers, etc.

An improvement in the signal/noise or signal/interference ratio at the receiver output has been brought about by the compression of the dynamic range of the programme at the transmitter, resulting in a considerably higher average modulation depth. This procedure has proved quite acceptable for many programmes, at l.f., m.f. and h.f.; it has in fact become almost an essential for the 'pop music' type of programme and at h.f., where received signal/noise ratios are sometimes poor, it is quite acceptable for the transmission of news and light entertainment.

The future holds many possibilities for the technical methods of sound broadcasting and it is perhaps permissible to indulge in speculation on these. Whether any of them will be put into service would depend largely on the demand and (improbable) international agreement. In the case of v.h.f. f.m. the addition to the service depended on the provision of an entirely new receiver but c.s.s.b. and stereo are compatible, that is to say, capable of reception on existing receivers. Perhaps such compatibility will not be an essential requirement in the future if multi-purpose receivers can be economically manufactured. The use of carrier-suppressed single-sideband systems for l.f. and m.f. broadcasting might then be envisaged with the advantage that at least twice the present total of 136 channels might be available for re-allocation by international agreement in Europe.

If further frequency bands should be available at u.h.f. or s.h.f. and be required for sound broadcasting, pulse modulation systems<sup>16, 17</sup> might be used. For broadcasting purposes this would merely be an extension of techniques already in use for other branches of telecommunications. These techniques might be particularly suitable for broadcasting from satellites.

### 8. Broadcasting from Satellites

A recent C.C.I.R. report<sup>18</sup> has reviewed the feasibility of direct sound and television broadcasting from satellites and provided some data on the parameters for a satellite broadcasting system to give a service either to the maximum possible area of the Earth's surface or for a more limited geographical coverage, e.g. an area approximately the size of Europe. It is as well to repeat the C.C.I.R. statement: 'Formidable technical problems remain to be solved before high-quality broadcasting from satellites can be established.'

The only feasible satellite position for normal uninterrupted broadcasting is a stationary equatorial orbit at approximately 22 300 miles (36 000 km) altitude. For limited sound broadcasting only, there might be some application for an inclined orbit with a period of revolution of 24 hours, or a lower-altitude orbit with a period equal to a sub-multiple of 24 hours, either of which could provide service successively to different regions for limited fixed periods of time each day.

In the case of satellite broadcasting, practically all listeners within the illuminated area would receive substantially the same signal strength and unfavourable comparison may be made with existing terrestrial broadcasting if a uniform but mediocre satellite service were made available alongside existing terrestrial services, such as would arise if the satellite service provided a signal/noise ratio similar to that in a terrestrial 'fringe' area. For this reason, in Table 4, the requirement of rather higher signal/noise ratios has been assumed than those given in the C.C.I.R. report.

#### 8.1. Usable Frequency Assignments for Satellite Sound Broadcasting

The assumption is made that frequency bands already allocated for broadcasting will be used for the satellite transmissions. There may be an agreement at some future international conference for the use of special bands for direct broadcasting from satellites; for example, the use of part of the spectrum between 1 and 10 GHz would alleviate some of the difficulties which result from any attempt to share frequency channels between satellite broadcasting stations and existing ground broadcasting stations. In Table 3, however, the bands considered for possible sound

**Table 3**  
Frequency bands considered for possible sound broadcasting from satellites

Band	Proposed use of band	Channel width	No. of channels
21.45–21.7 MHz	high quality a.m. sound	20 kHz	12
25.6–26.1 MHz	high quality a.m. sound	20 kHz	25
87.5–100 MHz	f.m. sound	200 kHz	62
11.7–12.7 GHz	f.m. sound	200 kHz	5000

broadcasting from satellites are listed, showing the suggested purpose to which each band might be put and the number of frequency channels which would be available. It has been assumed that the currently unallocated 11.7–12.7 GHz band could be used equally well for sound as for television although it is more likely to be in demand for television.

Transmissions from satellites at frequencies below about 100 MHz may at times be affected by the presence of the ionosphere, although sufficiently penetrating it for an adequate field-strength to be received. The effects to be taken into account would include variable absorption, refraction, scintillation and polarization changes,<sup>19</sup> and separately or collectively could limit coverage particularly where an oblique path through the ionosphere is involved as, for example, from a satellite in an equatorial orbit to a country at a high latitude on the Earth's surface.

The lowest available broadcast band in which transmissions from a satellite would be expected to penetrate the ionosphere at nearly all times is around 20 MHz. Transmissions in this band from a satellite in a stationary equatorial orbit would provide coverage to the limits of the northerly and southerly latitudes containing a high proportion of the Earth's population. A simple receiving aerial such as a horizontal dipole is assumed. A possible use for the two lowest bands is high-quality a.m. sound broadcasting; a total of 37 20-kHz channels is theoretically available for this purpose. Bearing in mind the use of both these h.f. bands by many ground stations at the sun-spot maximum epoch, co-channel and adjacent-channel interference would restrict satellite broadcasting at certain times of the day to an extent which would vary with season and the sun-spot cycle. At other times, however, particularly at night, the bands are little used by terrestrial services and could be used for satellite sound broadcasting leading to a much more efficient use of these bands. However, at the present time, only a small proportion of short-wave domestic receivers cover the top-frequency band, and a large number do not receive above 18 MHz.

**Table 4**  
Stationary Earth-satellite broadcasting

Frequency, MHz	20	100	12 000	
Receiving installation assumptions:				
Service (A)	a.m. <sup>a</sup> sound	f.m. sound	f.m. sound	
Effective noise bandwidth, MHz (B)	0.02	0.2	0.2	
Thermal noise, dB(W) (C)	-161	-151	-151	
Required signal/noise ratio in receiver, dB (D)	58 <sup>f</sup> †	34 <sup>g</sup> †	34 <sup>g</sup> †	
Noise factor plus feeder loss, dB (E)	20	10	10 <sup>b</sup>	
Atmospheric or galactic noise, dB above thermal (F)	35	7	—	
Total noise, referred to aerial, dB above thermal (G)	35	12	10	
Signal power at aerial, dB(W) (H)	-68	-105	-107	
Aerial gain, dB rel. λ/2 dipole (I)	0	6	30	
Aerial gain, dB rel. aerial of 1 m <sup>2</sup> effective area (J)	15	7	-11	
Flux density, dB rel. 1 watt/m <sup>2</sup>	-83	-112	-96	
Field strength, dB rel. 1 μV/m (L)	63	34	50	
Field strength, μV/m	1400	50	300	
Satellite transmitter assumptions:				
Directive radiated power (d.r.p.) needed <sup>c</sup> from 40 000 km range, dB (W) (M)	80	51	67	
Approximate aerial diameter, m <sup>d</sup> (N)				
17.5° beam	} See below	60	12	0.1
7° beam		150	30	0.25
2.5° beam		420	84	0.7
Transmitter power <sup>e</sup> , kW (P)				
17.5° beam	1250	1.6	60	
7° beam	200	0.25	10	
2.5° beam	25	0.032	1	
Transmitting aerial parameters, assuming circular aperture:				
Beam-width between -3 dB points	Maximum gain in dB referred to λ/2 dipole	Maximum gain in dB referred to isotropic radiator	Gain at -3 dB points dB referred to isotropic radiator	
17.5°	20	22	19	
7°	28	30	27	
2.5°	37	39	36	

† These signal/noise ratios, which are based on full (100%) modulation, refer to the signal and the noise as they would be measured in the intermediate frequency circuits of the receiver.

**Notes:**

- <sup>a</sup> Double sideband a.m. with 10 kHz modulation bandwidth.
- <sup>b</sup> Assuming low-noise amplifier or converter at the aerial.
- <sup>c</sup> D.r.p. is equivalent power from an isotropic radiator.
- <sup>d</sup> Assuming a uniformly illuminated circular aperture. Larger diameters may be needed if non-uniform, e.g. for purposes of reducing side-lobes. The e.r.p. is about 2 dB less than the d.r.p.
- <sup>e</sup> Transmitter power to provide d.r.p. out to the -3 dB beam edges. It is assumed that the receiving aerial matches the transmitted polarization.
- <sup>f</sup> For 'perceptible' random noise. For 'just perceptible' random noise, 69 dB would be required.
- <sup>g</sup> For 'just perceptible' random noise. For 'perceptible' random noise, 23 dB would be required.

**Formulae (units as given in Table):**

$$C = 10 \log B - 144 \text{ (based on } kTB \text{ available noise)}$$

$$G = 10 \log_{10}(10^{0.1E} + 10^{0.1P} - 1)$$

$$H = C + D + G$$

$$J = I + 10 \log_{10}(1.64 \lambda^2 / 4\pi)$$

where λ is wavelength in metres

$$K = H - J$$

$$L = 146 + K$$

$$M = 163 + K = 71 + K + 20 \log_{10} d$$

where d is in kilometres

In the v.h.f. band 62 channels are available in many parts of the world. Use of a particular channel for satellite broadcasting, which (as will be seen below) is at present considered practicable over a minimum area of some 800 000 square miles, will preclude the use of the same channel for any ground station within that area. Thus, if only one country of the many in an area such as Europe elected to fulfil its v.h.f. sound broadcasting requirements from an Earth satellite, it would not be possible to find an exclusive channel for this purpose within the band at present used. Furthermore, taking Europe as a whole, if every one of about 30 countries elected to go over to v.h.f. broadcasting from Earth satellites, and required three-programme transmission, the total number of channel requirements would be 90. Such an arrangement could not be fitted into the existing band since the same channel could not be used for more than one satellite transmission. Moreover, current receivers cannot reliably separate adjacent channels (200 kHz spacing) of equal strength so that further limitations in the use of the available 62 channels would arise. Such a project would therefore be quite impracticable for Europe. For a single large country such as Australia, Canada, the U.S.A., U.S.S.R. or China, sound broadcasting by this means at v.h.f. might be practicable, particularly within the limits of the field strength figures detailed in Table 4, provided that exclusive channels are allocated to the area over which the satellite is effectively above the horizon. Such allocations may require the use of a new frequency band or the extension of existing broadcasting bands.

### 8.2. Requirements for a Direct Broadcasting Satellite

The transmitter power requirements for direct satellite broadcasting on each of the frequency bands enumerated in Table 3 have been estimated after making assumptions concerning characteristics of the transmitting and receiving installations. Table 4 gives the assumptions made, the system parameters and finally the transmitter power required for each purpose. As far as the satellite-borne transmitter is concerned, many extremely difficult technical problems remain to be solved and it is not yet clear which are likely to be resolved within a reasonable time.

### 8.3. Coverage Obtainable with Direct Broadcasting from Satellites

For the transmitter power for the broadcasting satellite to be kept as low as possible the satellite transmitting aerial will be required to have a very high gain with consequent large aperture and small beam-width. The smallest beam-width considered in this paper for which values are given in Table 1 is  $2\frac{1}{2}^\circ$  to the half-power points and two other possible beam-widths for the transmitting aerial are also considered. The transmitter powers have been calculated from the require-

ment that the radiated powers at the half-power points must be sufficient to provide the minimum required field strength at the Earth's surface in the beam directions corresponding to the half-power points. A satellite to Earth range of 40 000 km has been assumed and allows for the fact that the maximum of the beam might be directed approximately towards latitude  $50^\circ$ , this latitude in the northern hemisphere being roughly that of the centre of Europe. For this particular case, the area bounded by the limiting field strength contour will be of a near-elliptical shape with a minimum width in an East-West direction of approximately 1000 miles giving coverage over some 800 000 square miles. This may in fact be the most practicable area of coverage in the first applications to broadcasting since if, on the one hand, the beam-width were decreased there would be greater difficulties in achieving stable orientation of the transmitting aerial while if, on the other hand, the beam-width were increased there would be greater difficulties in providing the transmitter power needed.

The maximum coverage that can be achieved without regard to power limitation of the satellite transmitter is clearly that part of the surface of the Earth visible from the satellite. It is in fact about one-third of the Earth's surface area and the calculations given in Table 4 for a  $17.5^\circ$  beam-width refer to this case. At the other extreme, should it become practicable to use transmitting aërials with very narrow beam widths, say, down to  $0.5^\circ$  for some or all of the frequency bands, coverage over smaller areas such as a single small country could be achieved with correspondingly lower satellite transmitter powers than those given in Table 4 but with more serious problems in transmitting aerial design and stabilization.

Whether broadcasting satellites can share frequency channels with each other or with ground transmitters will depend very largely on the interference range of the transmissions from the satellite. Even a satellite aerial having a beam-width of  $2\frac{1}{2}^\circ$  and serving an area on the Earth's surface of some 1000 square miles across will, because of side-lobe radiation, be a potential source of interference in any other part of the Earth's surface visible to the satellite.

In cases where the receiving aerial can play no useful part in discriminating against the interfering satellite transmission, the full protection against co-channel interference must be achieved by the satellite transmitting aerial. (This would apply in many cases when receiving existing terrestrial services, bearing in mind that even horizontally directed aërials may be 'looking towards' the satellite in those areas where the satellite appears low above the horizon.) The interference is thus likely to be appreciable except possibly in regions well away from the service zone towards which the side-lobe radiation might be reliably suppressed to

very much less than the level of  $-30$  dB relative to the radiation at the half-power point.

Co-channel working by sharing with terrestrial services must therefore be considered impracticable within an area such as Europe. On the other hand, where the receiving aerial directivity can play a significant part (e.g. for two services on higher frequencies from satellites well spaced in the equatorial orbit) the interference position would be more favourable.

Studying the parameters of satellite transmitter power and required aerial diameter, a judgment must be made as to what is practicable and what is impracticable. The author's estimate is that the stage of development of satellite construction, control, orientation, and launching is such that within ten years transmitter powers of up to 10 kW and satellite aerial diameters of up to 30 m will be possible. On this basis, it would seem that f.m. sound broadcasting of acceptable quality will be practicable over wide areas in the v.h.f. band with fairly wide-beam satellite transmitting aerials (small aerial diameters) although this would require receiving aerials adequate for the assumed field strength of  $50 \mu\text{V/m}$ . Problems of channel allocations in the range 87.5 to 100 MHz, with the present high usage of Band II on a world-wide scale, would be very severe. Should the s.h.f. band be developed for this purpose, broadcasting over smaller areas on the Earth's surface might be practicable but would, as Table 4 shows, require the use of a special receiving aerial of high gain.

### 9. Conclusions

The factors affecting the quality or acceptability of a sound broadcasting service may be summarized as those due to natural or man-made noise, limitations due to the transmitter and receiver, interference from other transmissions and the effects of the propagation medium.

If there is a demand for further sound broadcasting services it may be practicable to develop other methods than those at present in use, for example, direct broadcasting from satellites may become possible for limited uses within the next ten years.

### 10. Acknowledgments

The author wishes to thank the Director of Engineering, B.B.C., for permission to publish this paper.

### 11. References and Bibliography

1. 'World Distribution and Characteristics of Atmospheric Radio Noise', C.C.I.R. Report No. 322, Documents of the Xth Plenary Assembly of the C.C.I.R. (Geneva, 1963).

2. A. J. Gill and S. Whitehead, 'Electrical interference with radio reception', *J. Instn Elect. Engrs*, **83**, pp. 345-86, September 1938.
3. C.I.S.P.R. Publications Nos. 7, 8 and 9, 1st edition 1966. (Obtainable from B.S.I. Sales Office, Newton House, 101/113 Pentonville Road, London, N.1.)
4. C. W. Sowton, G. A. C. R. Britton *et al.*, 'Radio interference', *P.O. Elect. Engrs J.*, **50**, Part 4, January 1958; **51**, Parts 1, 2, 3, 1959 and **52**, Part 1, April 1960. (A series of 6 articles.)
5. 'Federal Communications Commission (U.S.A.) Rules and Regulations', Vol. III, Part 73, Section 182, pp. 44-45, January 1964.
6. 'Reference Data for Radio Engineers', 4th Edition, p. 763 (International Telephone and Telegraph Corporation).
7. 'NAB (National Association of Broadcasters) Engineering Handbook', 5th edition, p. 1-146 (McGraw-Hill, New York, 1960).
8. 'Standards for Frequency Modulation Sound Broadcasting in the V.H.F. (Metric) Band', C.C.I.R. Recommendation No. 412, Documents of the XIth Plenary Assembly, Vol. V, p. 30, Oslo, 1966.
9. C.C.I.R. Recommendation No. 448, 'L.F./M.F. Sound Broadcasting: Radio Frequency Protection Ratio', and C.C.I.R. Recommendation No. 449, 'Amplitude Modulation Sound Broadcasting: Radio-frequency Protection Ratio Curves', Documents of the XIth Plenary Assembly, Vol. V, pp. 34-36, Oslo, 1966.
10. L. J. Prechner, 'Propagational Factors in Short Wave Broadcasting Reception', B.B.C. Engineering Division Monograph, No. 43, August 1962.
11. E. W. Hayes and H. Page, 'The B.B.C. sound broadcasting service on very high frequencies', *Proc. I.E.E.*, **104**, Part B, No. 15, pp. 213-24 and 249-53, May 1957.
12. L. R. Kahn, 'Compatible single-sideband', *Proc. Inst. Radio Engrs*, **49**, No. 10, pp. 1503-27, 1961.
13. 'Stereophonic Systems for V.H.F. Frequency-Modulation Broadcasting', C.C.I.R. Recommendation No. 450, Documents of the XIth Plenary Assembly, p. 37, Oslo, 1966.
14. J. G. Spencer and G. J. Phillips, 'Stereophonic broadcasting and reception', *The Radio and Electronic Engineer*, **27**, No. 6, pp. 399-416, June 1964.
15. G. J. Phillips, 'Stereophonic broadcasting in Britain', *Electronics and Power*, **13**, pp. 287-91, August 1967.
16. Harold Black, 'Modulation Theory', (Van Nostrand, New York, 1953).
17. B. M. Oliver, J. R. Pierce and C. E. Shannon, 'The philosophy of p.c.m.', *Proc. I.R.E.*, **36**, No. 11, pp. 1324-31, November 1948.
18. 'Feasibility of Direct Sound and Television Broadcasting from Satellites', C.C.I.R. Report No. 215-1, Documents of the XIth Plenary Assembly, Vol. IV, Part 2, p. 444, Oslo, 1966.
19. R. S. Lawrence, C. G. Little and H. J. A. Chivers, 'A survey of ionospheric effects upon Earth-space radio propagation', *Proc. I.E.E.E.*, **52**, No. 1, pp. 4-27, January 1964.

*Manuscript received by the Institution on 6th November 1967. (Paper No. 1184/Com. 2.)*

© The Institution of Electronic and Radio Engineers, 1968

# A Simple Method for the Measurement of Varactor $Q$ -factor

By

R. B. SMITH,

B.Sc., Ph.D., C.Eng., M.I.E.E.†

**Summary:** In the proposed method, which is applicable to silicon varactors, measurement is made at a single frequency and the varactor is not matched to the measuring waveguide. The varactor  $Q$ -factor is determined from the change in phase of the reflection coefficient between two bias conditions and the voltage standing-wave ratio at one of these. The technique is suitable for production testing.

## List of Principal Symbols

$A, jB, jC, D$	constants of lossless transformer network
$\alpha$	transformer constant = $A/D$
$C_d$	depletion layer capacitance
$Q_d$	$Q$ -factor of semiconductor region
$Q_{d0}$	$Q$ -factor of semiconductor region for bias voltage at which the varactor is matched to the measuring waveguide
$Q_{dp}$	$Q$ -factor of semiconductor region for bias voltage at which $z_1$ is real
$\Delta\theta$	change in phase of the reflection coefficient between the $z_1 = r_1$ and $z_1 = jx_{1s}$ conditions
$R_d$	loss resistance of semiconductor region
$\rho$	complex reflection coefficient
$S$	voltage standing-wave ratio ( $S \geq 1.0$ )
$\omega$	angular frequency
$x_{1s}$	normalized reactance at reference plane in measuring waveguide when $Z_d = 0$
$z_1$	normalized impedance in the measuring waveguide ( $z_1 = r_1 + jx_1$ )
$Z_d$	impedance of semiconductor region ( $Z_d = R_d - j/\omega C_d$ )

## 1. Introduction

The impedance of the semiconductor region of a varactor diode cannot be directly measured in the microwave band because of the transforming effect of the diode encapsulation and its mount. To overcome this difficulty, several measurement techniques have been evolved and these fall into two categories, namely, transmission measurements and relative impedance measurements. For both, it is necessary to assume that for reverse bias voltages not exceeding the reverse breakdown voltage and for a single or small

range of frequencies, the impedance,  $Z_d$ , of the varactor semiconductor material can be equivalently represented by a simple series circuit. This circuit comprises the loss resistance,  $R_d$ , of the bulk semiconductor material on either side of the depletion layer and the dynamic capacitance,  $C_d$ , of the depletion layer. The capacitance  $C_d$  is a function of bias voltage and is generally assumed to be independent of frequency while  $R_d$  is assumed to be constant although it is potentially a function of both bias voltage and frequency.<sup>1</sup>

In transmission measurements, the parameters of the semiconductor region are determined from the transmission loss of the varactor as either frequency<sup>2</sup> or bias voltage<sup>3</sup> is varied. The varactor is mounted in reduced height waveguide or coaxial line, the characteristic impedance of which must be known, and the semiconductor region must form part of a resonant circuit, the mode of oscillation of which must be known or assumed.

Relative impedance measurements<sup>4,5</sup> do not rely on the semiconductor region forming part of a resonant circuit, but only enable the varactor  $Q$ -factor,  $Q_d = 1/\omega C_d R_d$ , to be found. The varactor is matched to the measuring waveguide using lossless matching elements and in this way  $Z_d$  is normalized to  $R_d$ . The measured impedance,  $z_1$ , at an appropriate reference plane is then given by,

$$z_1 = 1 + j(Q_{d0} - Q_d)$$

Here,  $Q_d$  is the varactor  $Q$ -factor at an arbitrary bias voltage and  $Q_{d0}$  its value at the bias voltage at which the varactor is matched. The change in varactor  $Q$ -factor,  $\Delta Q = Q_{d0} - Q_d$ , can be read directly from the locus of  $z_1$  or calculated from the magnitude of the reflection coefficient; although to find  $Q_{d0}$  from  $\Delta Q$ , the parameters of the depletion layer capacitance-voltage relationship must be known. However, if it is possible to make  $Z_d$  approximately equal to zero (which can be achieved with silicon but not with gallium arsenide varactors by passing high forward current through the junction),  $Q_{d0}$  can be found directly, since for this condition,  $z_1 = jQ_{d0}$ . To do this

† Postgraduate School of Studies in Electrical and Electronic Engineering, University of Bradford, Yorkshire.

it is necessary to plot an impedance locus over a range of bias conditions, including high forward current.

In making the relative impedance measurements outlined above, it is a common practice to match the varactor at some bias voltage which is often zero. However, Berlin and Davydov<sup>6</sup> have shown that this is not necessary in the measurement of  $\Delta Q$ . In this paper it is shown that the  $Q$ -factor of silicon varactors can also be found without matching the varactor to the measuring waveguide and moreover that it is then not necessary to plot an impedance locus. The proposed technique is simple to use and is suitable for production testing.

**2. Analysis of the Technique**

The varactor is mounted in a waveguide with suitable arrangements for the application of bias voltage. This waveguide is closed by a terminating short-circuit whose position is adjustable and there is no matching device between the varactor and the measuring waveguide. With the varactor mounted in this way, the impedance,  $Z_d$ , of the varactor semiconductor region is transformed into a normalized input impedance,  $z_1$ , at an arbitrary reference plane in the measuring waveguide. The transformer, which is here assumed to be lossless, can be represented by a two-port network as shown in Fig. 1. Since this network includes the terminating short-circuit, its parameters are a function of the short-circuit position.

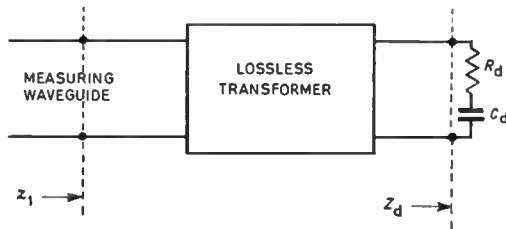


Fig. 1. Representation of the lossless transformation of the impedance of the semiconductor region.

For this lossless network and for any single frequency, the normalized input impedance,  $z_1$ , is related to the terminating impedance,  $Z_d$ , by the bi-linear relationship,

$$z_1 = \frac{AZ_d + jB}{jCZ_d + D} \dots\dots(1)$$

where  $A, B, C$  and  $D$  are real constants.

Equation (1) can be simplified if the reference plane in the measuring waveguide is chosen so that  $z_1 = \infty$  when  $Z_d = \infty$ . For this condition,

$$z_1 = A/jC = \infty$$

Hence  $C = 0$ , since  $A \neq \infty$ .

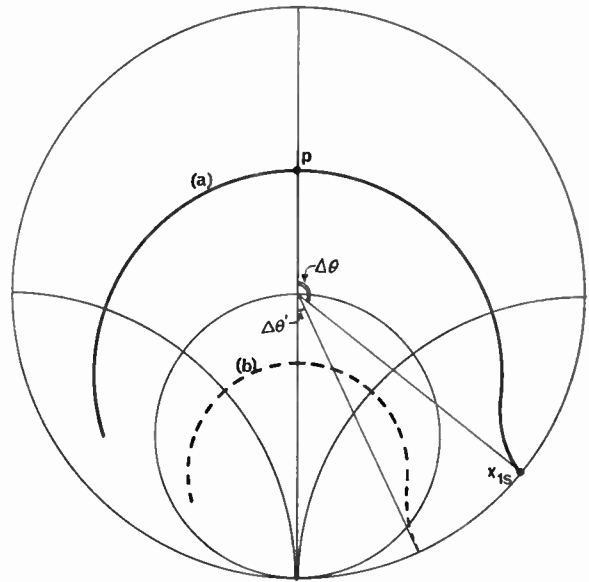


Fig. 2. Impedance loci.

(a) First type,  $r_1 < 1.0$ , (b) second type,  $r_1 > 1.0$ .

Substituting this condition in eqn. (1) and writing  $Z_d = R_d - j/\omega C_d$  gives

$$z_1 = \frac{A}{D} R_d \left\{ 1 + j \left( \frac{B}{AR_d} - \frac{1}{\omega C_d R_d} \right) \right\}$$

If  $z_1$  is real when  $C_d = C_{dp}$ , this becomes

$$z_1 = \alpha R_d \{ 1 + j(Q_{dp} - Q_d) \} \dots\dots(2)$$

where  $\alpha = A/D$  and  $Q_{dp} = 1/\omega C_{dp} R_d$  is the value of the varactor  $Q$ -factor when  $z_1$  is real. It also follows, when  $z_1$  is real, that

$$z_1 = r_1 = \alpha R_d \dots\dots(3)$$

By expressing the reflection coefficient in terms of the impedance given by eqn. (2), Berlin and Davydov<sup>6</sup> have shown that the change,  $\Delta Q$ , in  $Q_d$  between two bias voltages can be found from the voltage standing-wave ratios,  $S_1$  and  $S_2$  ( $S \geq 1.0$ ) at the two voltages and the corresponding change,  $\Delta\psi$ , in the phase of the reflection coefficient. Thus,

$$\Delta Q^2 = 2(p_1 p_2 - q_1 q_2 \cos \Delta\psi - 1) \dots\dots\dagger(4)$$

where

$$p_{1,2} = \frac{S_{1,2}^2 + 1}{2S_{1,2}}$$

and

$$q_{1,2} = \frac{S_{1,2}^2 - 1}{2S_{1,2}}$$

† This must be the equation obtained by Berlin and Davydov although it is not the equation given in their paper<sup>6</sup> in which there is presumably a typographical error.

As  $C_d$  is varied, it is seen from eqn. (2) that, if  $R_d$  is constant, the locus of  $z_1$  lies on a constant-resistance circle on the Smith Chart. This locus can be of two types. The first type which is shown as a full curve in Fig. 2 lies outside the unit-resistance circle; the second type, as shown by the dashed curve, lies inside the unit-resistance circle. In the following analysis it is assumed that the locus is of the first type but where differences occur, if the locus is of the second type, these are discussed.

If high forward current flows in the varactor and  $Z_d$  falls to zero, it follows from eqn. (2) that

$$z_1 = jx_{1s} = j\alpha R_d Q_{dp}$$

Substitution in this equation for  $\alpha R_d$  from eqn. (3) gives

$$Q_{dp} = \frac{x_{1s}}{r_1} \quad \dots\dots(5)$$

It should be noted that if the impedance locus is of the first type than  $r_1 < 1.0$ , and if it is of the second type,  $r_1 > 1.0$ , but that eqn. (5) holds for both types.

Although the varactor is not matched to the measuring waveguide at any bias voltage,  $Q_{dp}$  can be found using eqn. (5) from an impedance locus plotted relative to an appropriate reference plane. The impedance locus, relative to this reference plane, can be obtained by plotting the locus relative to an arbitrary reference plane and then rotating this about the centre of the Smith Chart for best coincidence with a constant-resistance circle. However, when the varactor is unmatched, it is not necessary to plot an impedance locus. For an impedance locus of the first type, the angle of the reflection coefficient corresponding to the  $z_1 = r_1$  condition is  $\pi$  radians and of the  $z_1 = jx_{1s}$  condition is  $(\pi - \Delta\theta)$  radians, where  $\Delta\theta$  is the difference between the angles of the reflection coefficients of the two conditions. The reflection coefficient of the  $z_1 = jx_{1s}$  condition, whose magnitude is unity, may be expressed in terms of  $jx_{1s}$ . Thus

$$\rho = \exp [j(\pi - \Delta\theta)] = \frac{jx_{1s} - 1}{jx_{1s} + 1}$$

and then

$$x_{1s} = \tan (\Delta\theta/2) \quad \dots\dots(6)$$

If the voltage standing-wave ratio is  $S_p$  when  $z_1 = r_1$ , then,

$$r_1 = \frac{1}{S_p} \quad \dots\dots(7)$$

Combining eqns (6) and (7) with eqn. (5) gives

$$Q_{dp} = S_p \tan (\Delta\theta/2) \quad \dots\dots(8)$$

If the impedance locus is of the second type, then this equation becomes

$$Q_{dp} = \frac{\cot (\Delta\theta'/2)}{S'_p} \quad \dots\dots(9)$$

The dashed symbols refer to the locus of the second type (Fig. 2).

### 3. Experimental Procedure

The varactor bias voltage is set to the value for which its  $Q$ -factor is required. The position of the terminating short-circuit is then adjusted for minimum standing-wave ratio in the measuring waveguide. Since any change in  $C_d$  will now result in an increase of the standing-wave ratio, the impedance at the reference plane in the measuring waveguide will correspond to point  $p$  on the impedance locus of Fig. 2. The value of  $S_p$  can therefore be measured directly and  $\Delta\theta$  determined from the change in phase of the standing-wave pattern when high forward current is passed through the varactor, i.e. when the  $z_1 = jx_{1s}$  condition is realized.  $Q_{dp}$  is then found using eqn. (8) or eqn. (9). To know which equation is applicable, the type of the impedance locus must be established and this is achieved, without plotting an impedance locus, in the following manner. On the application of high forward-current it is noted in which direction the standing-wave minimum moves. It can be deduced from Fig. 2 that the minimum moves towards the load if the locus is of the first type and towards the generator if the locus is of the second type. It may, however, be desirable to plot a complete locus for, perhaps, one out of a batch of varactors. In this way the type of the locus is clearly established and, further, some indication of the effect of loss in the measuring system can be obtained.<sup>7</sup>

Since a small error in  $\Delta\theta$  will give a relatively large error in  $Q_{dp}$  if  $\Delta\theta > \pi/2$ , it is necessary to establish  $\Delta\theta$  with the greatest possible accuracy. The phase of the standing-wave pattern for the high forward current condition can be measured with good accuracy since the standing-wave ratio is then large and the position of minima well defined. However, at  $p$  the standing-wave ratio is relatively small and phase measurement less accurate, although the method of equal responses can give considerable improvement. Furthermore, it can be seen from Fig. 2 that in the region of  $p$ , the standing-wave ratio varies slowly with bias voltage and the same is true for the variation with the position of the terminating short-circuit. Great care must therefore be taken in establishing the minimum voltage standing-wave ratio condition or serious errors will be incurred.

This difficulty can be overcome by making phase and standing-wave ratio measurements at two points on either side of  $p$  for which the standing wave ratio is the same. At these points the standing-wave ratio is varying rapidly with bias voltage and hence the

points are well defined. From these measurements and the phase measurement for the high forward-current condition, varactor  $Q$ -factor can be found using eqns. (4) and (8). However, the simplicity of the method is thereby lost, although accuracy is improved.

#### 4. Results

Measurements have been made of the  $Q$ -factor of silicon varactors using the proposed technique. These varactors were encapsulated in standard microwave cartridges. The results were compared with the  $Q$ -factor from an impedance locus obtained with and without matching the varactor to the measuring line. When care was taken in establishing the minimum standing-wave ratio condition, good agreement was obtained. The  $Q$ -factors at zero bias voltage for the varactor used ranged from 1.5 to 4.0 at a frequency of 9.5 GHz, which was also the measurement frequency.

#### 5. Conclusion

A simple measurement technique for determining the  $Q$ -factor of silicon varactors has been presented. Although the positioning of the terminating short-circuit requires care, the varactor is not matched to the measuring waveguide at any bias voltage. The varactor  $Q$ -factor is found from the change in the phase of the reflection coefficient between two bias conditions and the voltage standing wave ratio at one of these.

#### 6. Acknowledgments

The author wishes to acknowledge the benefit of discussions with his colleague, Mr. L. J. Hoyle, and the provision of varactors by The Marconi Company. He is also grateful to Professor G. N. Patchett for the generous facilities made available for the use of the author in the Postgraduate School of Studies in Electrical and Electronic Engineering at Bradford.

#### 7. References

1. C. Toker and F. J. Hyde, 'The series resistance of varactor diodes', *The Radio and Electronic Engineer*, **32**, pp. 165–8, September 1966.
2. B. C. DeLoach, 'A new microwave measurement technique to characterize diodes and an 800 Gc/s cutoff frequency varactor at zero volts bias', *Trans. Inst. Elect. Electronics Engrs on Microwave Theory and Technique*, **MTT-12**, p. 15, January 1964.
3. D. A. E. Roberts and K. Wilson, 'Evaluation of high-quality varactor diodes', *The Radio and Electronic Engineer*, **31**, pp. 277–85, May 1966.
4. N. Houlding, 'Measurement of varactor quality', *Microwave J.*, **3**, p. 40, January 1960.
5. R. I. Harrison, 'Parametric diode  $Q$  measurements', *Microwave J.*, **3**, p. 43, May 1960.
6. A. S. Berlin and V. M. Davydov, 'Method of measuring the quality factor of microwave varactor diodes without the use of standard resistors and alignment of the measuring chamber' *Radio Engineering and Electronic Physics.*, (English language edition of *Radiotekhnika i Elektronika*), **10**, p. 1780, November 1965.
7. F. J. Hyde and R. B. Smith, 'Effect of losses in varactor-diode impedance measurements', *Proc. Instn Elect. Engrs*, **111**, p. 471, March 1964.

*Manuscript first received by the Institution on 10th August 1967 and in revised form on 20th November 1967.*

(Contribution No. 102.)

© The Institution of Electronic and Radio Engineers, 1968